NUMERICAL OPTIMIZATION OF SHIP HULL FORMS FROM VIEWPOINT OF WAVEMAKING RESISTANCE BASED ON PANEL METHOD
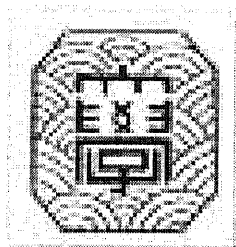
造波抵抗を考慮したパネル法に基づく船型の数値最適化

NUMERICAL OPTIMIZATION OF SHIP HULL FORMS FROM VIEW POINT OF WAVEMAKING RESISTANCE BASED ON PANEL METHOD

造波抵抗を考慮したパネル法に基づく船型の数値最適化

A Doctoral Dissertation

By

Goutam Kumar Saha

Graduate School of Engineering

Yokohama National University, Japan

September 2004

Numerical Optimization of Ship Hull Forms from View Point of Wavemaking Resistance Based on Panel Method

By

Goutam Kumar Saha

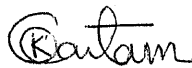B.Sc., Bangladesh University of Engineering and Technology, 1996

M.Sc., Bangladesh University of Engineering and Technology, 2000

A Thesis submitted to Graduate School of Engineering, Yokohama National University in partial Fulfillment of the Requirements for the Degree of

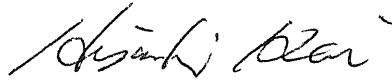**Doctor of Engineering**

September 2004

Signature of Author_____

Goutam Kumar Saha
Graduate School of Engineering
Yokohama National University
September 2004

Certified by _____

Professor Kazuo Suzuki
Thesis Supervisor
Department of Ocean and Space Engineering
Faculty of Engineering
Yokohama National University

Certified by _____

Dr. Hisashi Kai
Thesis Co-supervisor
Department of Ocean and Space Engineering
Faculty of Engineering
Yokohama National University

Certified by _____

Professor Tsugukiyo Hirayama
Member
Department of Ocean and Space Engineering
Faculty of Engineering
Yokohama National University

Certified by _____

Professor Makoto Arai
Member
Department of Ocean and Space Engineering
Faculty of Engineering
Yokohama National University

Certified by _____

Professor Kyoji Kamemoto
Member
Department Mechanical Engineering
Faculty of Engineering
Yokohama National University

Numerical Optimization of Ship Hull Forms from View Point of Wavemaking Resistance Based on Panel Method

By Goutam Kumar Saha

Abstract

A computational method is proposed for the analysis of hydrodynamic performance of ships and the design of optimized hull form in shallow water and deep water with respect to the wavemaking resistance is presented. The method involves coupled ideas from two distinct research fields: numerical ship hydrodynamics and nonlinear programming technique. Having the numerical tools for hydrodynamic analysis, a mathematical procedure for optimizing hull forms is developed. The optimal hull form design system enables the designer to include advanced resistance performance predictions at the early stage of design process, allowing a systematic evaluation of the resistance performance characteristics as a function of the hull geometry.

The wavemaking resistance of ships is estimated by means of Morino's panel method extended to free surface flow and into the influence of finite depth on the wave resistance of ships and PAFS is linked to the optimization procedure of Sequential Quadratic Programming (SQP) technique. An optimum hull form can be obtained through a series of iterative computation subject to some design constraints.

The developed optimization procedure in shallow water is demonstrated by choosing a mathematical Wigley (C_B = 0.444) hull and a standard Series 60 (C_B = 0.60) hull. The optimization in shallow water is carried out at Froude number of 0.316 and the wavemaking resistance taken as an objective function and the optimized hull forms are obtained for different depths of water. The specified Froude number corresponds to lower

I

than depth critical speed since most of ships operating in shallow water below depth critical speed. The sinkage is an important factor in shallow water and this method considered sinkage as a hydrodynamic design constraint during the optimization process. The numerical results of optimization procedure indicate that the optimized hull forms in shallow water yields a reduction in wavemaking resistance.

In the optimization of catamaran ship hull without and with airship forms bulb installed on the center plane of catamaran, a mathematical ship hull of cosine waterline and parabolic frame line has been chosen to carry out the fundamental study of the numerical optimization and the wavemaking resistance taken as the objective function. The optimization is carried out at two Froude numbers 0.45 and 0.50 respectively, which are around the last hump of the wavemaking resistance curve of catamaran ship and most of the catamaran ships are running in high-speed range. The optimized catamaran hulls without and with airship form bulbs show lower wavemaking resistance with original ones around the design speed.

The entire process of hydrodynamic analysis, geometrical modeling and optimization thus attempts to imitate the traditional hull form design procedure. The system of computer can be used to develop mathematically faired and hydrodynamically desirable hull forms from an existing ship.

Acknowledgement

Table of Contents

List of Figures

X

List of Tables

CHAPTER 1

Introduction

The numerical shape optimization technique is a promising method for the design problems in engineering because it can supplement an experience and guide when designing new geometries or trying to improve the efficiency of the existing ones. Approach of using a direct flow solver and general robust constraint methods is accepted in 3D industrial aerodynamics design, simple geometries and simple flow models such as 2D airfoils or wing profiles, the shape optimization methods are widely used.

The most fundamental and persistent problem in ship hydrodynamics is the design of a low resistance ship that satisfies given requirements of displacement volume and speed. Ship designers and ship hydrodynamicists have always been interested in finding ship forms of minimum resistance. The knowledge of the flow around the ship and its resistance components is very important in ship hull form development.

Traditionally naval architects design the ship hull form and perform the model tests to survey the wave property. If the results cannot meet the expectation, then they modify the hull form and execute another test, repeating the process until satisfactory result are obtained. This optimal cycles consumes time and cost. In recent years computational fluid dynamics (CFD) method were introduced into the design process to simulate the flow filed around the hull.

Numerical optimization is a well established mathematical filed and there are numerous references on the theory and application of numerical optimization technique. Many mathematical algorithms exist for solving optimization problems. However, they vary greatly in efficiency and quality of the final solution for a given number of function evaluations. No single technique is best for solving all problems.

1

An interesting possibility is to combine a CFD method and a numerical method together with a program for hull form variation. This procedure can be used to find a hull that is optimized with respect to properties computed by the CFD method, such as resistance, wave-height, sinkage, trim etc. One or more geometrical constraints for instance displacement and ship hull main dimensions and hydrodynamic constraints such as sinkage, trim etc. must be introduced to limit the modifications of the hull.

Many interesting works on hull optimization in deep water from hydrodynamic point of view have been presented through the years, both for conventional and unconventional ships (Hino 1996, Hino et al. 1998, Peri et al. 2001 and Tahara et al. 1998). Different hydrodynamic models for the flow prediction have been used, from thin ship theory for the wave resistance to more advanced CFD methods. Some of these attempts seem to be encouraging as numerical computations show improvements of the optimized design.

The term "shallow water" is used to describe a body of water in which the boundaries are close to the ship only in the vertical direction. When the water shallows, the resistance of the ship moving through it will become greater. The three-dimensional motion of the water will approach a two dimensional character. The pressure set up by the ship's motion will be greater and this extra pressure in shallow water causes waves larger than those in deep water. In shallow water the lengths of waves accompanying the ship at a given speed, are greater than for the same speed in deep water. Furthermore, the change in stream velocities past the surface of the ship when in shallow water will increase the resistance somewhat.

It is important to know what happened if a hull form optimized for deep water operates in shallow water. In shallow water there is a phenomena commonly referred to as squat that increases draft of a ship, while it is steaming in shallow water. Ship squat or decrease in under keel clearance when a ship moving in shallow water, is one of the most important and well known phenomena affecting safe operation of ships in restricted waters. Squat is present also in deep water. Sinkage and trim, or squat is important in very shallow water because of its practical consequences to under-keel clearance. In shallow water it is common for a vessel to reach a state of operation known as critical

speed where instead of a combination of diverging and transverse waves seen in deep water, a wave pattern is created and moves in the forward direction as the ship. This wave pattern is typically large and takes much energy to create and can lead to severe environmental problems near the shore. At speed greater or less than critical speed, the steepness of created waves and the resulting resistance are greatly reduced. Therefore, it is required to estimate the speed range through shallow water areas and the wave making resistance for primary hull form design.

It is necessary to mention here that Bangladesh is a riverine country. Some major rivers flow through this country and finally discharge into the Bay of Bengal, which surrounds the southern part. River craft, big and small play a very important role in the transportation of goods and passengers through the country. There is no doubt that the rivers and the Bay of Bengal are very significant in relation to the economic development. A striking feature of many rivers of Bangladesh is the vast shallow water areas, which necessitate strict draft requirement for ship.

The catamaran or twin hull concept has been employed in high-speed craft design for several decades, and both sailing as well as powered catamarans are used.   The resistance of a catamaran is mainly affected by the wetted surface ratio [wetted surface area/ (volume-displacement)$^{2/3}$], the slenderness ratio [length/(volume-displacement)$^{1/3}$], and the hull spacing . The wetted surface ratio is relatively high compared with mono-hulls of same displacement. Consequently catamarans show poor performance at low speed (F_n < 0.35) where skin friction is predominant. At higher speeds (in the hump region, $F_n \approx 0.5$) the low trim angles associated with the slender demi-hulls of the catamaran lead to a favorable performance. The hull spacing ratio is associated with the interference effects between the component hulls. These effects consist of wave interference effects and body interference effects. Wave interference effects are due to the superposition of two wave systems, each associated with a component hull in isolation. The body interference effects are caused by the change of flow around one demi-hull due to the presence of the other hull. The wave interference may influence the resistance to a large extent. Beneficial wave interference is achieved by the cancellation

of part of the divergent wave systems of each demi hulls, whereas adverse wave interference arises on interaction of the transverse wave system. The generation of vertical hydrodynamic lift and the associated change of hull form because of trim and rise of the center of gravity , may have a significant effect on the interference effects.

The wavemaking resistance characteristic of high-speed catamaran ship is improved by the use of hydrofoil, streamlined bodies of revolution placed between the demi-hulls, etc. Many ships operating on seaway now have conventional bulbous bow, which can reduce the wave resistance by hydrodynamic interaction of the waves between the main hull and the bulb. However, results of the minimum wave resistance theory show that the higher speed the optimum bulb radius becomes the larger. In a practical sense, those results are not applicable to most high-speed ships of displacement. In high-speed range, the wavelength of the elementary waves generated by a disturbance becomes so large that the so-called wavemaking length becomes large too. According to this consideration, the relative position of the bulb to the main hull is one of the important factors. In the case catamaran, airship form bulb is introduced instead of conventional bulb. The airship form bulb is expressed as an axis-symmetric streamline body formed by the combination of a hydrodynamic point source and line sink.

In order to solve a hydrodynamic optimization problem like ship hull forms optimization, following elementals are necessary; an evaluation method of an objective function related to a hydrodynamic performance, a numerical optimization technique of the objective function and a numerical shape deformation method of ship hull form in the optimization process.

1.1 Previous Research

1.1.1 Mono Hull in Shallow Water and Deep Water

The effect upon resistance due to the changes in flow in shallow water has attracted the interest of scientist for many years. Michell, J. H. (1898) first derived an analytical expression for the wave resistance of ship moving in calm water. Havelock, T. H. (1922) studied the effects of shallow water on the wave resistance and wave pattern for a point pressure impulse traveling over a free surface. Kinoshita M. & Inui, T. (1953) extended

Havelock's theory to satisfy bottom boundary condition more exactly. Kirsch, M. (1966) used linearized wave theory to calculate the wavemaking resistance for simplified hull form in different water depths and channel widths. Muller, E. (1985) carried out extensive experiments and theoretical calculations based on linearized wave theory to investigate the effect of shallow water on wavemaking resistance. Yasukawa, T. (1989) has developed first order panel method based on Dawson's approach for the linear free surface condition and shallow water effect is undertaken by replacing the bottom surface with Rankine sources. Tarafder, M.D., Suzuki, K. and Kai, H (2002, 2002) used Morino's panel method (1976) into the influence of finite depth on the wave resistance of ships. The other researchers who have important contribution in ship resistance in shallow water are Maruo and Tachibana (1981), Lee (1992), Kim et al. (1996) respectively.

1.1.2 Catamaran Hull

The wavemaking resistance characteristic of high-speed catamaran ship with airship form large bow and stern bulbs installed on the center plane of a catamaran are suggested and their wavemaking characteristics to reduce the wavemaking resistance acting on the catamaran in high speed range by means of model experiments and numerical analyses based on panel method has been investigated by Suzuki. K., Kai, H. and Tatsunami, H (2003, 2003) and about 40-45% reduction of wavemaking resistance can be expected. Also resistance characteristics of ship hull forms with airship form bulbs have been investigated and the airship form bulb which minimize the wave resistance in high speed range by hydrodynamic interaction with the main hull proposed by Suzuki, K. et. al (1994), Ikehata, M. and Suzuki, K. (1995).They found that the shape of the main hull becomes more slender and bulb size becomes larger according to the increment of design speed and if optimizing the bulb position, it changes and protrudes larger with increasing the design speed. Ando, J. and Nakatake, K. (2004) has been done hull form improvement of catamaran using genetic algorithm. Zotti, I. (2003) has investigated hydrodynamic improvement of catamaran with streamlined bodies of revolution having different length to diameter. Research on resistance reduction in catamaran also have been investigated by Söding, S. (1997) and Zotti, I. (1997) and made great contribution on the research of wave resistance of catamaran.

1.2 Present Research

1.2.1 Optimization of Mono Hull (Wigley and Series 60, $C_B = 0.6$) in Shallow Water

In this study, a hydrodynamic optimization is carried out at a design Froude no $F_n = 0.316$ on Wigley Mathematical hull ($C_B = 0.444$) and practical Series 60 ($C_B = 0.6$) in shallow water.

In the present, the hydrodynamic shape optimization system for three-dimensional bodies is constructed based on panel method, PAFS (Panel Applied to Free Surface Flow) and a numerical optimization method called SQP (Sequential Quadratic Programming). In the optimization procedure the wavemaking resistance has been selected as a single objective function. A body shape is defined by the design variables and the combinations of design variable which gives the body of hydrodynamic extremity such as minimum wave resistance under certain geometrical and hydrodynamical constraints is sought. If the sinkage is large, under-keel clearance will be low for a particular depth of water and may cause a ship to scrape the bottom. This circumstance should be borne in mind while ensuring the safety operation of ships with a restricted draft in the design process. So sinkage is an important factor in shallow water, this method specially considered as a hydrodynamic design constraint. The critical speed is related to the depth Froude Number. The critical depth Froude number is 1.0. The optimization is carried out at Froude number lower than critical depth Froude number since most of the ships operating in shallow water below critical speed at a particular depth of water.

1.2.2 Optimization of Catamaran Hull

A hydrodynamic optimization problem for catamaran ship hull with and without bow and stern bulbs installed on the center plane of demi-hulls has been treated. The body shape of demi-hull without and with airship forms bulbs installed on the center plane of demi-hull optimized to achieve lower wave resistance hull and to observe the hydrodynamic interaction between demi-hull and bulbs. Relatively high Froude numbers (0.45 and 0.50) are selected, as most of catamaran ships run in high-speed range and the selected Froude numbers are around the last hump of the wavemaking resistance curve.

6

In the optimization PAFS used as three-dimensional flow solver and SQP, a numerical optimization tool. Bulb position and bulbs size didn't optimize but only the body shape of main hull.

CHAPTER 2

Numerical Modeling of Potential Flow Method

2.1 General Nonlinear Boundary Value Problem

The flow around a ship moving with a steady forward speed U under the influence of incoming waves defines a boundary value problem for the velocity potential. The problem is analyzed by introducing two co-ordinate systems as show in Figure 2.1. The first is the inertial axis system x-y-z advancing in space with steady speed U in the positive x direction, y directed to starboard and z vertically upward. The origin of this system is in the plane of the undisturbed free surface above the center of gravity. The other axis system x-y'-z' is fixed to the body. The two systems coincide with each other when there is no motion. The fluid is assumed to be inviscid and incompressible and the flow is irrotational such that the velocity potential Φ can be defined as
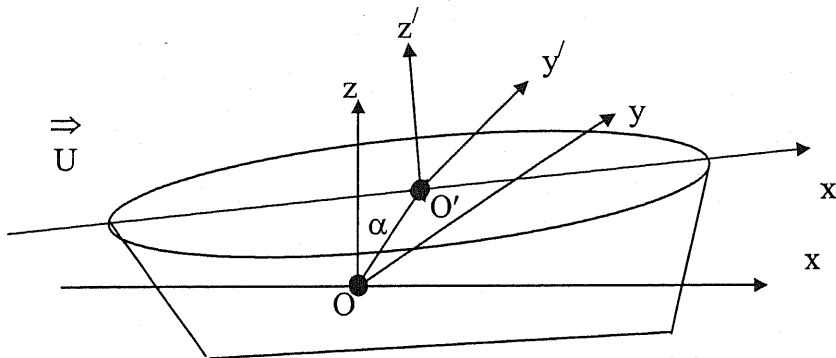
Fig. 2.1 Definition sketch of co-ordinate system

$$\Phi = U.x + \phi \tag{2.1.1}$$

where ϕ is the perturbation velocity potential due to the presence of the body. The velocity potential Φ satisfies the Laplace equation

$$\nabla^2 \Phi = 0 \tag{2.1.2}$$

in the fluid domain V. The hull boundary condition requires that normal velocity potential on the hull must be zero.

$$\nabla\Phi \cdot n = 0 \qquad\qquad (2.1.3)$$

The kinematic and dynamic boundary conditions on the free surface can be respectively written as:

$$\Phi_x \zeta_x + \Phi_y \zeta_y - \Phi_z = 0 \quad \text{at} \quad z = \zeta \qquad\qquad (2.1.4)$$

$$g\zeta + \frac{1}{2}\left[\nabla\Phi.\nabla\Phi - U^2\right] = 0 \quad \text{at} \quad z = \zeta \qquad\qquad (2.1.5)$$

Combining Equation (2.1.4) and Equation (2.1.5)

$$\nabla\Phi.\nabla\left[\frac{1}{2}(\nabla\Phi.\nabla\Phi)\right] + g\Phi_z = 0 \quad \text{at} \quad z = \zeta \qquad\qquad (2.1.6)$$

Finally energy condition requires that the velocity potential approaches the uniform onset flow potential. There are no waves far upstream of the ship and waves always travel in the downstream direction.

The problem described in equations (2.1.1) to (2.1.5) is nonlinear since the free surface conditions (2.1.4) and (2.1.5) themselves are nonlinear and should be satisfied on the true free surface which is unknown and should be obtained as a part of the solution.

◆ 2.1.1 Linearization of Free Surface Boundary Condition:

In order to analyze the above (Equation 2.1.4 and Equation 2.1.5) nonlinear free surface problem, the first step is to introduce appropriate smallness parameter, with respect to which the above expressions are to be perturbed. Here we define the smallness parameter $\varepsilon = B/L$, where B and L are the Beam and length of the ship. Then the surface of the ship can be written as

$$y = \varepsilon \, f(x,z)$$

◆ 2.1.2 Free Surface Boundary Condition for Uniform Flow

As the perturbation velocity potential of the fluid motion generated by a thin ship is small in order of ε, one can expand the velocity potential in a power of series such as (Maruo, 1966):

$$\phi = \varepsilon\phi_1 + \varepsilon^2\phi_2 + \ldots\ldots\ldots \qquad\qquad (2.1.7)$$

So the total velocity potential can be written as

$$\Phi = U.x + \varepsilon\phi_1 + \varepsilon^2\phi_2 + \ldots\ldots\ldots \qquad\qquad (2.1.8)$$

The corresponding wave elevation can be written as

$$\zeta = \varepsilon\zeta_1 + \varepsilon^2\zeta_2 + \ldots\ldots\ldots\ldots \tag{2.1.9}$$

Substituting equation (2.1.8) into equation (2.1.6)

$$\frac{1}{2}U.\nabla\left[U^2 + \varepsilon.2U.\nabla\phi_1 + \varepsilon^2\left(\nabla\phi_1.\nabla\phi_1 + 2U.\nabla\phi_2\right)\right] +$$

$$\frac{1}{2}\varepsilon\nabla\phi_1.\nabla\left[U^2 + \varepsilon.2U.\nabla\phi_1 + \varepsilon^2\left(\nabla\phi_1.\nabla\phi_1 + 2U.\nabla\phi_2\right)\right] + \tag{2.1.10}$$

$$\frac{1}{2}\varepsilon^2\nabla\phi_2.\nabla\left[U^2 + \varepsilon.2U.\nabla\phi_1\right] + g\left[\varepsilon\phi_{1z} + \varepsilon^2\phi_{2z}\right] + O(\varepsilon^3) = 0$$

Rearranging Equation (2.1.10) and obtain

$$\varepsilon\left[U.\nabla(U.\nabla\phi_1) + g\phi_{1z}\right]_{z=\zeta}$$

$$\varepsilon^2\left[U.\nabla(U.\nabla\phi_2) + g\phi_{2z} + \frac{1}{2}U.\nabla(\nabla\phi_1.\nabla\phi_1) + \nabla\phi_1.\nabla(U.\nabla\phi_1)\right]_{z=\zeta} \tag{2.1.11}$$

Using the following vector identities into Equation (2.1.11)

$$\frac{1}{2}U.\nabla(\nabla\phi_1.\nabla\phi_1) = \nabla\phi_1.\nabla(U.\nabla\phi_1)$$

$$U.\nabla(\nabla\phi_1.\nabla\phi_2) = \nabla\phi_2.\nabla(U.\nabla\phi_1) + \nabla\phi_1.\nabla(U.\nabla\phi_2)$$

we obtain

$$\left[\frac{1}{2}\nabla\Phi.\nabla(\nabla\Phi.\nabla\Phi) + g\Phi_z\right]_{z=\zeta} = \varepsilon\left[U.\nabla(U.\nabla\phi_1) + g\phi_{1z}\right]_{z=\zeta} +$$

$$\varepsilon^2\left[U.\nabla(U.\nabla\phi_2) + g\phi_{2z} + U.\nabla(\nabla\phi_1.\nabla\phi_1)\right]_{z=\zeta} = 0 \tag{2.1.12}$$

The boundary condition is to be evaluated at the unknown position, $z = \zeta$. To avoid the difficulties we choose to satisfy a boundary condition at mean value of ζ (at $z = 0$, still water plane) by using Taylor's theorem. The function $\Phi(x,y,z)$ can be written

$$\Phi(x,y,z) = \Phi(x,y,0) + \zeta\Phi_{1z}(x,y,0) + \frac{1}{2}\zeta^2\Phi_{2z}(x,y,0) + \ldots\ldots\ldots$$

Similarly

$$\left[\phi\right]_{z=\zeta} = \left[\phi\right]_{z=0} + \zeta\left[\phi_{1z}\right]_{z=0} + \frac{1}{2}\zeta^2\left[\phi_{2z}\right]_{z=0} + \ldots\ldots\ldots$$

Now expanding Equation (2.1.12) we obtain

$$\varepsilon[U.\nabla(U.\nabla\phi_1)+g\phi_{1z}]_{z=0}+\varepsilon\zeta\frac{\partial}{\partial z}[U.\nabla(U.\nabla\phi_1)+g\phi_{1z}]_{z=0}+$$

$$\varepsilon\frac{1}{2}\zeta^2\frac{\partial^2}{\partial z^2}[U.\nabla(U.\nabla\phi_1)+g\phi_{1z}]_{z=0}+\varepsilon^2[U.\nabla(U.\nabla\phi_2)+g\phi_{2z}+U.\nabla(\nabla\phi_1.\nabla\phi_1)]_{z=0}+ \quad (2.1.13)$$

$$\varepsilon^2\zeta\frac{\partial}{\partial z}[U.\nabla(U.\nabla\phi_2)+g\phi_{2z}+U.\nabla(\nabla\phi_1.\nabla\phi_1)]_{z=0}=0$$

Substituting Equation (2.1.9) into Equation (2.1.13) we get

$$\varepsilon[U.\nabla(U.\nabla\phi_1)+g\phi_{1z}]_{z=0}+\varepsilon^2\left[\zeta_1\frac{\partial}{\partial z}(U.\nabla(U.\nabla\phi_1)+g\phi_{1z})_{z=0}\right]_{z=0}+$$

$$\varepsilon^2[U.\nabla(U.\nabla\phi_2)+g\phi_{2z}+U.\nabla(\nabla\phi_1.\nabla\phi_1)]_{z=0}=0 \quad (2.1.14)$$

Now taking the coefficients of ε, ε^2 on each side of Equation (2.1.14) and substituting $g/U^2=K_0$, we have

$$\varepsilon:\quad U.\nabla(U.\nabla\phi_1)+g\phi_{1z}=0 \quad\quad \text{on}\quad z=0 \left.\begin{array}{c}\\\\\end{array}\right\}$$
$$\phi_{1xx}+K_0\phi_{1z}=0 \quad\quad \text{on}\quad z=0 \quad\quad\quad (2.1.15)$$

$$\varepsilon^2:\quad U.\nabla(U.\nabla\phi_2)+g\phi_{2z}=-U.\nabla(\nabla\phi_1.\nabla\phi_1)-\zeta_1\frac{\partial}{\partial z}[U.\nabla(U.\nabla\phi_1)+g\phi_{1z}]$$

$$\phi_{2xx}+K_0\phi_{2z}=f(\phi_1) \quad\quad \text{on}\quad z=0 \quad\quad\quad (2.1.16)$$

$$f(\phi_1)=-\frac{1}{U}\frac{\partial}{\partial x}(\phi_{1x}^2+\phi_{1y}^2+\phi_{1z}^2)-\zeta_1\frac{\partial}{\partial z}(\phi_{1xx}+K_0\phi_{1z})$$

Similarly expanding Equation (2.1.5) we obtain the equations of wave profiles for the 1st order, 2nd order approximation respectively as

$$\zeta_1=-\frac{1}{g}(U.\nabla\phi_1)=-\frac{U}{g}\phi_{1x}$$

$$\zeta_2=-\frac{1}{g}\left[\frac{1}{2}\nabla\phi_1.\nabla\phi_1+U.\nabla\phi_2+\zeta_1\frac{\partial}{\partial z}(U.\nabla\phi)\right]$$

$$=-\frac{1}{g}\left[U.\phi_{2x}+\frac{1}{2}(\phi_{1x}^2+\phi_{1y}^2+\phi_{1z}^2)+U\zeta_1\phi_{1xz}\right]$$

Finally the equations of the wave profiles

$$\zeta_1=-\frac{U}{g}\phi_{1x} \quad\quad\quad\quad\quad\quad\quad\quad\quad\quad (2.1.17)$$

$$\zeta_2=-\frac{U}{g}\phi_{2x}-\frac{U}{g}\zeta_1\phi_{1xz}-\frac{1}{2g}(\phi_{1x}^2+\phi_{1y}^2+\phi_{1z}^2) \quad\quad\quad\quad (2.1.18)$$

◆ 2.1.3 Free Surface Boundary Condition for Sinkage and Trim

The total velocity potential can be represented by means of two small parameters ε and δ, the first one ϕ pertaining to the steady motion due to uniform flow and second one φ to the first order oscillatory motion of the ship (Timman et al. 1985),

$$\Phi = U.x + \phi + \delta\varphi$$
$$= U.x + \sum_{n=1}^{\infty} \varepsilon^n \phi_n + \delta\left(s\varphi_s + t\varphi_t\right) \tag{2.1.19}$$

where φ_s is the steady potential due to unit sinkage and φ_t is the steady potential due to unit trim. s is the sinkage (positive upward) and t is the trim angle (trim by the stern is positive).

For the second order approximation $(\delta \approx \varepsilon^2)$ the velocity potential and the wave elevation are written as

$$\left. \begin{array}{l} \Phi = U.x + \varepsilon\phi_1 + \varepsilon^2\left(\phi_2 + s\varphi_s + t\varphi_t\right) \\ \zeta = \varepsilon\zeta_1 + \varepsilon^2\left(\zeta_2 + s\zeta_s + t\zeta_t\right) \end{array} \right\} \tag{2.1.20}$$

Substituting the second order terms of velocity potential and wave elevation in Equation (2.1.16) and (2.1.18), we have

$$\varepsilon^2 : \varphi_{sxx} + K_0\varphi_{sz} = 0 \quad \text{for sinkage}$$

$$\varphi_{txx} + K_0\varphi_{tz} = 0 \quad \text{for trim}$$

$$\varepsilon^2 : \quad \zeta_s = -\frac{U}{g}\varphi_{sx} \quad \text{for sinkage}$$

$$\zeta_t = -\frac{U}{g}\varphi_{tx} \quad \text{for trim}$$

◆ 2.1.4 Linearization of Body Boundary Condition

The second order fluid velocity vector on the instantaneous wetted surface S_H can be obtained as

$$\nabla\Phi = W + \varepsilon^2\left(\nabla\phi_2 + \nabla\varphi\right) \tag{2.1.21}$$

where

$$W = Ux + \varepsilon\nabla\phi_1$$

12

The local velocity vector $\nabla\Phi$ on the instantaneous wetted surface S_H of the ship may be expanded about the mean position of the body surface S_0 using the vector form of Taylor's theorem as:

$$[\nabla\Phi]_{S_H} = [\nabla\Phi]_{S_0} + (\alpha.\nabla)[\nabla\Phi]_{S_0} + \frac{1}{2}(\alpha.\nabla)^2[\nabla\Phi]_{S_0} + \ldots\ldots\ldots$$
$$= [\nabla\Phi]_{S_0} + (\alpha.\nabla)[\nabla\Phi]_{S_0} + O(\delta^2)$$

(2.1.22)

α is the oscillatory displacement of the ship and will be obtained from the transformation of co-ordinate system. The normal vector on the instantaneous hull surface S_H is

$n_H = (n + \Omega \times n)_{S_0}$ for first order approximation.

Ω denotes the rotation of the ship. Neglecting second order terms of Equation (2.1.22) the linearized body boundary condition at the wetted surface reduces to

$$[\nabla\Phi + (\alpha.\nabla)\nabla\Phi][n + \Omega \times n] = 0$$

$$\nabla\Phi.n + (\alpha.\nabla)\nabla\Phi.n + \nabla\Phi.(\Omega \times n) + O(\delta^2) = 0$$

Substituting the value of $\nabla\Phi$ we get

$$W.n + \nabla\phi_2 \cdot n + \nabla\varphi.n + \{(\alpha.\nabla)W\} \cdot n + \{W.(\Omega \times n)\} = 0$$

$$\nabla\varphi \cdot n = [\Omega \times W - (\alpha.\nabla)W] \cdot n$$

$$\nabla\varphi \cdot n = [\nabla \times (\alpha \cdot W)] \cdot n$$

The body boundary condition derived by Timman and Newman (1962) to account in a consistent manner for the interaction between the steady and oscillatory flow field. Accrording to Ogilvie and Tuck (1969) the body boundary conditions for the steady oscillatory motions of the ships can be expressed as

$$\frac{\partial\varphi_j}{\partial n} = m_j$$

with
$$m_1 i + m.j + m_3.k = -(n \cdot \nabla)W$$
$$m_4 i + m_5 j + m_6 k = -(n \cdot \nabla)(x \times W)$$

(2.1.23)

W is the fluid velocity due to the steady forward motion of the vessel in the ship fixed co-ordinate frame. The normal derivative of the steady potential due to oscillatory motion of the ship represents the change in the local steady flow field due to the motion of the body. The m-terms are written in terms of derivatives of the steady potential and normal vector consist of second derivatives of the steady potential.

2.2 Potential Flow Hydrodynamics in Deep Water

◆ 2.2.1 Linear Boundary Value Problem in Deep Water

Consider a closed three-dimensional domain V with boundary S, the unit normal vector n to S being oriented to V as shown in Figure 2.2. The boundary surface S is composed of hull surface S_H, wake surface S_W, free surface S_F and a large hemi-sphere S_R in the lower half space. The body is subject to the inflow velocity U. With the assumption that the fluid is incompressible, inviscid and irrotational, there exists a velocity potential
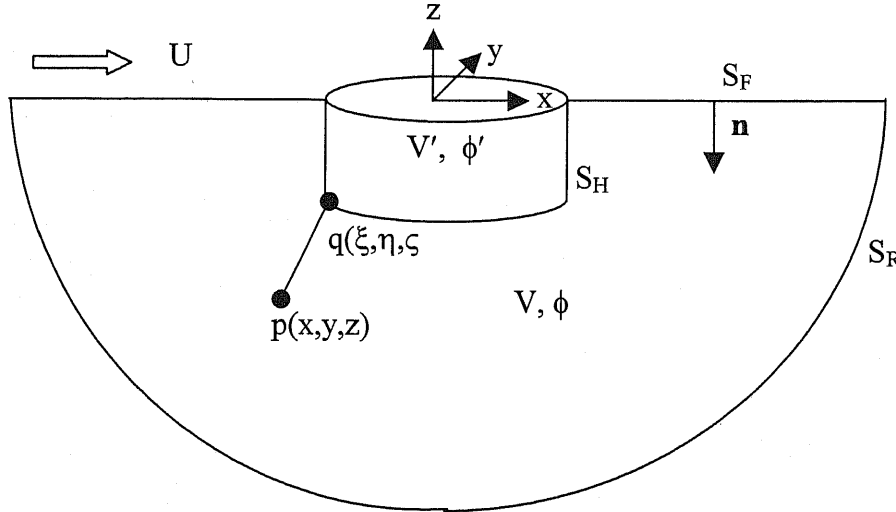
Fig 2.2 Application of Green's theorem for a body in deep water

$$\Phi = U.x + \phi + \delta\varphi$$
$$= U \cdot x + \varepsilon\phi_1 + \varepsilon^2\left(\phi_2 + s\varphi_s + t\varphi_t\right) \tag{2.2.1}$$

which satisfy the Laplace equation

$$\nabla^2\Phi = 0 \quad \text{in the fluid domain} \quad V \tag{2.2.2}$$

A boundary value problem can be constructed by specifying boundary conditions on the boundary as follows:

(a) The boundary condition on the hull surface requires that the normal velocity component of the fluid particle at the wetted surface of the ship must be zero.

14

$$\varepsilon : \nabla\phi_1 \cdot n = -U \cdot n_x$$

$$\varepsilon^2 : \nabla\phi_2 \cdot n = 0$$

and with respect to sin kage and trim

$$\varepsilon^2 : \nabla\varphi_s \cdot n = m_3$$

$$\varepsilon^2 : \nabla\varphi_t \cdot n = m_5$$

$$\left.\begin{array}{l}\end{array}\right\} \qquad (2.2.3)$$

in which $n = n_x i + n_y j + n_z k$ denotes the unit normal vector on the hull surface and is positive into the fluid.

(b) The free surface boundary conditions are

$$\varepsilon : \phi_{1xx} + K_0 \phi_{1z} = 0$$

$$\varepsilon^2 : \phi_{2xx} + K_0 \phi_{2z} = f(\phi_1)$$

with respect to sin kage and trim $\left.\begin{array}{l}\end{array}\right\}$ on z = 0

$$\varepsilon^2 : \varphi_{sxx} + K_0 \varphi_{sz} = 0$$

$$\varepsilon^2 : \varphi_{txx} + K_0 \varphi_{tz} = 0$$

$$\qquad (2.2.4)$$

(c) The wake surface S_W is assumed to have zero thickness. The normal velocity jump and the pressure jump across S_W is zero, while a jump in the potential is allowed

$$(\Delta p)_{on\ S_W} = p^+ - p^- = 0$$

$$\Delta\left(\frac{\partial\phi}{\partial n}\right)_{on\ S_W} = \left(\frac{\partial\phi}{\partial n}\right)^+ - \left(\frac{\partial\phi}{\partial n}\right)^- = 0$$

$$\Delta\left(\frac{\partial\varphi}{\partial n}\right)_{on\ S_W} = \left(\frac{\partial\varphi}{\partial n}\right)^+ - \left(\frac{\partial\varphi}{\partial n}\right)^- = 0$$

$$\left.\begin{array}{l}\end{array}\right\} \qquad (2.2.5)$$

(d) For the steady lifting problem, the potential jump across the wake surface is same as the circulation around the body and is constant in the stream-wise direction.

$$(\Delta\phi)_{on\ S_W} = \phi^+ - \phi^- = \Gamma$$

$$(\Delta\varphi)_{on\ S_W} = \varphi^+ - \varphi^- = \Gamma$$

$$\left.\begin{array}{l}\end{array}\right\} \qquad (2.2.6)$$

A kutta condition is required at the trailing edge to uniquely specify the circulation. In its most general form, it states that the flow velocity at the trailing edge remains bounded

15

$$\left.\begin{array}{l}\left|\nabla\phi\right|_{TE} \prec \infty \\ \left|\nabla\varphi\right|_{TE} \prec \infty\end{array}\right\} \qquad (2.2.7)$$

(e) In addition, it is necessary to impose a radiation condition to ensure that the free surface waves vanish upstream of the disturbance.

◆ 2.2.2 Solution of Free Surface Problem in Deep Water:

The boundary value problem for the velocity potential outside the body surface can be transformed into an integral equation, upon consideration of a fictitious fluid V', which is the domain internal to the body surface S_H. Thus the velocity potential any point p within the fluid domain V can be expressed as

$$4\pi E\phi(p) = \int_{S_H}[\phi(q) - \phi'(q)]\frac{\partial G}{\partial n_q}dS - \int_{S_H}\frac{\partial}{\partial n_q}[\phi(q) - \phi'(q)]GdS +$$

$$\int_{S_W}\Delta\phi(q)\frac{\partial G}{\partial n_q}dS - \int_{S_F}\frac{\partial\phi(q)}{\partial n_q}GdS \qquad (2.2.8)$$

From the condition at infinity for G and ϕ, it is easy to see that the integral on S_R goes to zero as $R \to \infty$. The source potential can be written as

$$G = \frac{1}{R_0(p;q)} + \frac{1}{R_1(p;q)} \qquad (2.2.9)$$

where

p(x,y,z) = field point where influence coefficient is calculated

q(ξ,η,ς) = source point where singularity is located.

$$R_0 = \sqrt{(x-\xi)^2 + (y-\eta)^2 + (z-\varsigma)^2}$$
$$R_1 = \sqrt{(x-\xi)^2 + (y-\eta)^2 + (z+\varsigma)^2}$$

But it is mentioned here that ς is zero on the free surface and R_1 will be equal to R_0. In order to obtain an approximate solution of the integral equation, the internal velocity potential ϕ' is assumed to be zero and the surfaces S_H, S_W and S_F are divided into small quadrilateral elements. The values of ϕ and $(\partial\phi/\partial n)$ are constants over each elements. The integral equation is to be satisfied at the centriod of each element and may be written as

$$4\pi E\phi(p) = \sum_{j=1}^{N_H} \int_{S_H} \phi(q)\frac{\partial G}{\partial n_q}\,dS - \sum_{j=1}^{N_H} \int_{S_H}\frac{\partial}{\partial n_q}\phi(q)G\,dS +$$

$$\sum_{j=1}^{N_W} \int_{S_W} \Delta\phi(q)\frac{\partial G}{\partial n_q}\,dS - \sum_{j=1}^{N_F} \int_{S_F}\frac{\partial\phi(q)}{\partial n_q}G\,dS$$

(2.2.10)

where , $E = \begin{cases} \frac{1}{2} & \text{on} \quad S_H \text{ and } S_W \\ 1 & \text{on} \quad S_F \end{cases}$

N_H, N_F and N_w are the number of element of hull surface, free surface and wake surface respectively. The normal velocity component on the free surface can be written as

$$\frac{\partial\phi}{\partial z} = -\frac{\partial\phi}{\partial n} = -\frac{\sigma}{2}$$

(2.2.11)

Introducing the normal velocity components given by (2.2.3) into integral equation (2.2.10) and substituting equation (2.2.10) into equation (2.2.4) one can find for

◆ 2.2.3 First Order Linear Equation in Deep Water

$$\phi_1(p) = \frac{1}{2\pi}\int_{S_H}\phi_1(q)\frac{\partial G}{\partial n_q}\,dS + \frac{1}{2\pi}\int_{S_H}(U\cdot n_x)G\,dS + \frac{1}{2\pi}\int_{S_W}\Delta\phi_1(q)\frac{\partial G}{\partial n_q}\,dS -$$

$$\frac{1}{2\pi}\int_{S_F}\frac{\sigma_1(q)}{2}G\,dS \quad \text{on} \quad S_H$$

$$\frac{1}{2\pi}\int_{S_H}\phi_1(q)\frac{\partial^2}{\partial x^2}\left(\frac{\partial G}{\partial n_q}\right)dS + \frac{1}{2\pi}\int_{S_H}(U\cdot n_x)\frac{\partial^2 G}{\partial x^2}\,dS + \frac{1}{2\pi}\int_{S_W}\Delta\phi_1(q)\frac{\partial^2}{\partial x^2}\left(\frac{\partial G}{\partial n_q}\right)dS -$$

$$\frac{1}{4\pi}\int_{S_F}\frac{\sigma_1(q)}{2}\frac{\partial^2 G}{\partial x^2}\,dS \quad - K_0\frac{\sigma_1(q)}{2} = 0 \quad \text{on} \quad S_F$$

◆ 2.2.4 Second Order Linear Equation in Deep Water

$$\phi_2(p) = \frac{1}{2\pi}\int_{S_H}\phi_2(q)\frac{\partial G}{\partial n_q}\,dS + \frac{1}{2\pi}\int_{S_W}\Delta\phi_2(q)\frac{\partial G}{\partial n_q}\,dS - \frac{1}{2\pi}\int_{S_F}\frac{\sigma_2(q)}{2}G\,dS \quad \text{on} \quad S_H$$

$$\frac{1}{2\pi}\int_{S_H}\phi_2(q)\frac{\partial^2}{\partial x^2}\left(\frac{\partial G}{\partial n_q}\right)dS + \frac{1}{2\pi}\int_{S_W}\Delta\phi_2(q)\frac{\partial^2}{\partial x^2}\left(\frac{\partial G}{\partial n_q}\right)dS -$$

$$\frac{1}{4\pi}\int_{S_F}\frac{\sigma_2(q)}{2}\frac{\partial^2 G}{\partial x^2}dS - K_0\frac{\sigma_2(q)}{2} = f(\phi_1) \quad \text{on} \quad S_F$$

◆ 2.2.5 Second Order Linear Equation for Sinkage in Deep Water

$$\varphi_s(p) = \frac{1}{2\pi}\int_{S_H}\varphi_s(q)\frac{\partial G}{\partial n_q}dS + \int_{S_H}m_3 G dS + \frac{1}{2\pi}\int_{S_W}\Delta\varphi_s(q)\frac{\partial G}{\partial n_q}dS -$$

$$\frac{1}{2\pi}\int_{S_F}\frac{\sigma_s(q)}{2}G dS \quad \text{on} \quad S_H$$

$$\frac{1}{2\pi}\int_{S_H}\varphi_s(q)\frac{\partial^2}{\partial x^2}\left(\frac{\partial G}{\partial n_q}\right)dS + \int_{S_H}m_3\frac{\partial^2 G}{\partial x^2}dS + \frac{1}{2\pi}\int_{S_W}\Delta\varphi_s(q)\frac{\partial^2}{\partial x^2}\left(\frac{\partial G}{\partial n_q}\right)dS -$$

$$\frac{1}{4\pi}\int_{S_F}\frac{\sigma_s(q)}{2}\frac{\partial^2 G}{\partial x^2}dS - K_0\frac{\sigma_s(q)}{2} = 0 \quad \text{on} \quad S_F$$

◆ 2.2.6 Second Order Linear Equation for Trim in Deep Water:

$$\varphi_t(p) = \frac{1}{2\pi}\int_{S_H}\varphi_t(q)\frac{\partial G}{\partial n_q}dS + \int_{S_H}m_5 G dS + \frac{1}{2\pi}\int_{S_W}\Delta\varphi_t(q)\frac{\partial G}{\partial n_q}dS -$$

$$\frac{1}{2\pi}\int_{S_F}\frac{\sigma_t(q)}{2}G dS \quad \text{on} \quad S_H$$

$$\frac{1}{2\pi}\int_{S_H}\varphi_t(q)\frac{\partial^2}{\partial x^2}\left(\frac{\partial G}{\partial n_q}\right)dS + \int_{S_H}m_5\frac{\partial^2 G}{\partial x^2}dS + \frac{1}{2\pi}\int_{S_W}\Delta\varphi_t(q)\frac{\partial^2}{\partial x^2}\left(\frac{\partial G}{\partial n_q}\right)dS -$$

$$\frac{1}{4\pi}\int_{S_F}\frac{\sigma_t(q)}{2.}\frac{\partial^2 G}{\partial x^2}dS - K_0\frac{\sigma_t(q)}{2} = 0 \quad \text{on} \quad S_F$$

The resulting algebraic system of equations can be written in the matrix form as

◆2.2.7 Matrix Form of First Order Linear Equation in Deep Water

$$\begin{bmatrix}(\delta - D_H) & S_F \\ -D_{Hxx} & 0.5(K_0\delta + S_{Fxx})\end{bmatrix}\begin{Bmatrix}\phi_{1j} \\ \sigma_{1j}\end{Bmatrix} = \begin{bmatrix}S_H \\ S_{Hxx}\end{bmatrix}\{U \cdot n_x\} + \begin{bmatrix}D_W \\ D_{Wxx}\end{bmatrix}\{\Delta\phi_{1j}\} \qquad (2.2.12)$$

18

where δ means the Dirac delta function and the other symbols represent the influence coefficients at the collocation point I due to sources and dipoles distributed on panel j and are defined as

$$\delta = \begin{cases} 0 & \text{if} \quad i \neq j \\ 1 & \text{if} \quad i = j \end{cases}$$

$$D_H = \frac{1}{2\pi} \int_{S_H} \frac{\partial}{\partial n_q} \left(\frac{1}{R_0} + \frac{1}{R_1} \right) dS$$

$$D_{Hxx} = \frac{1}{2\pi} \int_{S_H} \frac{\partial^2}{\partial x^2} \frac{\partial}{\partial n_q} \left(\frac{1}{R_0} + \frac{1}{R_1} \right) dS$$

$$S_H = \frac{1}{2\pi} \int_{S_H} \left(\frac{1}{R_0} + \frac{1}{R_1} \right) dS$$

$$S_{Hxx} = \frac{1}{2\pi} \int_{S_H} \frac{\partial^2}{\partial x^2} \left(\frac{1}{R_0} + \frac{1}{R_1} \right) dS$$

$$D_W = \frac{1}{2\pi} \int_{S_W} \frac{\partial}{\partial n_q} \left(\frac{1}{R_0} + \frac{1}{R_1} \right) dS$$

$$D_{Wxx} = \frac{1}{2\pi} \int_{S_W} \frac{\partial^2}{\partial x^2} \frac{\partial}{\partial n_q} \left(\frac{1}{R_0} + \frac{1}{R_1} \right) dS$$

$$S_F = \frac{1}{2\pi} \int_{S_H} \frac{1}{R_0} dS$$

$$S_{Fxx} = \frac{1}{2\pi} \int_{S_H} \frac{\partial^2}{\partial x^2} \left(\frac{1}{R_0} \right) dS$$

♦ 2.2.8 Matrix Form of Second Order Linear Equation in Deep Water

$$\begin{bmatrix} (\delta - D_H) & S_F \\ -D_{Hxx} & 0.5(K_0 \delta + S_{Fxx}) \end{bmatrix} \begin{Bmatrix} \phi_{2j} \\ \sigma_{2j} \end{Bmatrix} = \begin{bmatrix} 0 \\ -f(\phi_1) \end{bmatrix} + \begin{bmatrix} D_W \\ D_{Wxx} \end{bmatrix} \{\Delta\phi_{2j}\} \tag{2.2.13}$$

The matrices given by Equations (2.2.12) and (2.2.13) are built up by the Green's function and its derivatives. The Coefficients D_H, D_W, S_H, S_F and the derivatives are calculated according to Morino's analytical formula based on the assumption of quadrilateral elements as described in Appendix B. In order to satisfy the radiation condition, the second derivatives of D_H, D_W, S_H and S_F are computed by Dawson's upstream finite difference operator given in Appendix C. The circulation $\nabla\phi_1$ or $\nabla\phi_2$ is unknown and will be determined as described in Appendix D.

◆ 2.2.9 Matrix Form of Second Order Linear Equation for Sinkage in Deep Water

$$\begin{bmatrix} (\delta - D_H) & S_F \\ -D_{Hxx} & 0.5(K_0\delta + S_{Fxx}) \end{bmatrix} \begin{Bmatrix} \varphi_{sj} \\ \sigma_{sj} \end{Bmatrix} = \begin{bmatrix} S_H \\ S_{Hxx} \end{bmatrix} m_{3j} + \begin{bmatrix} D_W \\ D_{Wxx} \end{bmatrix} \{\Delta\varphi_{sj}\} \qquad (2.2.14)$$

◆ 2.2.10 Matrix Form of Second Order Linear Equation for Trim in Deep Water

$$\begin{bmatrix} (\delta - D_H) & S_F \\ -D_{Hxx} & 0.5(K_0\delta + S_{Fxx}) \end{bmatrix} \begin{Bmatrix} \varphi_{tj} \\ \sigma_{tj} \end{Bmatrix} = \begin{bmatrix} S_H \\ S_{Hxx} \end{bmatrix} m_{5j} + \begin{bmatrix} D_W \\ D_{Wxx} \end{bmatrix} \{\Delta\varphi_{tj}\} \qquad (2.2.15)$$

The *m*-terms are derived from normal derivatives of the fluid velocities due to the steady flow on the body surface. The velocity potentials of the fluid velocities on the body and in the fluid a small distance Δn away from the body along the normal direction can be computed from the known solution to the steady Newman- Kelvin problem. Once the velocity potentials are known, a simple finite difference can be used to determine the required derivatives.

The derivatives of the velocity potentials with respect to x and y (such as ϕ_x, ϕ_y) are computed by fitting a 2nd degree polynomial function passing through the potentials at the centroids of the three adjacent panels on the surfaces. For the evaluation of ϕ_n, the velocity potentials are calculated at three different positions along the normal direction and the same procedure applied to get the derivative. The matrix of linear system of equations is solved by LU decomposition method.

◆ 2.2.11   First Order Wave Profile Equation in Deep Water
The equation for the first order wave elevation is

$$\zeta_1 = -\frac{U}{g}\phi_{1x} \qquad (2.2.16)$$

Differentiating Equation (2.2.10) with respect to x and get

$$\frac{\partial \phi_1(p)}{\partial x} = \frac{1}{2\pi} \int_{S_H} \phi_1(q) \frac{\partial}{\partial x_p} \left(\frac{\partial G}{\partial n_q} \right) dS + \frac{1}{2\pi} \int_{S_H} (U \cdot n_x) \frac{\partial G}{\partial x_p} dS + \frac{1}{2\pi} \int_{S_W} \Delta \phi_1(q) \frac{\partial}{\partial x_p} \left(\frac{\partial G}{\partial n_q} \right) dS$$

$$- \frac{1}{4\pi} \int_{S_F} \frac{\sigma_1(q)}{2} \frac{\partial G}{\partial x_p} dS \quad \text{on} \quad z = 0$$

The above equation can be written as

$$\phi_{1x} = \sum_{j=1}^{N_H} \left[\phi_j D_{Hx} + (U \cdot n_x) \cdot S_{Hx} \right] + \sum_{j=1}^{N_W} \Delta \phi_j D_{Wx} - \frac{1}{2} \sum_{j=1}^{N_F} \sigma_j S_{Fx}$$

where

$$D_{Hx} = \frac{1}{2\pi} \int_{S_H} \frac{\partial}{\partial x} \frac{\partial}{\partial n_q} \left(\frac{1}{R_0} + \frac{1}{R_1} \right) dS \qquad S_{Hx} = \frac{1}{2\pi} \int_{S_H} \frac{\partial}{\partial x} \left(\frac{1}{R_0} + \frac{1}{R_1} \right) dS$$

$$D_{Wx} = \frac{1}{2\pi} \int_{S_W} \frac{\partial}{\partial x} \frac{\partial}{\partial n_q} \left(\frac{1}{R_0} + \frac{1}{R_1} \right) dS \qquad S_{Fx} = \frac{1}{2\pi} \int_{S_H} \frac{\partial}{\partial x} \left(\frac{1}{R_0} \right) dS$$

♦ 2.2.12 Second Order Wave Profile Equation in Deep Water

The Equation for second order wave elevation can be obtained as

$$\zeta = \zeta_1 + \zeta_2$$
$$\qquad = \zeta_1 + \zeta_2 + s\zeta_s + t\zeta_t \qquad\qquad\qquad\qquad\qquad (2.2.17)$$

where

$$\zeta_1 = -\frac{U}{g} \phi_{1x}$$

$$\zeta_2 = -\frac{U}{g} \phi_{2x} - \frac{U}{g} \zeta_1 \phi_{1xz} - \frac{1}{2g} \left(\phi_{1x}^2 + \phi_{1y}^2 + \phi_{1z}^2 \right)$$

$$\zeta_s = -\frac{U}{g} \varphi_{sx}$$

$$\zeta_t = -\frac{U}{g} \varphi_{tx}$$

Differentiating equation (2.2.10) with respect to x and y

21

$$\frac{\partial \phi_1(p)}{\partial x_p} = \frac{1}{2\pi} \int_{S_H} \phi_1(q) \frac{\partial}{\partial x_p}\left(\frac{\partial G}{\partial n_q}\right) dS + \frac{1}{2\pi} \int_{S_H} (U \cdot n_x)\left(\frac{\partial G}{\partial x_p}\right) dS +$$

$$\frac{1}{2\pi} \int_{S_W} \Delta\phi_1(q) \frac{\partial}{\partial x_p}\left(\frac{\partial G}{\partial n_q}\right) dS - \frac{1}{4\pi} \int_{S_F} \frac{\sigma_1(q)}{2} \frac{\partial G}{\partial x_p} dS \quad \text{on} \quad z = 0$$

$$\frac{\partial \phi_1(p)}{\partial y_p} = \frac{1}{2\pi} \int_{S_H} \phi_1(q) \frac{\partial}{\partial y_p}\left(\frac{\partial G}{\partial n_q}\right) dS + \frac{1}{2\pi} \int_{S_H} (U \cdot n_x)\left(\frac{\partial G}{\partial y_p}\right) dS +$$

$$\frac{1}{2\pi} \int_{S_W} \Delta\phi_1(q) \frac{\partial}{\partial y_p}\left(\frac{\partial G}{\partial n_q}\right) dS - \frac{1}{4\pi} \int_{S_F} \frac{\sigma_1(q)}{2} \frac{\partial G}{\partial y_p} dS \quad \text{on} \quad z = 0$$

The above equation can be written as

$$\phi_{1x} = \sum_{j=1}^{N_H} \left[\phi_j D_{Hx} + (U \cdot n_x) S_{Hx} \right] + \sum_{j=1}^{N_W} \Delta\phi_j D_{Wx} - \frac{1}{2} \sum_{j=1}^{N_F} \sigma_j S_{Fx}$$

$$\phi_{1y} = \sum_{j=1}^{N_H} \left[\phi_j D_{Hy} + (U \cdot n_x) S_{Hy} \right] + \sum_{j=1}^{N_W} \Delta\phi_j D_{Wy} - \frac{1}{2} \sum_{j=1}^{N_F} \sigma_j S_{Fy}$$

$$\frac{\partial \phi_1}{\partial z} = -\frac{\partial \phi_1}{\partial n} = -\frac{\sigma_1}{2}$$

2.3 Potential Flow Hydrodynamics in Shallow Water

♦ 2.3.1 Linear Boundary Value Problem in Shallow Water

Consider a closed three-dimensional domain V with boundary S, the unit normal vector n to S being oriented to V as shown in Figure 2.3. The boundary surface S is composed of the hull surface S_H, wake surface S_w, vertical cylindrical surface S_∞ far away from the body, the mean free surface S_F, and sea bottom S_B inside S_∞. The body is subjected to the inflow velocity U. With the assumption that the fluid is incompressible, inviscid and irrotational, there exists a velocity potential

$$\Phi = Ux + \phi + \delta\varphi$$
$$= Ux + \varepsilon\phi_1 + \varepsilon^2\left(\phi_2 + s\varphi_s + t\varphi_t\right) \tag{2.3.1}$$

which satisfies the Laplace equation

$$\nabla^2\Phi = 0 \text{ in the fluid domain V} \tag{2.3.2}$$
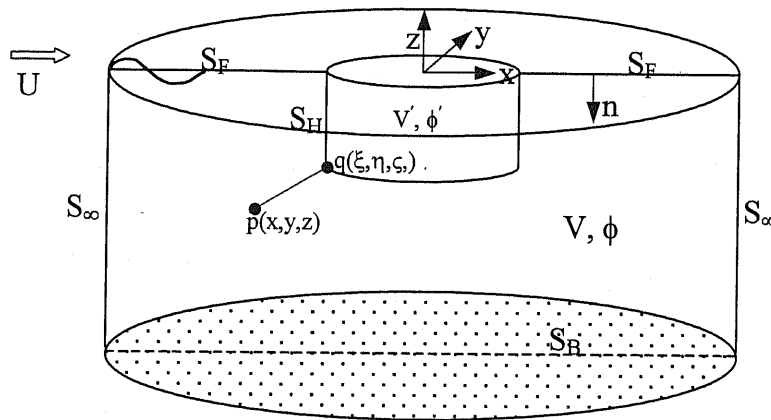
Figure 2.3. Application of Green's theorem for a body in shallow water

A boundary value problem can be constructed by specifying boundary conditions on the boundary as follows:

(a) The boundary condition on the hull surface requires that the normal velocity component of the water particles at the wetted surface of the ship must be equal to zero.

$\varepsilon : \nabla\phi_1 \cdot n = -U \cdot n_x$

$\varepsilon^2 : \nabla\phi_2 \cdot n = 0$

with respect to sinkage and trim

$\varepsilon^2 : \nabla\varphi_s \cdot n = m_3$

$\varepsilon^2 : \nabla\varphi_t \cdot n = m_5$

(2.3.3)

in which $n = n_x i + n_y j + n_z k$ denotes the unit normal vector on the surface and is positive into fluid.

(b) The free surface boundary conditions are

$\varepsilon : \phi_{1xx} + K_0\phi_{1z} = 0$

$\varepsilon^2 : \phi_{2xx} + K_0\phi_{2z} = f(\phi_1)$

with respect to sinkage and trim at $z = 0$

$\varepsilon^2 : \varphi_{sxx} + K_0\varphi_{sz} = 0$

$\varepsilon^2 : \varphi_{txx} + K_0\varphi_{tz} = 0$

(2.3.4)

(c) The boundary condition on sea bottom

$\varepsilon : \nabla\phi_1 \cdot n = 0$

$\varepsilon^2 : \nabla\phi_2 \cdot n = 0$

with respect to sinkage and trim

$\varepsilon^2 : \nabla\varphi_s \cdot n = 0$

$\varepsilon^2 : \nabla\varphi_t \cdot n = 0$

(2.3.5)

(d) The wake surface S_W is assumed to have zero thickness. The normal velocity jump and the pressure jump across S_W is zero, while a jump in the potential is allowed

$(\Delta p)_{\text{on } S_W} = p^+ - p^- = 0$

$\Delta\left(\dfrac{\partial\phi}{\partial n}\right)_{\text{on } S_W} = \left(\dfrac{\partial\phi}{\partial n}\right)^+ - \left(\dfrac{\partial\phi}{\partial n}\right)^- = 0$

$\Delta\left(\dfrac{\partial\varphi}{\partial n}\right)_{\text{on } S_W} = \left(\dfrac{\partial\varphi}{\partial n}\right)^+ - \left(\dfrac{\partial\varphi}{\partial n}\right)^- = 0$

(2.3.6)

(e) For the steady lifting problem, the potential jump across the wake surface is same as the circulation around the body and is constant in the stream-wise direction.

$$\left(\Delta\phi\right)_{\text{on } S_W} = \phi^+ - \phi^- = \Gamma \left.\right\}$$
$$\left(\Delta\varphi\right)_{\text{on } S_W} = \varphi^+ - \varphi^- = \Gamma \left.\right\}$$

(2.3.7)

A kutta condition is required at the trailing edge to uniquely specify the circulation. In its most general form, it states that the flow velocity at the trailing edge remains bounded

$$\left|\nabla\phi\right|_{\text{TE}} \prec \infty \left.\right\}$$
$$\left|\nabla\varphi\right|_{\text{TE}} \prec \infty \left.\right\}$$

(2.3.8)

(f) In addition, it is necessary to impose a radiation condition to ensure that the free surface waves vanish upstream of the disturbance.

◆ 2.3.2 Solution of Free Surface Problem in Shallow Water

The boundary value problem for the velocity potential outside the body surface can be transformed into an integral equation, upon consideration of a fictitious fluid V', which is the domain internal to the body surface S_H. Thus the velocity potential any point p within the fluid domain V can be expressed as

$$4\pi E\phi(p) = \int_{S_H}[\phi(q) - \phi'(q)]\frac{\partial G}{\partial n_q}dS - \int_{S_H}\frac{\partial}{\partial n_q}[\phi(q) - \phi'(q)]GdS + \int_{S_W}\Delta\phi(q)\frac{\partial G}{\partial n_q}dS$$
$$- \int_{S_F}\frac{\partial\phi(q)}{\partial n_q}GdS + \int_{S_B}\phi(q)\frac{\partial G}{\partial n_q}dS - \int_{S_B}\frac{\partial\phi(q)}{\partial n_q}GdS$$

(2.3.9)

The control S_∞ is a control surface at a large distance from the body and is chosen as the surface of circular cylinder of large radius. So the integral over the surface S_∞ must be zero as the radius of cylinder increases infinitely. The Green's function G satisfies the Laplace equation and can be approximated as

$$G = \frac{1}{R_0(p;q)} + \frac{1}{R_1(p;q)}$$

(2.3.10)

In order to obtain an approximate solution of the integral equation, the internal velocity potential ϕ' is assumed to be zero and the surfaces S_H, S_W, S_B and S_F are divided into small

quadrilateral elements. The values of ϕ and $(\partial\phi/\partial n)$ are constants over each elements. The integral equation is to be satisfied at the centriod of each element and may be written as

$$4\pi E\phi(p) = \sum_{j=1}^{N_H} \int_{S_H} \phi(q)\frac{\partial G}{\partial n_q}dS - \sum_{j=1}^{N_H} \int_{S_H}\frac{\partial}{\partial n_q}\phi(q)GdS + \sum_{j=1}^{N_W} \int_{S_W}\Delta\phi(q)\frac{\partial G}{\partial n_q}dS$$

$$- \sum_{j=1}^{N_F} \int_{S_F}\frac{\partial\phi(q)}{\partial n_q}GdS + \sum_{j=1}^{N_B} \int_{S_B}\phi(q)\frac{\partial G}{\partial n_q}dS - \sum_{j=1}^{N_B} \int_{S_B}\frac{\partial\phi(q)}{\partial n_q}GdS$$

(2.3.11)

where, $E = \begin{cases} \frac{1}{2} & \text{on} \quad S_H, S_B \text{ and } S_W \\ 1 & \text{on} \quad S_F \end{cases}$

N_H, N_F, N_B and N_w are the number of element of hull surface, free surface, bottom surface and wake surface respectively. The normal velocity component on the free surface can be written as

$$\frac{\partial\phi}{\partial z} = -\frac{\partial\phi}{\partial n} = -\frac{\sigma}{2}$$

(2.3.12)

Introducing the normal velocity components given by Equations (2.3.3) and (2.3.5) into integral Equation (2.3.11) and substituting Equation (2.3.11) into Equation (2.3.4) one can find for

◆ 2.3.3 First Order Linear Equation in Shallow Water

$$\phi_1(p) = \frac{1}{2\pi}\int_{S_H}\phi_1(q)\frac{\partial G}{\partial n_q}dS + \frac{1}{2\pi}\int_{S_H}(U\cdot n_x)GdS + \frac{1}{2\pi}\int_{S_W}\Delta\phi_1(q)\frac{\partial G}{\partial n_q}dS +$$

$$\frac{1}{2\pi}\int_{S_B}\phi_1(q)\frac{\partial G}{\partial n_q}dS - \frac{1}{2\pi}\int_{S_F}\frac{\sigma_1(q)}{2}GdS \quad \text{on} \quad S_H$$

$$\phi_1(p) = \frac{1}{2\pi}\int_{S_H}\phi_1(q)\frac{\partial G}{\partial n_q}dS + \frac{1}{2\pi}\int_{S_H}(U\cdot n_x)GdS + \frac{1}{2\pi}\int_{S_W}\Delta\phi_1(q)\frac{\partial G}{\partial n_q}dS +$$

$$\frac{1}{2\pi}\int_{S_B}\phi_1(q)\frac{\partial G}{\partial n_q}dS - \frac{1}{2\pi}\int_{S_F}\frac{\sigma_1(q)}{2}GdS \quad \text{on} \quad S_B$$

$$\frac{1}{2\pi}\int_{S_H}\phi_1(q)\frac{\partial^2}{\partial x^2}\left(\frac{\partial G}{\partial n_q}\right)dS + \frac{1}{2\pi}\int_{S_H}(U\cdot n_x)\frac{\partial^2 G}{\partial x^2}dS + \frac{1}{2\pi}\int_{S_W}\Delta\phi_1(q)\frac{\partial^2}{\partial x^2}\left(\frac{\partial G}{\partial n_q}\right)dS +$$

$$\frac{1}{2\pi}\int_{S_B}\phi_1(q)\frac{\partial^2}{\partial x^2}\left(\frac{\partial G}{\partial n_q}\right)dS - \frac{1}{4\pi}\int_{S_F}\frac{\sigma_1(q)}{2}\frac{\partial^2 G}{\partial x^2}dS - K_0\frac{\sigma_1(q)}{2} = 0 \quad \text{on} \quad S_F$$

◆2.3.4 Second Order Linear Equation in Shallow Water

$$\phi_2(p) = \frac{1}{2\pi}\int_{S_H}\phi_2(q)\frac{\partial G}{\partial n_q}dS + \frac{1}{2\pi}\int_{S_W}\Delta\phi_2(q)\frac{\partial G}{\partial n_q}dS + \frac{1}{2\pi}\int_{S_B}\phi_2(q)\left(\frac{\partial G}{\partial n_q}\right)dS -$$

$$\frac{1}{2\pi}\int_{S_F}\frac{\sigma_2(q)}{2}GdS \quad \text{on} \quad S_H$$

$$\phi_2(p) = \frac{1}{2\pi}\int_{S_H}\phi_2(q)\frac{\partial G}{\partial n_q}dS + \frac{1}{2\pi}\int_{S_W}\Delta\phi_2(q)\frac{\partial G}{\partial n_q}dS + \frac{1}{2\pi}\int_{S_B}\phi_2(q)\left(\frac{\partial G}{\partial n_q}\right)dS -$$

$$\frac{1}{2\pi}\int_{S_F}\frac{\sigma_2(q)}{2}GdS \quad \text{on} \quad S_B$$

$$\frac{1}{2\pi}\int_{S_H}\phi_2(q)\frac{\partial^2}{\partial x^2}\left(\frac{\partial G}{\partial n_q}\right)dS + \frac{1}{2\pi}\int_{S_W}\Delta\phi_2(q)\frac{\partial^2}{\partial x^2}\left(\frac{\partial G}{\partial n_q}\right)dS + \frac{1}{2\pi}\int_{S_B}\phi_2(q)\frac{\partial^2}{\partial x^2}\left(\frac{\partial G}{\partial n_q}\right)dS -$$

$$\frac{1}{4\pi}\int_{S_F}\frac{\sigma_2(q)}{2}\frac{\partial^2 G}{\partial x^2}dS \quad - K_0\frac{\sigma_2(q)}{2} = f(\phi_1) \quad \text{on} \quad S_F$$

◆ 2.3.5 Second Order Linear Equation for Sinkage in Shallow Water

$$\varphi_s(p) = \frac{1}{2\pi}\int_{S_H}\varphi_s(q)\frac{\partial G}{\partial n_q}dS + \int_{S_H}m_3 GdS + \frac{1}{2\pi}\int_{S_W}\Delta\varphi_s(q)\frac{\partial G}{\partial n_q}dS + \frac{1}{2\pi}\int_{S_B}\varphi_s(q)\frac{\partial G}{\partial n_q}dS -$$

$$\frac{1}{2\pi}\int_{S_F}\frac{\sigma_s(q)}{2}GdS \quad \text{on} \quad S_H$$

$$\varphi_s(p) = \frac{1}{2\pi}\int_{S_H}\varphi_s(q)\frac{\partial G}{\partial n_q}dS + \int_{S_H}m_3 GdS + \frac{1}{2\pi}\int_{S_W}\Delta\varphi_s(q)\frac{\partial G}{\partial n_q}dS + \frac{1}{2\pi}\int_{S_B}\varphi_s(q)\frac{\partial G}{\partial n_q}dS -$$

$$\frac{1}{2\pi}\int_{S_F}\frac{\sigma_s(q)}{2}GdS \quad \text{on} \quad S_B$$

$$\frac{1}{2\pi}\int_{S_H}\varphi_s(q)\frac{\partial^2}{\partial x^2}\left(\frac{\partial G}{\partial n_q}\right)dS + \int_{S_H}m_3\frac{\partial^2 G}{\partial x^2}dS + \frac{1}{2\pi}\int_{S_W}\Delta\varphi_s(q)\frac{\partial^2}{\partial x^2}\left(\frac{\partial G}{\partial n_q}\right)dS +$$

$$\frac{1}{2\pi}\int_{S_B}\varphi_s(q)\frac{\partial^2}{\partial x^2}\left(\frac{\partial G}{\partial n_q}\right)dS - \frac{1}{4\pi}\int_{S_F}\frac{\sigma_s(q)}{2}\frac{\partial^2 G}{\partial x^2}dS \quad - K_0\frac{\sigma_s(q)}{2} = 0 \quad \text{on} \quad S_F$$

♦ 2.3.6 Second Order Linear Equation for Trim in Shallow Water

$$\varphi_t(p) = \frac{1}{2\pi} \int_{S_H} \varphi_t(q) \frac{\partial G}{\partial n_q} dS + \int_{S_H} m_5 G dS + \frac{1}{2\pi} \int_{S_W} \Delta\varphi_t(q) \frac{\partial G}{\partial n_q} dS + \frac{1}{2\pi} \int_{S_B} \varphi_t(q) \frac{\partial G}{\partial n_q} dS -$$

$$\frac{1}{2\pi} \int_{S_F} \frac{\sigma_t(q)}{2} G dS \quad \text{on} \quad S_H$$

$$\varphi_t(p) = \frac{1}{2\pi} \int_{S_H} \varphi_t(q) \frac{\partial G}{\partial n_q} dS + \int_{S_H} m_5 G dS + \frac{1}{2\pi} \int_{S_W} \Delta\varphi_t(q) \frac{\partial G}{\partial n_q} dS + \frac{1}{2\pi} \int_{S_B} \varphi_t(q) \frac{\partial G}{\partial n_q} dS -$$

$$\frac{1}{2\pi} \int_{S_F} \frac{\sigma_t(q)}{2} G dS \quad \text{on} \quad S_B$$

$$\frac{1}{2\pi} \int_{S_H} \varphi_t(q) \frac{\partial^2}{\partial x^2}\left(\frac{\partial G}{\partial n_q}\right) dS + \int_{S_H} m_5 \frac{\partial^2 G}{\partial x^2} dS + \frac{1}{2\pi} \int_{S_W} \Delta\varphi_t(q) \frac{\partial^2}{\partial x^2}\left(\frac{\partial G}{\partial n_q}\right) dS +$$

$$\frac{1}{2\pi} \int_{S_B} \varphi_t(q) \frac{\partial^2}{\partial x^2}\left(\frac{\partial G}{\partial n_q}\right) dS - \frac{1}{4\pi} \int_{S_F} \frac{\sigma_t(q)}{2} \frac{\partial^2 G}{\partial x^2} dS - K_0 \frac{\sigma_t(q)}{2} = 0 \quad \text{on} \quad S_F$$

The resulting algebraic system of equations can be written in the matrix form as

♦ 2.3.7 Matrix Form of First Order Linear Equation in Shallow Water

$$\begin{bmatrix} (\delta - D_H) & -D_B & S_F \\ -D_H & (\delta - D_B) & S_F \\ -D_{Hxx} & -D_{Bxx} & 0.5(K_0\delta + S_{Fxx}) \end{bmatrix} \begin{Bmatrix} \phi_{1j} \\ \phi_{1j} \\ \sigma_{1j} \end{Bmatrix} = \begin{bmatrix} S_H \\ S_H \\ S_{Hxx} \end{bmatrix} \{U \cdot n_x\} + \begin{bmatrix} D_W \\ D_W \\ D_{Wxx} \end{bmatrix} \{\Delta\phi_{1j}\} \qquad (2.3.13)$$

where δ means the Dirac delta function and the other symbols represent the influence coefficients at the collocation point I due to sources and dipoles distributed on panel j and are defined as

$$\delta = \begin{cases} 0 & \text{if} \quad i \neq j \\ 1 & \text{if} \quad i = j \end{cases}$$

$$D_H = \frac{1}{2\pi} \int_{S_H} \frac{\partial}{\partial n_q}\left(\frac{1}{R_0} + \frac{1}{R_1}\right) dS \qquad D_{Hxx} = \frac{1}{2\pi} \int_{S_H} \frac{\partial^2}{\partial x^2} \frac{\partial}{\partial n_q}\left(\frac{1}{R_0} + \frac{1}{R_1}\right) dS$$

$$D_B = \frac{1}{2\pi} \int_{S_B} \frac{\partial}{\partial n_q}\left(\frac{1}{R_0} + \frac{1}{R_1}\right) dS \qquad D_{Bxx} = \frac{1}{2\pi} \int_{S_B} \frac{\partial^2}{\partial x^2} \frac{\partial}{\partial n_q}\left(\frac{1}{R_0} + \frac{1}{R_1}\right) dS$$

28

$$S_H = \frac{1}{2\pi} \int_{S_H} \left(\frac{1}{R_0} + \frac{1}{R_1} \right) dS \qquad S_{Hxx} = \frac{1}{2\pi} \int_{S_H} \frac{\partial^2}{\partial x^2} \left(\frac{1}{R_0} + \frac{1}{R_1} \right) dS$$

$$D_W = \frac{1}{2\pi} \int_{S_W} \frac{\partial}{\partial n_q} \left(\frac{1}{R_0} + \frac{1}{R_1} \right) dS \qquad D_{Wxx} = \frac{1}{2\pi} \int_{S_W} \frac{\partial^2}{\partial x^2} \frac{\partial}{\partial n_q} \left(\frac{1}{R_0} + \frac{1}{R_1} \right) dS$$

$$S_F = \frac{1}{2\pi} \int_{S_H} \frac{1}{R_0} dS \qquad S_{Fxx} = \frac{1}{2\pi} \int_{S_H} \frac{\partial^2}{\partial x^2} \left(\frac{1}{R_0} \right) dS$$

♦ 2.3.8 Matrix Form of Second Order Linear Equation in Shallow Water

$$\begin{bmatrix} (\delta - D_H) & -D_B & S_F \\ -D_H & (\delta - D_B) & S_F \\ -D_{Hxx} & -D_{Bxx} & 0.5(K_0\delta + S_{Fxx}) \end{bmatrix} \begin{Bmatrix} \phi_{2j} \\ \phi_{2j} \\ \sigma_{2j} \end{Bmatrix} = \begin{bmatrix} 0 \\ 0 \\ -f(\phi_1) \end{bmatrix} + \begin{bmatrix} D_W \\ D_W \\ D_{Wxx} \end{bmatrix} \{\Delta\phi_{2j}\} \qquad (2.3.14)$$

The matrices given by equations (2.3.13) and (2.3.14) are built up by the Green's function and its derivatives. The Coefficients D_H, D_W, S_H, S_F and the derivatives are calculated according to Morino's analytical formula based on the assumption of quadrilateral elements as described in Appendix B. In order to satisfy the radiation condition, the second derivatives of D_H, D_W, S_H and S_F are computed by Dawson's upstream finite difference operator given in Appendix C. The circulation $\nabla\phi_1$ or $\nabla\phi_2$ is unknown and will be determined as described in Appendix D.

♦ 2.3.9 Matrix Form of Second Order Linear Equation for Sinkage in Shallow Water

$$\begin{bmatrix} (\delta - D_H) & -D_B & S_F \\ -D_H & (\delta - D_B) & S_F \\ -D_{Hxx} & -D_B & 0.5(K_0\delta + S_{Fxx}) \end{bmatrix} \begin{Bmatrix} \varphi_{sj} \\ \varphi_{sj} \\ \sigma_{sj} \end{Bmatrix} = \begin{bmatrix} S_H \\ S_H \\ S_{Hxx} \end{bmatrix} m_{3j} + \begin{bmatrix} D_W \\ D_W \\ D_{Wxx} \end{bmatrix} \{\Delta\varphi_{sj}\} \qquad (2.3.15)$$

♦ 2.3.10 Matrix form of Second Order Linear Equation for Trim in Shallow Water

$$
\begin{bmatrix}
(\delta - D_H) & -D_B & S_F \\
-D_H & (\delta - D_B) & S_F \\
-D_{Hxx} & -D_B & 0.5(K_0\delta + S_{Fxx})
\end{bmatrix}
\begin{Bmatrix}
\varphi_{tj} \\
\varphi_{tj} \\
\sigma_{tj}
\end{Bmatrix}
=
\begin{bmatrix}
S_H \\
S_H \\
S_{Hxx}
\end{bmatrix}
m_{5j}
+
\begin{bmatrix}
D_W \\
D_W \\
D_{Wxx}
\end{bmatrix}
\{\Delta\varphi_{tj}\}
\qquad (2.3.16)
$$

The *m*-terms are derived from normal derivatives of the fluid velocities due to the steady flow on the body surface. The velocity potentials of the fluid velocities on the body and in the fluid a small distance Δn away from the body along the normal direction can be computed from the known solution to the steady Newman- Kelvin problem. Once the velocity potentials are known, a simple finite difference can be used to determine the required derivatives.

The derivatives of the velocity potentials with respect to x and y (such as ϕ_x, ϕ_y) are computed by fitting a 2nd degree polynomial function passing through the potentials at the centroids of the three adjacent panels on the surfaces. For the evaluation of ϕ_n, the velocity potentials are calculated at three different positions along the normal direction and the same procedure applied to get the derivative. The matrix of linear system of equations is solved by LU decomposition method.

♦ 2.3.11 First Order Wave Profile Equation in Shallow Water

The equation for the first order wave elevation is

$$
\zeta_1 = -\frac{U}{g}\phi_{1x}
\qquad (2.3.17)
$$

Differentiating Equation (2.3.11) with respect to x and get

$$
\frac{\partial \phi_1(p)}{\partial x} = \frac{1}{2\pi}\int_{S_H}\phi_1(q)\frac{\partial}{\partial x_p}\left(\frac{\partial G}{\partial n_q}\right)dS + \frac{1}{2\pi}\int_{S_H}(U\cdot n_x)\frac{\partial G}{\partial x_p}dS + \frac{1}{2\pi}\int_{S_W}\Delta\phi_1(q)\frac{\partial}{\partial x_p}\left(\frac{\partial G}{\partial n_q}\right)dS
$$

$$
+\frac{1}{2\pi}\int_{S_B}\phi_1(q)\frac{\partial}{\partial x_p}\left(\frac{\partial G}{\partial n_q}\right)dS - \frac{1}{4\pi}\int_{S_F}\frac{\sigma_1(q)}{2}\frac{\partial G}{\partial x_p}dS \quad on \quad z=0
$$

The above equation can be written as

$$\phi_{1x} = \sum_{j=1}^{N_H} \left[\phi_j D_{Hx} + (U \cdot n_x) \cdot S_{Hx} \right] + \sum_{j=1}^{N_B} \phi_j D_{Bx} + \sum_{j=1}^{N_W} \Delta\phi_j D_{Wx} - \frac{1}{2} \sum_{j=1}^{N_F} \sigma_j S_{Fx}$$

where

$$D_{Hx} = \frac{1}{2\pi} \int_{S_H} \frac{\partial}{\partial x} \frac{\partial}{\partial n_q} \left(\frac{1}{R_0} + \frac{1}{R_1} \right) dS \qquad S_{Hx} = \frac{1}{2\pi} \int_{S_H} \frac{\partial}{\partial x} \left(\frac{1}{R_0} + \frac{1}{R_1} \right) dS$$

$$D_{Bx} = \frac{1}{2\pi} \int_{S_B} \frac{\partial}{\partial x} \frac{\partial}{\partial n_q} \left(\frac{1}{R_0} + \frac{1}{R_1} \right) dS \qquad D_{Wx} = \frac{1}{2\pi} \int_{S_W} \frac{\partial}{\partial x} \frac{\partial}{\partial n_q} \left(\frac{1}{R_0} + \frac{1}{R_1} \right) dS$$

$$S_{Fx} = \frac{1}{2\pi} \int_{S_H} \frac{\partial}{\partial x} \left(\frac{1}{R_0} \right) dS$$

♦ 2.3.12 Second Order Wave Profile Equation in Shallow Water

The Equation for second order wave elevation can be obtained as

$$\begin{aligned} \zeta &= \zeta_1 + \zeta_2 \\ &= \zeta_1 + \zeta_2 + s\zeta_s + t\zeta_t \end{aligned}$$

(2.3.18)

where

$$\zeta_1 = -\frac{U}{g}\phi_{1x}$$

$$\zeta_2 = -\frac{U}{g}\phi_{2x} - \frac{U}{g}\zeta_1\phi_{1xz} - \frac{1}{2g}\left(\phi_{1x}^2 + \phi_{1y}^2 + \phi_{1z}^2 \right)$$

$$\zeta_s = -\frac{U}{g}\varphi_{sx}$$

$$\zeta_t = -\frac{U}{g}\varphi_{tx}$$

Differentiating equation (2.3.11) with respect to x and y

$$\frac{\partial \phi_1(p)}{\partial x_p} = \frac{1}{2\pi} \int_{S_H} \phi_1(q) \frac{\partial}{\partial x_p} \left(\frac{\partial G}{\partial n_q} \right) dS + \frac{1}{2\pi} \int_{S_H} (U \cdot n_x) \left(\frac{\partial G}{\partial x_p} \right) dS + \frac{1}{2\pi} \int_{S_B} \phi_1(q) \frac{\partial}{\partial x_p} \left(\frac{\partial G}{\partial n_q} \right) dS$$

$$\frac{1}{2\pi} \int_{S_W} \Delta\phi_1(q) \frac{\partial}{\partial x_p} \left(\frac{\partial G}{\partial n_q} \right) dS - \frac{1}{4\pi} \int_{S_F} \frac{\sigma_1(q)}{2} \frac{\partial G}{\partial x_p} dS \quad \text{on} \quad z = 0$$

31

$$\frac{\partial \phi_1(p)}{\partial y_p} = \frac{1}{2\pi} \int_{S_H} \phi_1(q) \frac{\partial}{\partial y_p}\left(\frac{\partial G}{\partial n_q}\right) dS + \frac{1}{2\pi} \int_{S_H} (U \cdot n_x)\left(\frac{\partial G}{\partial y_p}\right) dS + \frac{1}{2\pi} \int_{S_B} \phi_1(q) \frac{\partial}{\partial y_p}\left(\frac{\partial G}{\partial n_q}\right) dS$$

$$\frac{1}{2\pi} \int_{S_W} \Delta\phi_1(q) \frac{\partial}{\partial y_p}\left(\frac{\partial G}{\partial n_q}\right) dS - \frac{1}{4\pi} \int_{S_F} \frac{\sigma_1(q)}{2} \frac{\partial G}{\partial y_p} dS \quad \text{on} \quad z = 0$$

The above equation can be written as

$$\phi_{1x} = \sum_{j=1}^{N_H} \left[\phi_j D_{Hx} + (U \cdot n_x) S_{Hx}\right] + \sum_{j=1}^{N_B} \phi_j D_{Bx} + \sum_{j=1}^{N_W} \Delta\phi_j D_{Wx} - \frac{1}{2}\sum_{j=1}^{N_F} \sigma_j S_{Fx}$$

$$\phi_{1y} = \sum_{j=1}^{N_H} \left[\phi_j D_{Hy} + (U \cdot n_x) S_{Hy}\right] + \sum_{j=1}^{N_B} \phi_j D_{By} + \sum_{j=1}^{N_W} \Delta\phi_j D_{Wy} - \frac{1}{2}\sum_{j=1}^{N_F} \sigma_j S_{Fy}$$

$$\frac{\partial \phi_1}{\partial z} = -\frac{\partial \phi_1}{\partial n} = -\frac{\sigma_1}{2}$$

2.4 Sinkage and Trim Calculation

In order to calculate the forces and moments on the ship, the pressure must be evaluated on the actual instantaneous position of the ship hull. However, it is quite inconvenient to have a changing domain of integration, especially since finding domain is part of the problem. A priori, the location and orientation of the ship at any instant are unknown and so one does not know where to evaluate the pressure. Therefore, we choose to express the pressure at a point of the hull surface S_H in terms of the pressure at the corresponding point of S_0, the undisturbed position of the hull.

The fluid pressure acting on the instantaneous wetted surface S_H during oscillatory motions of the ship can be written by Bernoulli's equation

$$p - p_\infty = \frac{1}{2}\rho(U^2 - \nabla\Phi \cdot \nabla\Phi) - \rho gz \tag{2.4.1}$$

Unfortunately knowledge of the position of S_H is necessary if this expression is to be used. Newman (1978) suggests that this difficulty may be overcome by relating the pressure on the surface S_H to the pressure on the surface S_0 by Taylor series expansion. Thus

$$[p - p_\infty]_{S_H} = \left[1 + (\alpha \cdot \nabla) + \frac{1}{2}(\alpha \cdot \nabla)^2 + \ldots\ldots\ldots \right][p - p_\infty]_{S_0} \tag{2.4.2}$$

Now the total fluid velocity vector on the instantaneous wetted surface for second order approximation S_H can be obtained as

$$\nabla\Phi = W + \varepsilon^2(\nabla\phi_2 + \nabla\varphi)$$
$$\text{with} \quad W = U.i + \varepsilon\nabla\phi_1 \tag{2.4.3}$$

It is assumed that the oscillatory motions of the ship is so small that the second order terms of the unsteady components may be neglected, then the linearized form of the pressure on the wetted surface S_H becomes

$$p - p_\infty = \frac{1}{2}\rho(U^2 - \nabla\Phi \cdot \nabla\Phi) + \frac{1}{2}\rho(\alpha \cdot \nabla)(U^2 - \nabla\Phi \cdot \nabla\Phi) - \rho gz$$

$$= -\rho\left[\frac{1}{2}(W^2 - U^2) + W \cdot \nabla\phi_2 \right] - \rho gz - \rho[s \cdot (W \cdot \nabla\varphi_s) + t \cdot (W \cdot \nabla\varphi_t)] \tag{2.4.4}$$

$$- \left\{ tz'\frac{\partial}{\partial x} + (s - tx)\frac{\partial}{\partial z} \right\}\frac{1}{2}\rho W^2 + O(\alpha^2)$$

33

This approximation implies that the oscillatory flow and the motion of the ship are linearized but steady flow due to steady forward motion remains nonlinear. The hydrodynamic forces (k = 1, 2, 3 indicates surge, sway and heave) and moments (k = 4, 5, 6 indicates rolling, pitching and yawing) in the kth direction can be represented as (Yasukawa, 1993):

$$F_k = -\int (p - p_\infty) n_k dS \approx F_k^0 + s F_k^s + t F_k^t \tag{2.4.5}$$

where

$$F_k^0 = \rho \int \left[\frac{1}{2} (W^2 - U^2) + W \cdot \nabla \phi_2 \right] \cdot n_k dS$$

$$F_k^s = \rho \int \left[W \cdot \nabla \varphi_s + \frac{1}{2} \frac{\partial}{\partial z} W^2 \right] \cdot n_k dS$$

$$F_k^t = \rho \int \left[W \cdot \nabla \varphi_t + \frac{1}{2} \left(z' \frac{\partial}{\partial x} - x' \frac{\partial}{\partial z} \right) W^2 \right] \cdot n_k dS$$

and $n_4 i + n_5 j + n_6 k = r \times n, \, r = x' i + y' j + z' k$

The "sinkage" and "trim" of a ship moving in shallow water can be computed by equating the vertical force and pitch moment to the hydrostatic restoring force and moment. The resulting calculations are practical importance in predicting the "squat" of a ship, and ultimately the occurrence of grounding due to increased draft. The theory is invalid near the critical Froude number $F_h = 1$, but in other respects it agrees fairly well with the experiments. For typical ships the vertical "sinkage" is the dominant effect in the subcritical regime, whereas "trim" is dominant in the supercritical regime.

Suppose the ship responds to these forces and experiences a sinkage s defined as the downward vertical displacement at $x = 0$ and trim t defined as the bow up angle of rotation about $y = 0$. Now the following equations are obtained from the static equilibrium of forces:

$$\left. \begin{array}{l} F_3 = \rho g \int\limits_{-L/2}^{L/2} (s - tx) f_w (x) dx \\[2em] = \rho g s \int\limits_{-L/2}^{L/2} f_w (x) dx - t\rho g \int\limits_{-L/2}^{L/2} f_w (x) x dx \end{array} \right\} \tag{2.4.6}$$

$$F_5 = -\rho g \int_{-L/2}^{L/2} (s - tx) f_w(x) x \, dx$$

$$= -\rho g s \int_{-L/2}^{L/2} f_w(x) x \, dx + t \rho g \int_{-L/2}^{L/2} f_w(x) x^2 \, dx$$

(2.4.7)

$f_w(x)$ is the width of the water plane area at the still water level and L denotes the length of the ship. Combining equations (2.4.5), (2.4.6) and (2.4.7) we have

$$s\left(F_3^s - H_0\right) + t\left(F_3^t + H_1\right) = -F_3^0$$
$$s\left(F_5^s - H_1\right) + t\left(F_5^t - H_2\right) = -F_5^0$$

(2.4.8)

The values of s and t are obtained from these two simultaneous equations. The symbols are defined as

$$H_0 = \rho g \int_{-L/2}^{L/2} f_w(x) \, dx$$

$$H_1 = \rho g \int_{-L/2}^{L/2} f_w(x) x \, dx$$

$$H_2 = \rho g \int_{-L/2}^{L/2} f_w(x) x^2 \, dx$$

(2.4.9)

2.5 Pressure Computation on Hull Surface

♦ 2.5.1 Direct Method

After computing the discrete values of the potentials on the boundary surfaces, the pressure distribution on the surface can be determined by applying Bernoulli's equation. In accordance with the pressure along the stream surfaces remain constant:

$$\frac{p_\infty}{\rho} + \frac{1}{2}U^2 = \text{Constant} \qquad (2.5.1)$$

where U is the inflow velocity and p_∞ the pressure far away from the body. The total velocity vector can be decomposed as:

$$\left.\begin{array}{l} V = U + \nabla\phi \\ \text{with sinkage and trim} \\ V = U + \nabla\phi + \delta\nabla\varphi \end{array}\right\} \qquad (2.5.2)$$

To determine the pressure distribution on the body, it is first necessary to determine the velocity V at the control points on its surface. If n is the unit normal vector on the surface of the body, then according to kinematic boundary condition on the body

$$(U + \nabla\phi).n = 0 \qquad (2.5.3)$$

The perturbation velocity can be written as

$$\nabla\phi = \nabla_t\phi + \nabla_n\phi \quad \text{on S} \qquad (2.5.4)$$

where the term $\nabla_t\phi$ correspond to the component of perturbation velocity tangential to the body surface.

$$(\nabla_n\phi) = \left(\frac{\partial\phi}{\partial n}\right)n = -[U\cdot n]\cdot n \qquad (2.5.5)$$

Combining equations (2.5.4) and (2.5.5) we have

$$V = U - [U\cdot n]n + \nabla_t\phi \qquad (2.5.6)$$

if ξ and η are the unit vectors tangential to the surface along the two grid directions as shown in Figure 2.4 , the following equations are obtained:

$$\phi_\xi = \frac{\partial\phi}{\partial\xi} = \xi\nabla_t\phi \qquad (2.5.7)$$

$$\phi_\eta = \frac{\partial\phi}{\partial\eta} = \eta\nabla_t\phi \qquad (2.5.8)$$

By using equations (2.5.7) and (2.5.8) $\nabla_t\phi$ can be express

$$\nabla_t\phi = \frac{\frac{\partial\phi}{\partial\xi}[\xi-(\xi\cdot\eta)\eta]+\frac{\partial\phi}{\partial\eta}[\eta-(\eta\cdot\xi)\xi]}{|\xi\times\eta|^2}$$

(2.5.9)

The quantities $\left(\dfrac{\partial\phi}{\partial\xi}\right)$ and $\left(\dfrac{\partial\phi}{\partial\eta}\right)$ correspond to the projections of the perturbation velocity along the two grid directions and these will be obtained numerically from the derivative of the 2nd degree polynomial function passing through the potentials along each circumferential strip.
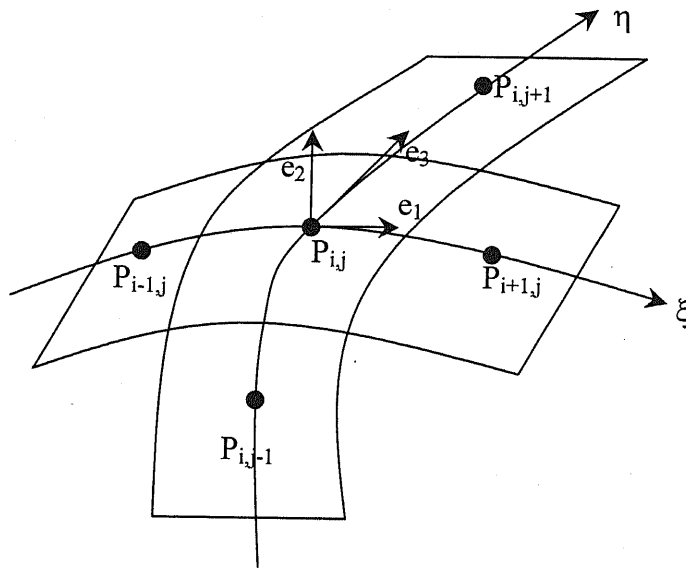
Fig 2.4 Definition sketch of the local coordinate system (ξ,η) and panel distributions

If we consider the sinkage and trim to be order of second, the fluid velocity vector will be obtained as

$$V = U -[U\cdot n]n +m_3\cdot n +\nabla_t(\phi+\phi)\quad\text{for sinkage}$$

(2.5.10)

$$V = U -[U\cdot n]n +m_5\cdot n +\nabla_t(\phi+\phi)\quad\text{for trim}$$

(2.5.11)

The pressures are finally expressed in terms of the pressure coefficient C_P that is defined as:

$$C_p = 1-\left(\frac{V}{U}\right)^2$$

♦2.5.2 Yanagizawa's Differentiation Scheme

The velocity and pressure on the surface can be obtained by numerically differentiation of velocity potential over the body surfaces as proposed by Yanagizawa (Hoshino, 1989). The distribution of the velocity potential ϕ is approximated by a quadratic equation passing through the potentials at the centroids of three adjacent panels as

$$\phi = as^2 + bs + c \tag{2.5.12}$$

where s is the surface distance and a, b, c are the coefficients of the quadratic equation. Then the derivative of the potential tangential to the surface can be written as

$$\frac{\partial \phi}{\partial s} = 2as + b \tag{2.5.13}$$

In terms of local coordinate system ξ-η, the perturbation velocity potential can be expressed as

$$\left. \begin{array}{l} \phi = a_1 \xi^2 + b_1 \xi + c_1 \\ \phi = a_2 \eta^2 + b_2 \eta + c_2 \end{array} \right\} \tag{2.5.14}$$

Differentiation of the above equation yields the velocity along the tangent direction ξ and η to the body surface respectively,

$$\left. \begin{array}{l} \dfrac{\partial \phi}{\partial \xi} = \phi_\xi = 2a_1 \xi + b_1 \\[2mm] \dfrac{\partial \phi}{\partial \eta} = \phi_\eta = 2a_2 \eta + b_2 \end{array} \right\} \tag{2.5.15}$$

After making a circle passing through the centriods of the three adjacent panels the position vector R_0 can be expressed as (Figure 2.5)

$$R_0 = \alpha + s_c \beta + t_c \gamma \tag{2.5.16}$$

where

$$s_c = \frac{|\beta|^2 - (\beta \cdot \gamma)|\gamma|^2}{2\left[|\beta|^2 |\gamma|^2 - (\beta \cdot \gamma)^2 \right]}$$

$$t_c = \frac{(\beta \cdot \gamma) - |\gamma|^2 |\beta|^2}{2\left[(\beta \cdot \gamma)^2 - |\beta|^2 |\gamma|^2 \right]}$$

The unit vectors n_r, n_n and λ are defined as

$$n_r = \frac{\alpha - R_0}{|\alpha - R_0|} \qquad n_n = \frac{\beta \times \gamma}{|\beta \times \gamma|} \qquad \lambda = \frac{b}{|b|}$$

38

Let e_1 and e_3 be the unit vector in the direction of ξ and η respectively and e_2 is in the direction perpendicular to e_1 as shown in Figure 2.4. The derivative of the potential along e_1 and e_2 can be expressed as

$$\phi_{e_1} = \frac{\partial \phi}{\partial \xi} \tag{2.5.17}$$
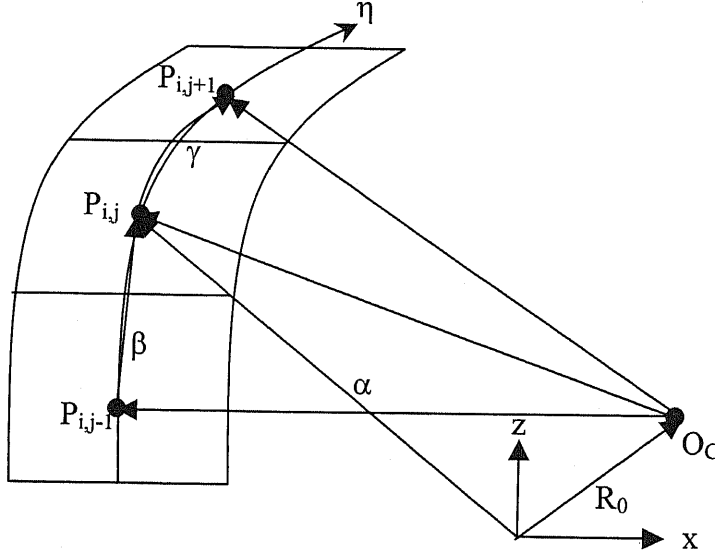
Fig. 2.5 Yanagizawa's differentiation scheme

$$\phi_{e_2} = \frac{\phi_{e_3} - (e_1 \cdot e_3)\phi_{e_1}}{e_3 \cdot e_2}$$

$$= \frac{1}{1 - (\xi \cdot \eta)^2}\left(\frac{\partial \phi}{\partial \eta} - (\xi \cdot \eta)\frac{\partial \phi}{\partial \xi}\right) \tag{2.5.18}$$

The perturbation velocity tangential to the body surfaces can be obtained by

$$\nabla_t \phi = \phi_{e_1} \cdot e_1 + \phi_{e_2} \cdot e_2 \tag{2.5.19}$$

Rewriting the Equations (2.5.19) as

$$\nabla_t \phi = \phi_{e_1} \cdot \xi + \phi_{e_2} \cdot [\eta - (\xi \cdot \eta)\xi] \tag{2.5.20}$$

Adding the tangential component of inflow velocity U we obtain the total velocity tangential to the body surface as

$$V = U - (U \cdot n)n + \nabla_t \phi$$

$$= U - (U \cdot n)n + \phi_{e_1} \cdot \xi + \phi_{e_2} \cdot [\eta - (\xi \cdot \eta)\xi] \tag{2.5.21}$$

where $n = e_1 \times e_2$ and the terms ξ and η can be found as

39

$$\left. \begin{array}{l} \xi = n_{n\xi} \times n_{r\xi} \\ \eta = n_{n\eta} \times n_{r\eta} \end{array} \right\}$$ (2.5.22)

If we consider the sinkage and trim to be of second order, the fluid velocity vectors will be obtained as

$$V = U - (U \cdot n) \cdot n + m_3 \cdot n + (\phi + \varphi)_{e_1} \xi + (\phi + \varphi)_{e_2} \{\eta - (\xi \cdot \eta) \cdot \xi\}$$ (2.5.23)

$$V = U - (U \cdot n) \cdot n + m_5 \cdot n + (\phi + \varphi)_{e_1} \xi + (\phi + \varphi)_{e_2} \{\eta - (\xi \cdot \eta) \cdot \xi\}$$ (2.5.24)

The pressure on the body surface can be written as

$$C_p = 1 - \left(\frac{V}{U}\right)^2$$ (2.5.25)

2.6 Calculation of Wave Making Resistance of Ships

◆2.6.1 Wavemaking Resistance in Fixed Condition

The pressure at any point on the hull surfaces can be expressed as

$$p - p_\infty = \frac{1}{2}\rho(U^2 - \nabla\Phi \cdot \nabla\Phi) - \rho gz \qquad (2.6.1)$$

where

$$\nabla\Phi = U + \nabla\varphi_1 + \nabla\varphi_2 \qquad \text{for } 2^{nd} \text{ order approximation}$$

$$\nabla\Phi = U + \nabla\phi_1 + (\nabla\phi_2 + \nabla\varphi) \text{ for } 2^{nd} \text{ order approximation with sinkage and trim}$$

The hydrodynamic force in the x-direction is obtained by integrating the pressure over the instantaneous wetted hull surface as follows:

$$R_W = -\int_{S+S'}(p - p_\infty)n_x dS \qquad (2.6.2)$$

$$R_w = -\int_S\left[\frac{1}{2}\rho(U^2 - \nabla\Phi \cdot \nabla\Phi) - \rho gz\right]n_x dS - \int_{S'}\left[\frac{1}{2}\rho(U^2 - \nabla\Phi \cdot \nabla\Phi) - \rho gz\right]n_x dS \qquad (2.6.3)$$

where S is the mean wetted surface and S' is the fluctuating part of the wetted surface between still water plane , $z = 0$ and the waterline along the hull , $z = \zeta$. For the simplicity, let the body have a vertical wall near the water line. The second integral can be transformed into a line integral along the water line. The pressure along the water line, $p = p_\infty$.

$$\frac{1}{2}\rho(U^2 - \nabla\Phi \cdot \nabla\Phi) - \rho g\zeta = 0$$

$$\frac{1}{2}\rho(U^2 - \nabla\Phi \cdot \nabla\Phi) = \rho g\zeta$$

The force on the hull surface in the x-direction can be expressed as

$$R_w = -\int_S\left[\frac{1}{2}\rho(U^2 - \nabla\Phi \cdot \nabla\Phi) - \rho gz\right]n_x dS - \int_{S'}(\rho g\zeta - \rho gz)n_x dz\, dL \qquad (2.6.4)$$

$$R_w = -\int_S\left[\frac{1}{2}\rho(U^2 - \nabla\Phi \cdot \nabla\Phi) - \rho gz\right]n_x dS - \frac{1}{2}\rho g\int_{wL}\zeta_r^2 n_x\, dL \qquad (2.6.5)$$

ζ_r is the relative wave elevation. After calculating the pressure coefficient on the hull surface by Equation (2.5.25) the wave making resistance coefficient can be obtained as

41

$$C_w = \frac{R_w}{\frac{1}{2}\rho S U^2}$$

$$= -\frac{\sum_{j=1}^{N_H} C_{pj} n_{xj} \Delta S_j}{\sum_{j=1}^{N_H} \Delta S_j} - \frac{\rho g \oint_{wL} \zeta_r^2 n_x dL}{\rho S U^2} \qquad (2.6.6)$$

where N_H is the number of panels on the hull surfaces, n_x is the x component of normal and ΔS_j is the area of j panel respectively.

♦2.6.2 Wavemaking Resistance in Free Condition:

After calculating the values of sinkage and trim, the wavemaking resistance can be obtained from Equation (2.4.6) as follows:

$$R_w = F_1^0 + s F_1^s + t F_1^t \qquad (2.6.7)$$

The displacement of ship in relation to steady moving coordinate system can be expressed as (described Appendix A)

$$\alpha = \xi(\xi_1, \xi_2, \xi_3) + \Omega(\xi_4, \xi_5, \xi_6) \times x' + O(\delta^2)$$
$$= (\xi_1 + \xi_5 z - \xi_6 y)\mathbf{i} + (\xi_2 + \xi_6 x - \xi_4 z)\mathbf{j} + (\xi_3 + \xi_4 y - \xi_5 x)\mathbf{k} \qquad (2.6.8)$$

So the relative wave elevation due to the motion of the body and wave system is given by

$$\zeta_r = \zeta - (\xi_3 + \xi_4 y - \xi_5 x)$$
$$= \zeta - (s - tx) \quad \text{for sinkage and trim} \qquad (2.6.9)$$

Now the total wavemaking resistance can be defined as

$$R_w = F_1^0 + s F_1^s + t F_1^t - \frac{1}{2}\rho g \int_{wL} \zeta^2 n_x \, dL - \oint_{wL} F_1^0 (s - tx) n_x dL \qquad (2.6.10)$$

The 4th term of Equation (2.6.10) is the correction factor due to the difference between the real and still water level and 5th term is due to changes of sinkage and trim. We can use ($F_1^0 + s F_1^s + t F_1^t$) instead of F_1^0. But as we have considered the sinkage and trim to be of second order or higher order, it is reasonable to take F_1^0.

42

CHAPTER 3

Nonlinear Optimization Technique

Optimization might be defined as the science of determining the best solutions to certain mathematically defined problems, which are often models of physicals reality. It involves the study of optimality criteria for problems, the determination of algorithmic methods of solution, the study of the structure of such methods, and computer experimentation with methods both under trail conditions and on real life problems. There is an extremely diverse range of practical applications. The applicability of optimization methods is widespread, reaching into almost every activity in which numerical information is processed (Science, Engineering, Mathematics, Economics, Commerce, etc.). Optimization techniques, is used effectively, can greatly reduce the engineering design time and yield improved, efficient, and economical designs.

Numerical optimization techniques offer a logical approach to design automation, and many algorithms have been proposed in recent years. Some of these techniques, such as linear, quadratic, dynamic, and geometric programming algorithms, have been developed to deal with specific classes of optimization problems. A more general category of algorithms referred to as nonlinear programming has evolved for the solution of general optimization problems. As is frequently the case with nonlinear problems, there is no single method that is clearly better than others. Methods for numerical optimization are referred to collectively as mathematical programming techniques.

Sequential Quadratic Programming (SQP) has arguably the most successful method for solving nonlinearly constrained optimization problems. The SQP is a general method for solving nonlinear optimization problems with constraints. The mathematical formulation of the present design oriented (SQP) problem, which finds an optimum shape of the ship with minimum resistance subject to geometric and hydrodynamic constraints can be expressed as

Minimize $f(x)$ (3.1)

Subjected to $h_i(x) = 0, \quad i = 1, N$
$g_i(x) \leq 0, \quad i = 1, M$

where x is a vector representation of design variables defining the hull surface and hull form characteristics. The ship wave making resistance is used as an objective function f. The geometrical and hydrodynamical design constraints about the hull surface are contained in both the equality (h_i) and inequality (g_i) constraints, N is the number of equality constraint and M is the number of inequality constraints respectively.

At first this design-constrained problem is converted to an unconstrained one associating penalty for any constraint violation. Thus the Equation (3.1) is transformed into the following function

$$F(x) = f(x) + \sum_{i=1}^{N_{Tc}} \delta_i \phi_i(x)$$ (3.2)

where N_{TC} is the total number of constraint, δ_I is the penalty coefficients for constraint i and $\phi_i(x)$ is a penalty term related to the ith constraint.

F is a nonlinear optimization problem since the objective function, the wavemaking resistance of ship and the constraints are implicit, non-linear functions of the design variable x. F is in many cases non-convex and has often multiple minima. In fact, there is no general reliable optimization method available to find a global minimum and no general agreement on the best approach to solve non-linear multivariable constrained problems. A method that works well on one problem may perform very poorly on another problem of same kind.

Merit Function:

The SQP algorithm can be made more robust by adding a step-length control. Thus, the basic iteration of a practical method for solving nonlinear constrained problems is written as follows:

$$x^{(k+1)} = x^{(k)} + \alpha d$$ (3.3)

The direction d is computed by solving the quadratic programming sub problem. In the case of unconstrained problems, the step length is computed by minimizing the objective function along the computed direction. In the case of constrained problem, a

44

merit function that takes into consideration both the constraints and the objective function is used during step length calculations. The following merit function is commonly used with the SQP method:

$$\phi(\alpha) \equiv F\left(x^k + \alpha d\right) + r\left[\sum_{i=1}^{N}\left|h_i\left(x^k + \alpha d\right)\right| + \sum_{i=1}^{M}\left|\min\left\{0, g_i\left(x^k + \alpha d\right)\right\}\right|\right] \qquad (3.4)$$

where r is a scalar penalty parameter,

An inequality constraint is violated if $g_i > 0$. For equality constraint, any nonzero value indicates a violation of that constraint. Hence, for equality constraints, an absolute value is used in the above definition. If all constraints are satisfied (all $g_i \leq 0$ and $h_i = 0$), then the merit function is the same as the objective function. The penalty parameter r is introduced to allow for an additional control over the definition of ϕ.

Minimizing the merit function:

To determine a suitable step length α along a computed direction d, the merit function $\phi(\alpha)$ needs to be minimized. Theoretically, this is the same as the one-dimensional line search presented for unconstrained problems. But constrained problem a numerical search procedure is used because from the definition of $\phi(\alpha)$ it is not a differentiable function. In the numerical search procedure the following line search procedure is based on Armijo's rule for unconstrained problems.

Approximate Line-Search Procedure

The procedure starts by first computing the merit function value with $\alpha = 0$. This value is identified as $\phi_0(\alpha)$ and

$$\phi_0(\alpha) = F\left(x^k\right) + r\left[\sum_{i=1}^{N}\left|h_i\left(x^k\right)\right| + \sum_{i=1}^{M}\left|\min\left\{0, g_i\left(x^k\right)\right\}\right|\right] \qquad (3.5)$$

Then

$$\phi(\alpha) \equiv F\left(x^k + \alpha d\right) + r\left[\sum_{i=1}^{N}\left|h_i\left(x^k + \alpha d\right)\right| + \sum_{i=1}^{M}\left|\min\left\{0, g_i\left(x^k + \alpha d\right)\right\}\right|\right] \qquad (3.6)$$

45

values are computed successively with $\alpha =1, 1/2, 1/4 ,..$ until an α is found that satisfies the following criteria.

$$\phi(\alpha) \le \phi_0(\alpha) - \alpha\omega\|d\|^2$$

where ω is an additional parameter introduced to provide further control over search process. ω is typically set to 0.5. As can be seen from this criterion, instead of finding the true minimum of $\phi(\alpha)$, in this line search we accept α that reduces the initial value of ϕ by a factor $\alpha\omega\|d\|^2$. Since α is included in this factor, as the trial step length is reduced, the expected reduction becomes small as well. Hence , as long as d is a decent direction, the test must pass after a finite number of iterations.

SQP Algorithm

Given the penalty parameter r (r =1) and step length parameter ω ($\omega = 0.5$)

Step 1. Set an iteration counter k = 0. Starting initial estimates x^0, u^0, v^0 and a symmetric positive definite matrix H^0.

Step 2. Solve the problem

Minimize $\quad P(d) = F\left(x^{(k)}\right) + \nabla F^T\left[x^{(k)}\right] \cdot d + \frac{1}{2} d^T \cdot H^{(k)} \cdot d$

Subjected to $\quad \begin{aligned} & h_i\left[x^{(k)}\right] + \nabla h_i^T\left[x^{(k)}\right] \cdot d = 0 \quad i = 1, N \\ & g_i\left[x^{(k)}\right] + \nabla g_i^T\left[x^{(k)}\right] \cdot d \le 0 \quad i = 1, M \end{aligned}$

Solving Kuhn-Tucker conditions for the original problem using Newton's method for solving nonlinear equations directly leads to above form in which matrix H represents the Hessian of the Lagrangian

$$H = \nabla^2 F + \sum_{i=1}^{N} u_i \nabla^2 h_i + \sum_{i=1}^{M} v_i \nabla^2 g_i$$

where $u = (u_1, u_2, u_3 \dots u_N)^T$ and $v = (v_1, v_2, v_3 \dots v_M)^T$ are the Lagrangian multiplier for equality and inequality constraints respective. The Lagrangian function is defined in terms of variables x, and Lagrangian multipliers

(u, v), so a feature of the resulting methods is that a sequence of approximations $x^{(k)}$, $u^{(k)}$, and $v^{(k)}$ to both the solution vector x and the vector of optimum Lagrange multipliers (u, v) is generated.

Step 4. Update the penalty parameter r

(i)   Set $r^{k+1} = 4.0\left\{1.0 + \dfrac{1}{4}\left[\displaystyle\sum_{i=1}^{M} abs(v_i) + \sum_{i=1}^{N} u_i\right]\right\}$

(ii) $F(x^k) + r^{k+1}V(x^k) > F(x^k) + r^k V(x^k)$ need to restart, go to step 1. Otherwise, continue to step 5.

Step 5. Compute the step length α using approximation line search as follows:

(i)   Compute $\phi_0(\alpha) = F(x^k) + r\left[\displaystyle\sum_{i=1}^{N}|h_i(x^k)| + \sum_{i=1}^{M}|min\{0, g_i(x^k)\}|\right]$. Set i = 0.

(ii)   Set $\alpha = (1/2)^i$

(iii)   Compute $\phi(\alpha) \equiv F(x^k + \alpha d) + r\left[\displaystyle\sum_{i=1}^{N}|h_i(x^k + \alpha d)| + \sum_{i=1}^{M}|min\{0, g_i(x^k + \alpha d)\}|\right]$

(iv)   If $\phi(\alpha) \le \phi_0 - \alpha\omega\|d\|^2$ then accept α. Otherwise set i=i+1 and go to step (ii)

Step 6. Set the new point as

$$x^{(k+1)} = x^{(k)} + \alpha d$$

Step 7. Check for convergence. If $\|d\| \le$ tol (a small number), then stop. Otherwise go to Step 8.

Step 8. Update the $H^{(k)}$ in such a way that $H^{(k+1)}$ remains positive definite. Then set k = K+1 and go to Step 2.

The Hessian matrix is updated by using the BFGS (Broyden, Fletcher, Goldfarb and Shanon) method as follows:

$$H^{(k+1)} = H^k + \frac{\gamma\gamma^T}{q^T s} - \frac{H^{(k)}ss^T H^{(k)}}{s^T H^{(k)} s}$$

where

47

$$s = x^{(k+1)} - x^{(k)} \qquad q = \nabla_x L^{(k+1)} - \nabla_x L^{(k)}$$

$$\nabla_x L = \nabla F + \sum_{i=1}^{N_e} u_i \nabla h_i + \sum_{i=1}^{M_i} v_i \nabla g_i$$

$$\gamma = \theta q + (1 - \theta) H^{(K)} \cdot s$$

$$\theta = \left(\begin{array}{ll} 1.0 & \text{if } q^T s \geq 0.2 s^T H^{(k)} s \\[2mm] \dfrac{0.8 s^T H^{(k)} \cdot s}{s^T H^{(k)} s - q^T s} & \text{if } \quad q^T s < 0.2 s^T H^{(k)} s \end{array} \right)$$

CHAPTER 4

Results and Discussions

4.1 Optimization Method for Hull Form

The numerical optimization can be carried out by systematically iterative evaluations of the objective function as shown in Figure 4.1. In the general engineering optimization problem, the objective functions are nonlinear with respect to the design variables and complex design constraints are imposed. To solve those optimization problems a nonlinear programming (NLP) techniques should be employed. In the present study, SQP (ASNOP, 1991 & Bhati, 2000) (Sequential Quadratic Programming) is selected as one of NLP to minimize the objective function under design constraints.

The method of finding a form with lower resistance is as follows. Optimization is carried out so as to yield the hull form with lower resistance. The objective function is the wave resistance coefficient.
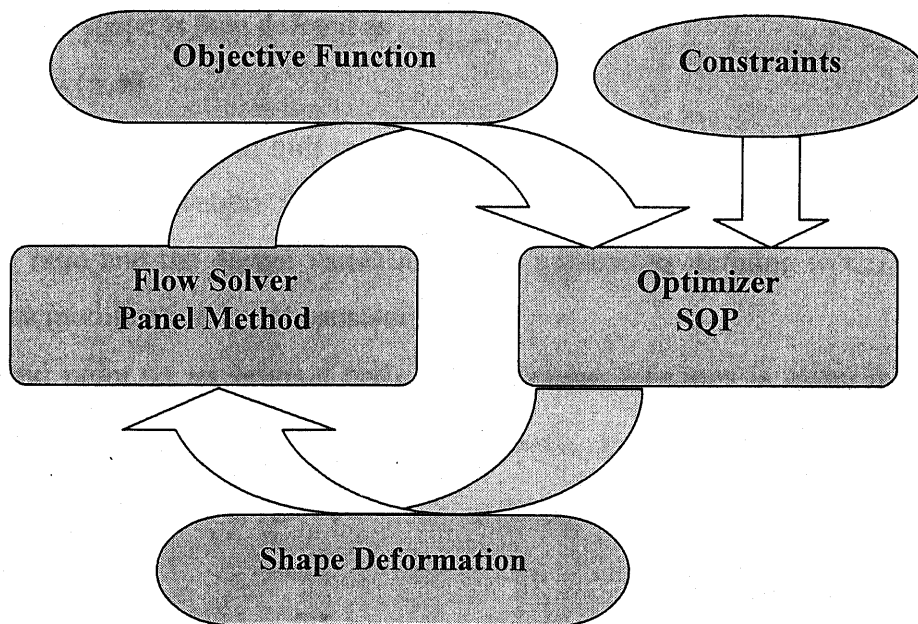
Fig. 4.1 Iterative process of shape optimization

4.2 Hull Form Deformation Function

The role of a shape modification function is to provide a link between the design variables and the body shape, which should be defined geometrically. In an optimization system, design variables and shape modification method should be selected with a compromise between flexibility and simplicity. Since an optimization procedure searches an optimal solution in the space defined by the design variables, the final shape is optimal among the shapes, which can be defined by the combination of design variable values. Thus the design variables and a shape modification method should be flexible and enough to cover a wide variety of body shapes. On the other hand, the number of design variables should be as small as possible and shape modification should be as simple as possible from the efficiency point of view.

The shape modification method used here is based on a weight function. First the initial ship hull form is assumed to be

$$y = f_0(x, z) \tag{4.1}$$

In case of practical ship hull form, $f_0(x,z)$ does not necessarily take an explicit functional form. Instead it is given numerically as the coordinates of a body surface grid.

The modified shape is then defined as

$$y = f_0(x, z)w(x, z) \tag{4.2}$$

where $f_0(x,z)$ is the original hull surface defined in longitudinal and vertical coordinates (x, z). $w(x,z)$ is a weight function to provide transverse-directional expansion and reduction ratio and the design variables are the parameters defining $w(x,z)$. In this form depth-wise modification is not considered.

Thus a grid point on an original body surface whose locations is given by (x_0, y_0, z_0) moves to $(x_0, w(x_0, y_0)y_0, z_0)$ on a modified body. A new surface grid is obtained with the re-distribution of surface grid points along the grid lines in the girth direction.

♦ 4.2.1 Weight Function of Hull Form Deformation of Monohull

The weight functions of hull deformation during the optimization procedure of Wigley hull and the Series 60 hull are expressed below:

For fore body

$$w(x,z) = 1 - \sum_{m=1}\sum_{n=1}\alpha_{mn}\sin\left\{\pi\left(\frac{x-x_0}{x_{min}-x_0}\right)^{m+2}\right\}$$
$$\times \sin\left\{\pi\left(\frac{\beta-z}{\beta+T}\right)^{n+2}\right\} \qquad -L/2 \le x \le 0 \tag{4.3}$$

and for aft body

$$w(x,z) = 1 - \sum_{m=1}\sum_{n=1}\alpha_{mn}\sin\left\{\pi\left(\frac{x-x_0}{x_{max}-x_0}\right)^{m+2}\right\}$$
$$\times \sin\left\{\pi\left(\frac{\beta-z}{\beta+T}\right)^{n+2}\right\} \qquad 0 \le x \le L/2 \tag{4.4}$$

where x_0, x_{max}, x_{min}, T are parameters for characterizing the hull form modification (hull form parameters) and α_{mn} and β are taken as the design variables in the optimization procedure.

◆ 4.2.2 Weight Function of Hull Form Deformation of Catamaran Hull

The weight functions of catamaran hull deformation of inside and outside part expressed as for fore body

$$w^{I,O}(x,z) = 1 - \sum_{m=1}\sum_{n=1}\alpha_{mn}\sin\left\{\pi\left(\frac{x-x^{I,O}_0}{x^{I,O}_{min}-x^{I,O}_0}\right)^{m+2}\right\}$$
$$\times \sin\left\{\pi\left(\frac{\beta^{I,O}-z}{\beta^{I,O}+T}\right)^{n+2}\right\} \qquad -L/2 \le x \le 0 \tag{4.5}$$

and for aft body

$$w^{I,O}(x,z) = 1 - \sum_{m=1}\sum_{n=1}\alpha_{mn}\sin\left\{\pi\left(\frac{x-x^{I,O}_0}{x^{I,O}_{max}-x^{I,O}_0}\right)^{m+2}\right\}$$
$$\times \sin\left\{\pi\left(\frac{\beta^{I,O}-z}{\beta^{I,O}+T}\right)^{n+2}\right\} \qquad 0 \le x \le L/2 \tag{4.6}$$

where $x_0^{I,O}$, $x_{max}^{I,O}$, $x_{min}^{I,O}$, T are parameters for characterizing the hull form modification (hull form parameters) and α_{mn} and β are taken as the design variables in the optimization procedure.

4.3 Optimization of Wigley Hull in Shallow Water

In the optimization of mono hull in shallow water, first a mathematical Wigley hull is used to carry out the numerical optimization. The equation of this type of hull surface is

$$y(x,z) = \frac{B}{2}S(z)\left[1 - \frac{x^2}{(L/2)^2}\right] \tag{4.7}$$

where L, B, and T are the ship length, beam and draft and $S(z)$ is a function define the frame line of ship cross-section. For rectangular cross-sections $S(z) = 1$, for triangular cross-sections $S(z) = 1 + z/T$, and for parabolic cross-section $S(z) = 1 - (z/T)^2$. The symmetric parabolic frame lines and parabolic waterlines are used in the present numerical optimization procedure. The principal particulars and the design speed and design constraints for optimization problem of Wigley hull are shown in Tables 4.1 and 4.2.

Table 4.1 Principal Particulars of Wigley Hull

Particulars	Wigley hull
L/B	10
L/T	16
Block coefficient C_B	0.444
Midship coefficient C_M	0.667
Waterplane area coefficient C_w	0.667

Since the body is symmetric about the center plane of ship, one half of the computational domain is used for the numerical calculation. The panels from 1.5L upstream to 3.0L downstream cover the free surface domain. The free surface domain along the transverse direction is 1.5L. The domain of sea bottom along the longitudinal direction is $5.0L \geq x \geq -3.0L$ and along the transverse direction is $0 \geq y \geq -2.0L$. The number of panel on the ship hull, the free surface and the bottom surface are 40x10, 70x15 and 40x10 respectively. The panel distributions of the Wigley hull, the free surface and the sea bottom surface are shown in Figure 4.2. The total number of design variables is 10.
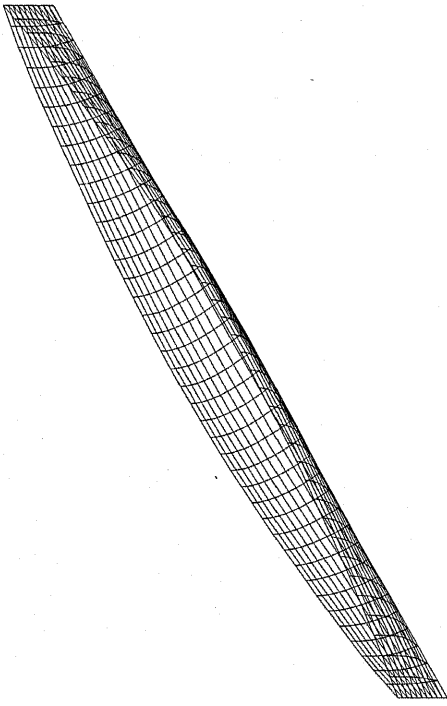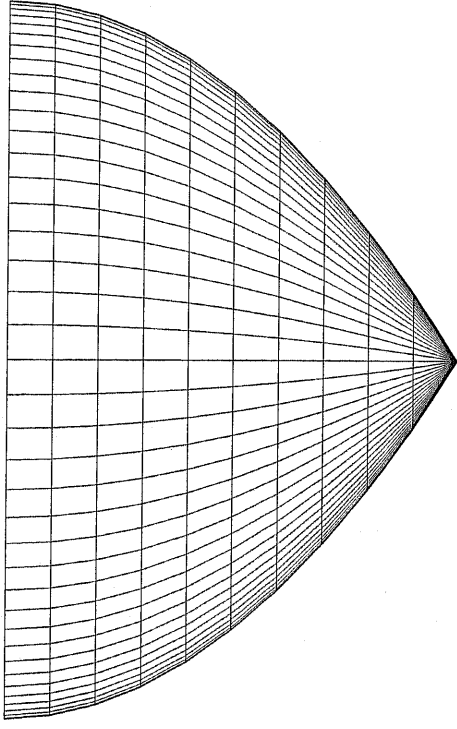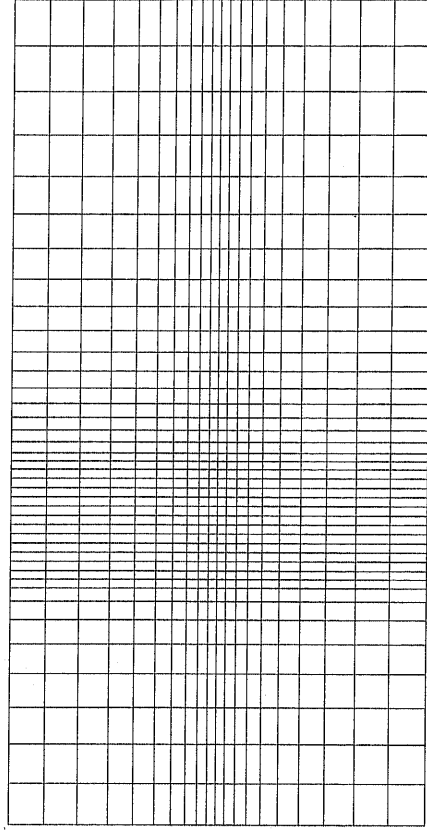
Body plan of Wigley model

Sea Bottom Surface
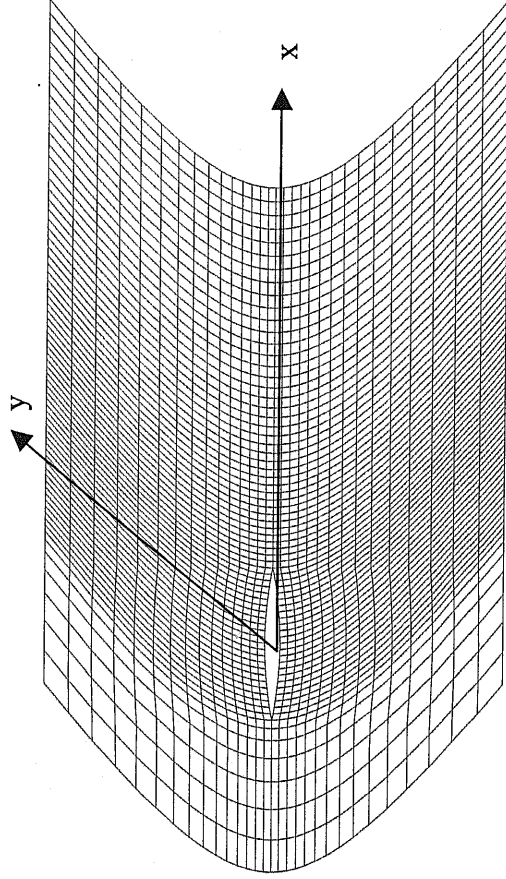
3-D view of Wigley model

Free Surface

Figure 4.2 Panel distribution of Wigley model, Free Surface and Sea Bottom Surface in Shallow water

53

Table 4.2 Design Speed and Constraints for Wigley Hull

Particulars	Constraints
Hull surface	$y(x,z) > 0$
Volume Displacement (∇)	$0.0995\nabla_0 < \nabla < 1.005\nabla_0$
Longitudinal Center of Buoyancy, LCB	$LCB_0 \pm 0.02\ L_{pp}$
Water plane area coefficient, C_W	$C_W > C_{W0}$
Sinkage, s	$s < s_0$
F_n	0.316

The first application is for the optimization of Wigley hull ($C_B = 0.444$) form with respect to the minimum wavemaking resistance. This hull form is optimized at water depths $h/T = 2.5$, 3.0, 4.0, 5.0 and deep water in order to compare the hydrodynamic behavior in shallow and deep water.

Convergence histories of the wavemaking resistance and sinkage of Wigley hull of SQP process are shown in Figure 4.3 and 4.4 respectively. Optimized at $h/T = 2.5$, 3.0, 4.0, 5.0 and deep water yield converged solution at 8, 4, 4, 10 and 5 optimization cycles respectively. The wave resistance decreased approximately 8% at $h/T = 2.5$, approximately 6% at $h/T = 3.0$ and 4.0, approximately 17% at $h/T = 5.0$ and approximately 10% at $h/T = \infty$.

The application of the optimization procedure produced optimal hulls with the original body-plans shown in Figure 4.5, Figure 4.6, Figure 4.7, Figure 4.8 and Figure 4.9 at depth of water $h/T = 2.5$, 3.0, 4.0, 5.0 and deep water, respectively. The resulting forms are entirely dictated by the hydrodynamic behavior associated with the changes in hull shape and optimized hull form has scarcely deviated from the original hull.

Figure 4.10 shows comparisons of sectional areas between the original one and the optimized hulls at different depth of water. The sectional area is decreased near amidships region and is increased towards the FP and AP.

The comparisons between the calculated wave profiles of optimized and original body along the hull are shown in Figure 4.11, Figure 4.12, Figure 4.13, Figure 4.14, and Figure 4.15 at $h/T = 2.5$, 3.0, 4.0, 5.0 and deep water respectively. The wave profiles were taken from the free surface elevation at the panels adjacent to the ship hull surface.

The optimized hull generates a slightly greater wave height at bow than the original hull. This is due to the increase of steepness of creative waves at the bow. The amplitude of stern waves is lower than the original hull and this is due to the reduction of transverse wave system.

Figure 4.16, Figure 4.17. Figure 4.18, Figure 4.19 and Figure 4.20 give the contours of the calculated non-dimensional wave pattern for optimized hulls (upper) and the corresponding wave patterns for original hull (lower) at depth of water $h/T = 2.5$, 3.0, 4.0, 5.0 and deep water respectively. The difference of wave fields generated by the optimized hulls and the original hull are clearly observed.

Finally Figure 4.21 shows the comparisons of the wavemaking resistance coefficient for the optimized hull and original one. It is seen that the reduction in the wavemaking resistance coefficient has been achieved. Although the wave height at bow is slightly higher than original one and the hull form has been optimized for a single speed (F_n =0.316) corresponds to lower critical speed for different depth of water, the optimized forms have less wave resistance over the wide range of design speed.
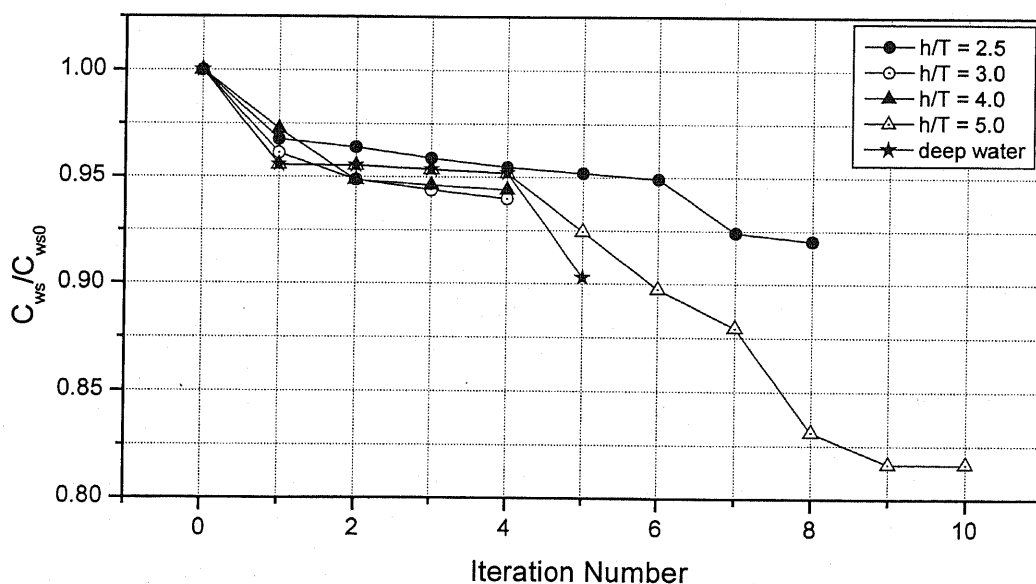
Fig. 4.3 Convergence history of wavemaking resistance of Wigley hull at $F_n = 0.316$
for different depths of water
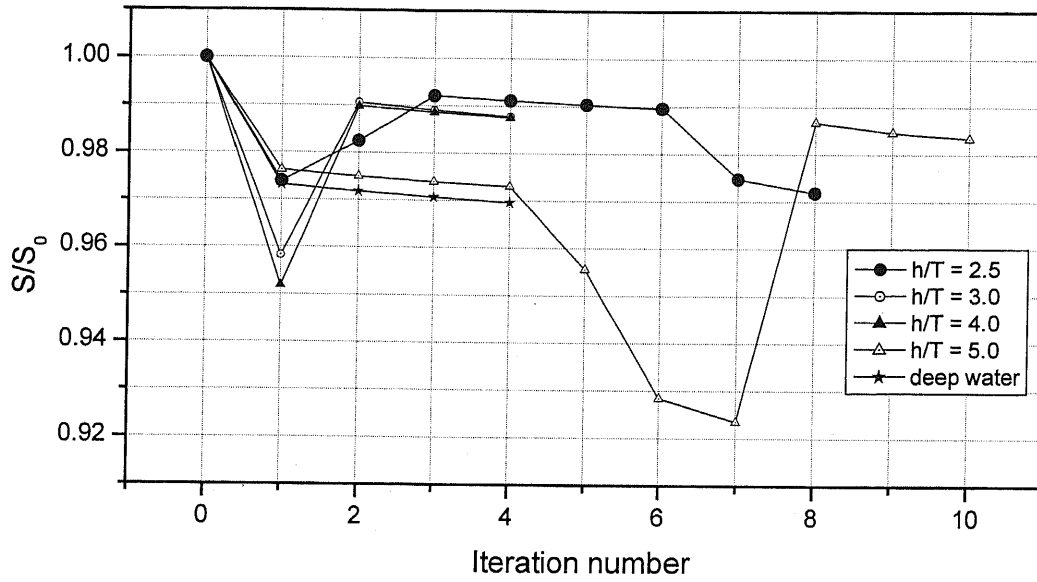
Fig. 4.4 Convergence history of sinkage of Wigley hull at $F_n = 0.316$ for different depths of water
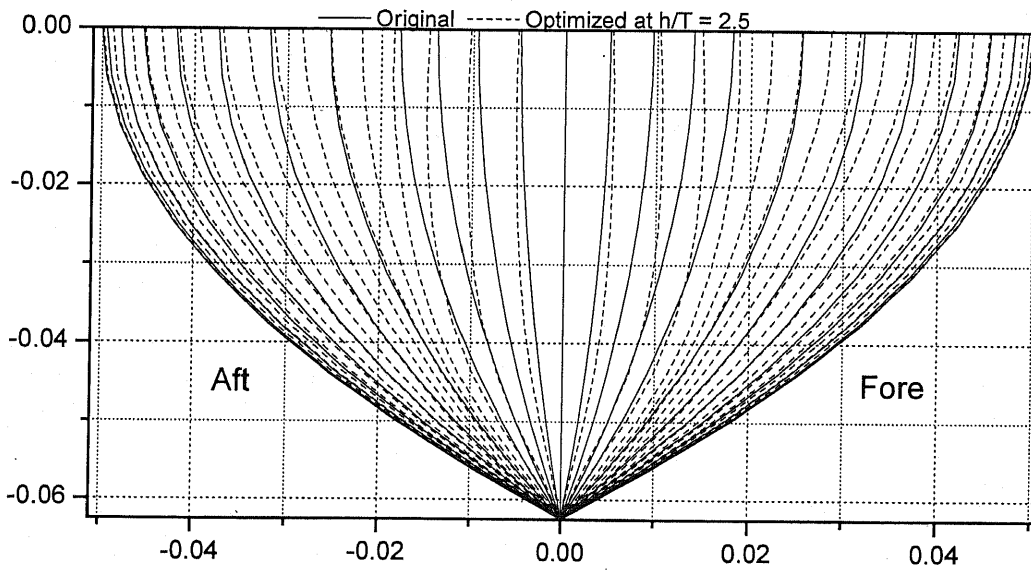
Fig. 4.5 Comparisons of body plans of Wigley hull optimized at $F_n = 0.316$ at depth of water $h/T = 2.5$.
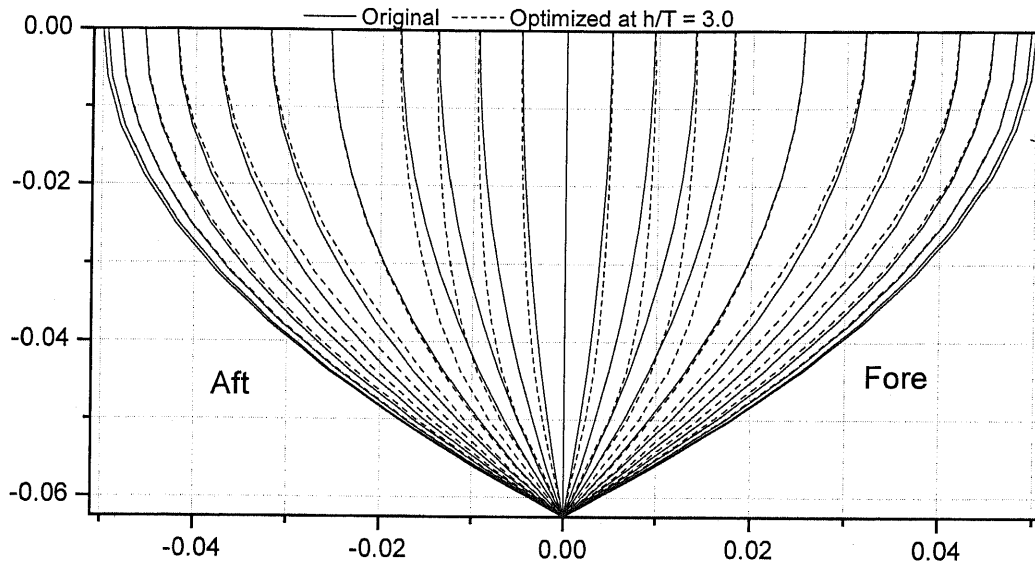
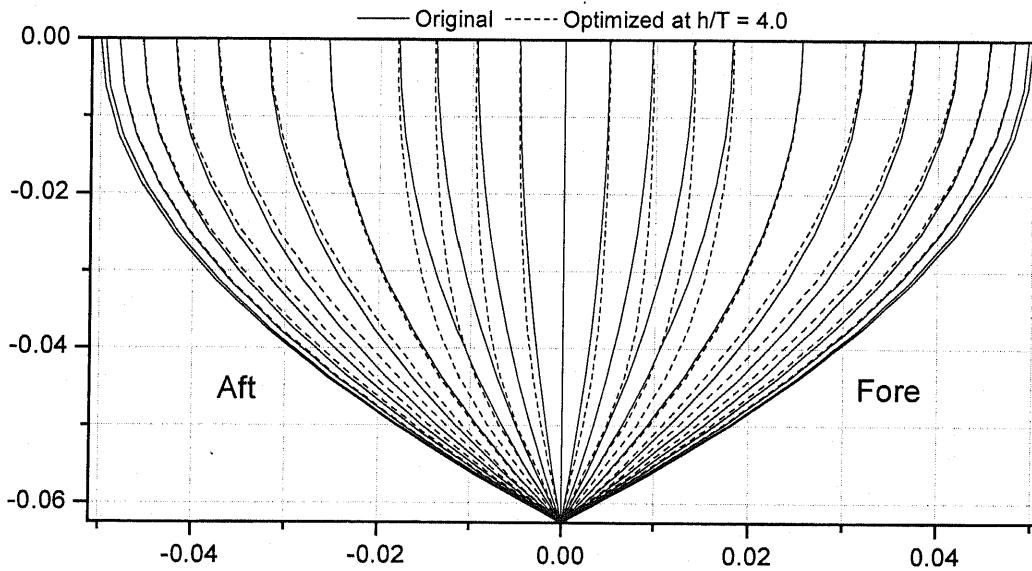Fig. 4.6 Comparisons of body plans of Wigley hull optimized at $F_n = 0.316$ at depth of water $h/T = 3.0$.

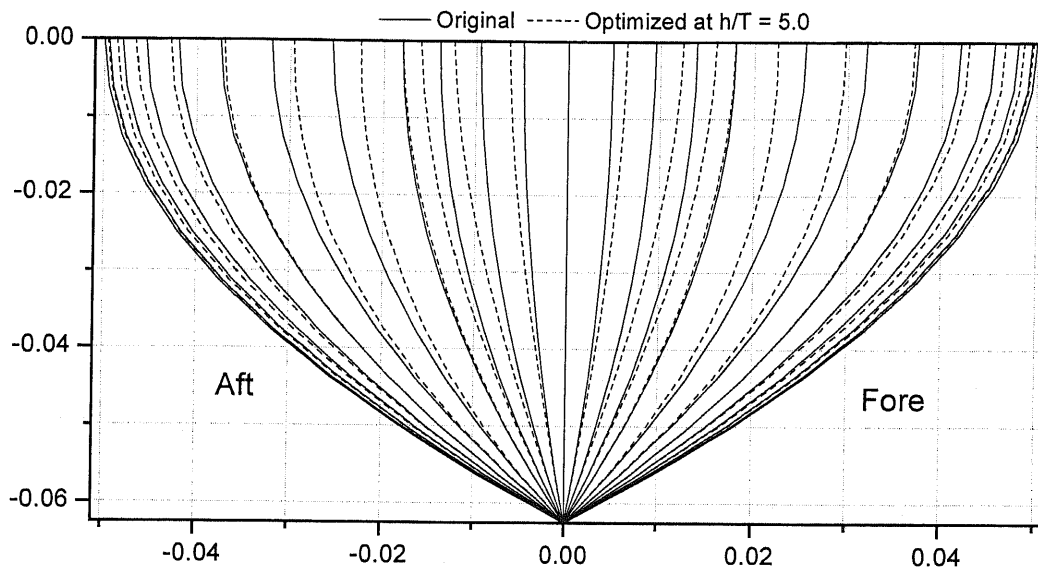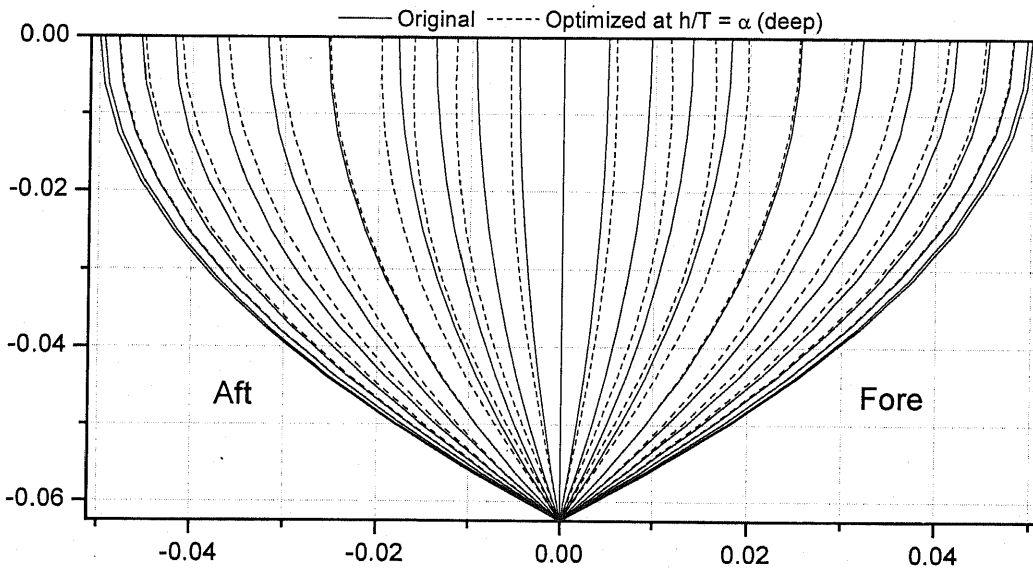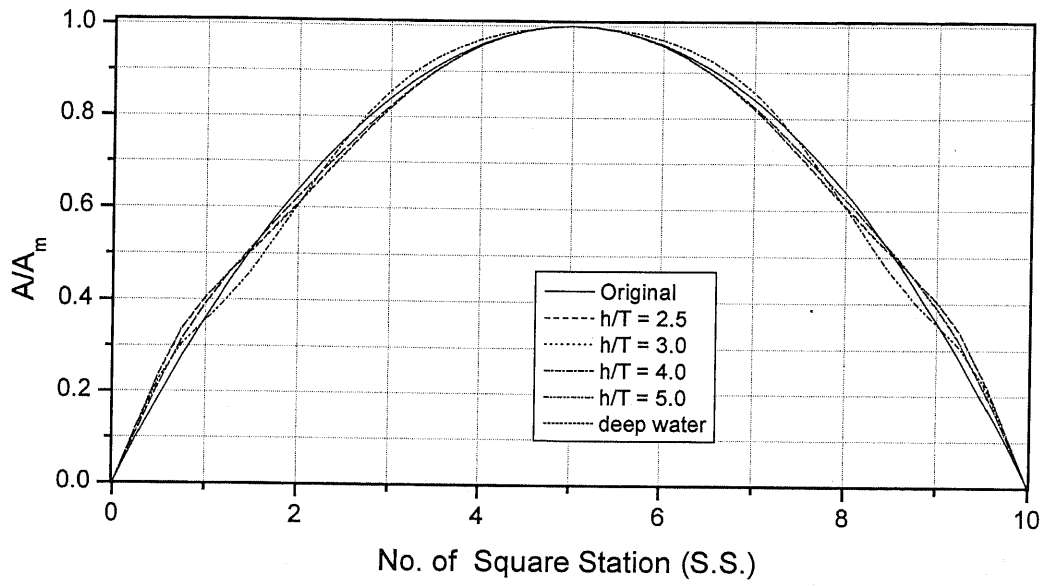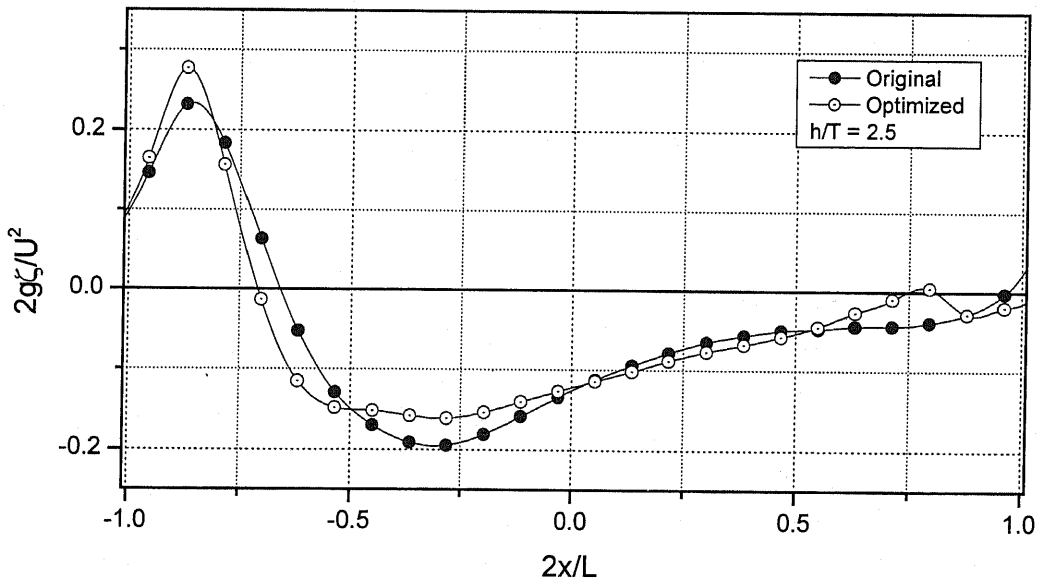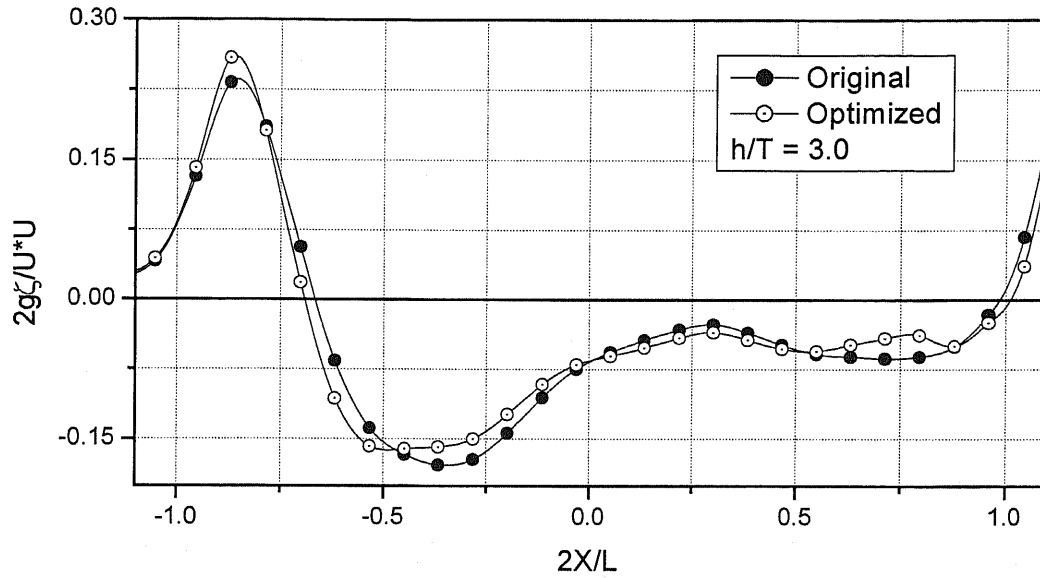Fig. 4.7 Comparisons of body plans of Wigley hull optimized at $F_n = 0.316$ at depth of water $h/T = 4.0$.

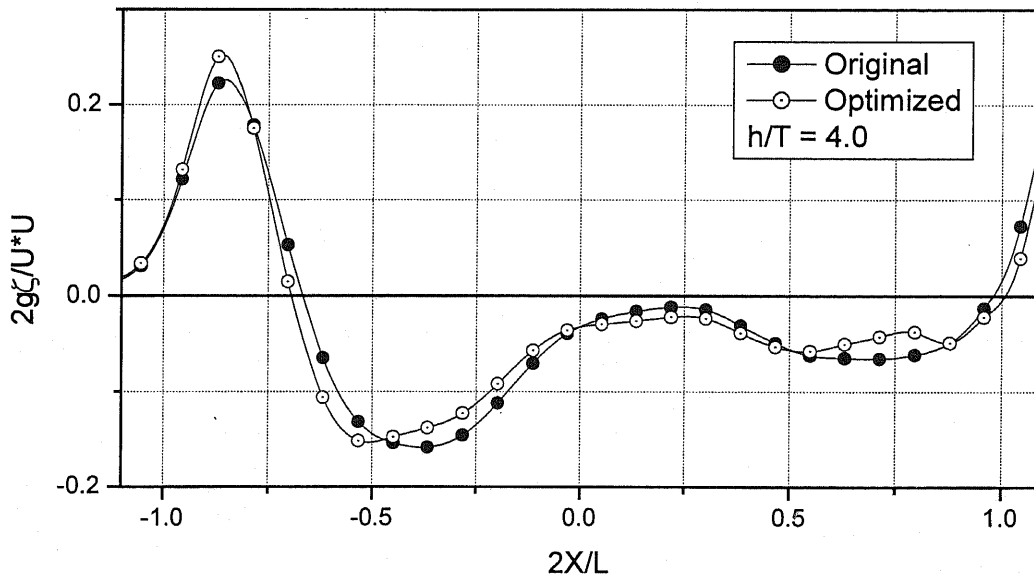Fig. 4.8 Comparisons of body plans of Wigley hull optimized at $F_n = 0.316$ at depth of water $h/T = 5.0$.

Fig. 4.9 Comparisons of body plans of Wigley hull optimized at $F_n = 0.316$ at deep water.

Fig. 4.10 Comparisons of sectional areas of Wigley hull optimized at $F_n = 0.316$ for different depths of water.
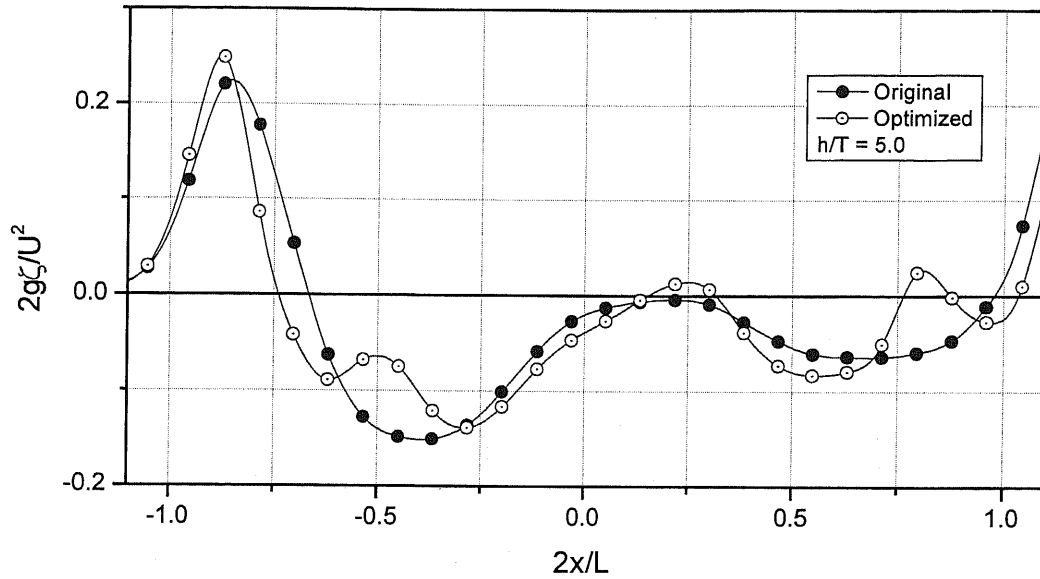

Fig. 4.11 Comparisons of wave profiles of Wigley hull optimized at $F_n = 0.316$ at depth of water h/T = 2.5.

59

Fig. 4.12 Comparisons of wave profiles of Wigley hull optimized at F_n = 0.316 at depth of water h/T = 3.0.

Fig. 4.13 Comparisons of wave profiles of Wigley hull optimized at F_n = 0.316 at depth of water h/T = 4.0.

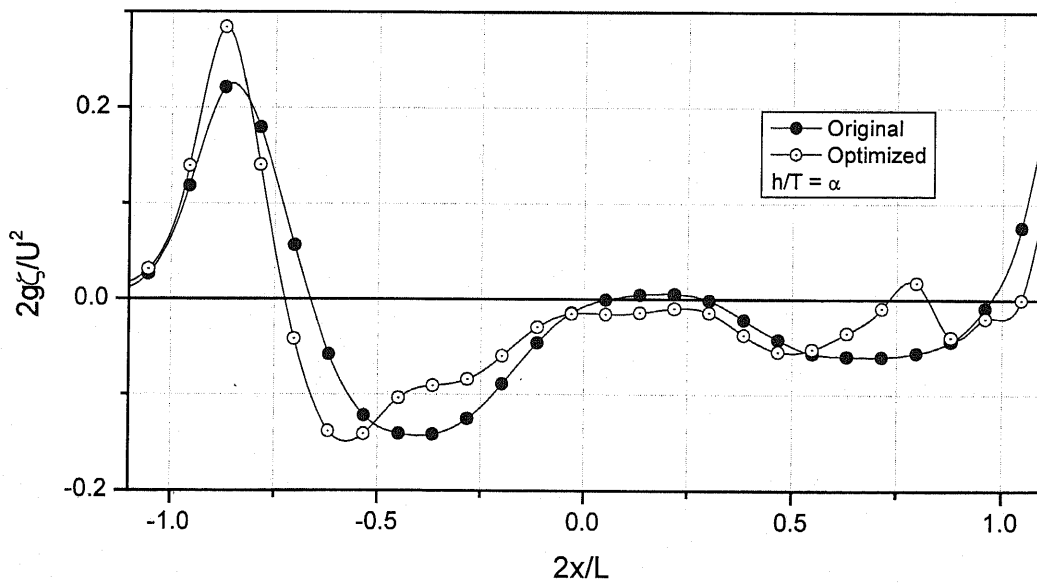Fig. 4.14 Comparisons of wave profiles of Wigley hull optimized at $F_n = 0.316$ at depth of water h/T = 5.0.

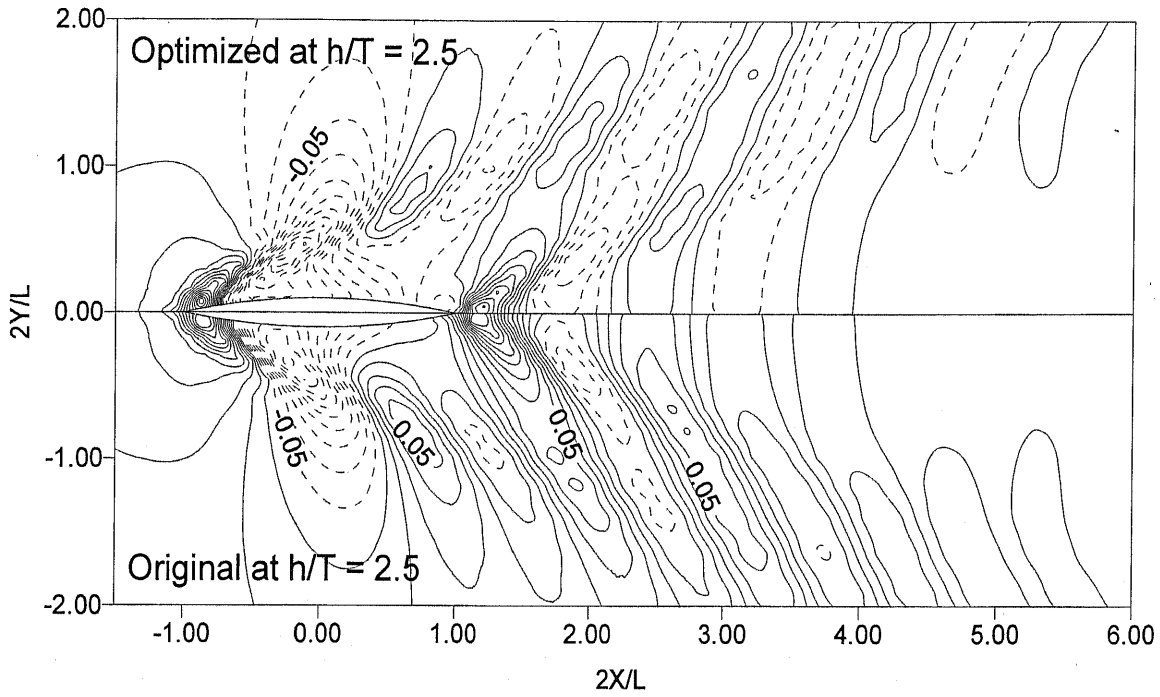Fig. 4.15 Comparisons of wave profiles of Wigley hull optimized at $F_n = 0.316$ at deep water.

Fig. 4.16 Comparisons of wave patterns ($2g\zeta/U^2$) of Wigley hull optimized at
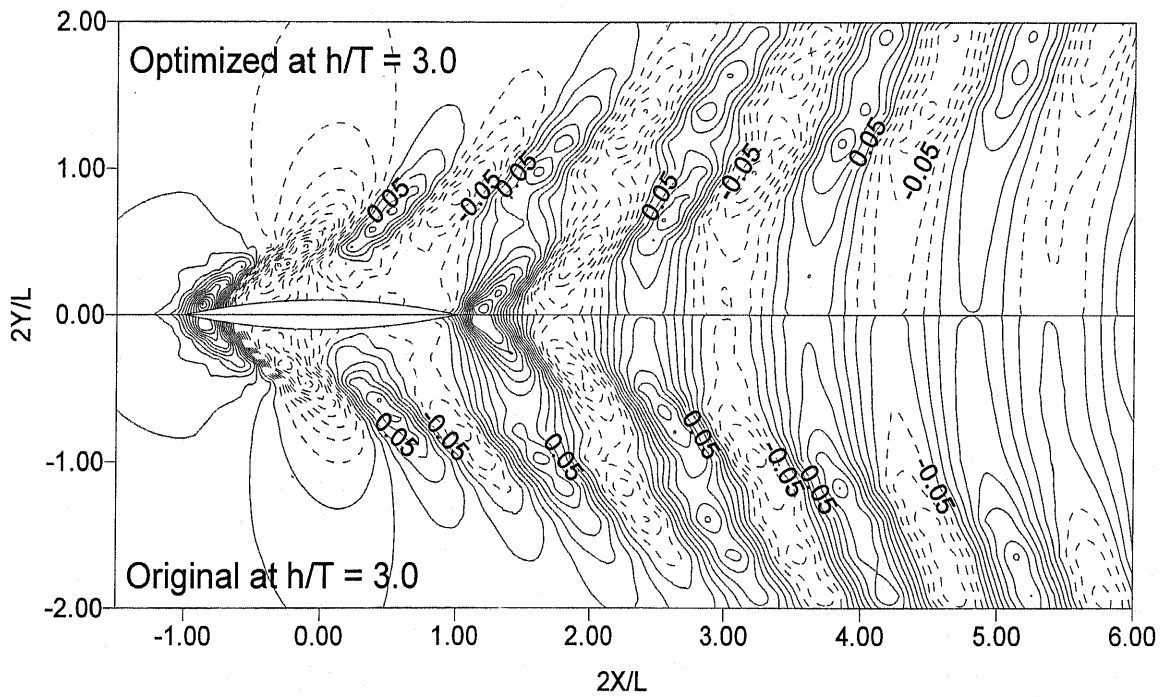$F_n = 0.316$ at depth of water h/T = 2.5.

Fig. 4.17 Comparisons of wave patterns ($2g\zeta/U^2$) of Wigley hull optimized at
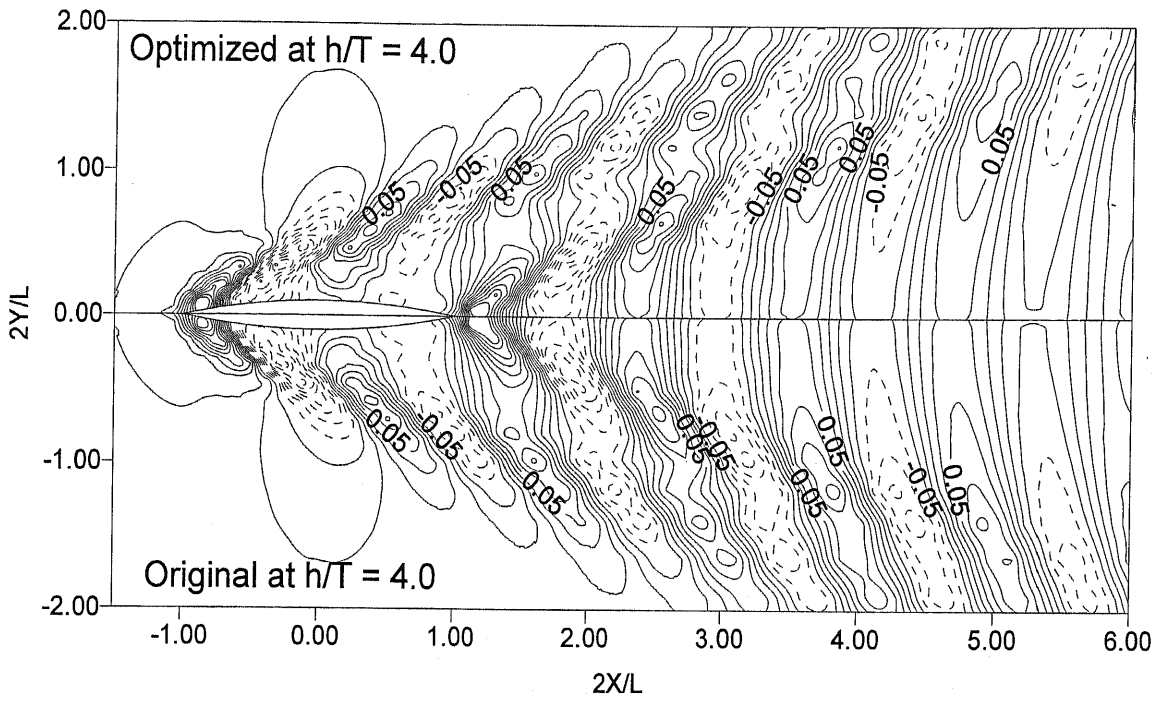$F_n = 0.316$ at depth of water h/T = 3.0.

Fig. 4.18 Comparisons of wave patterns ($2g\zeta/U^2$) of Wigley hull optimized at
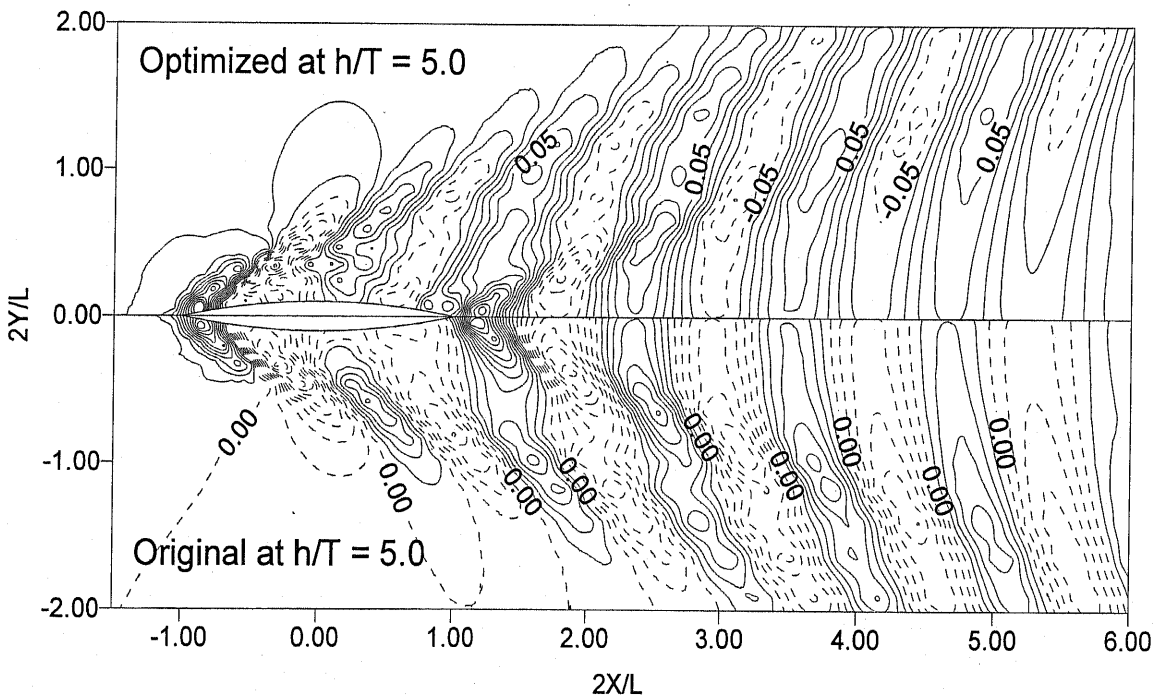$F_n = 0.316$ at depth of water h/T = 4.0.

Fig. 4.19 Comparisons of wave patterns ($2g\zeta/U^2$) of Wigley hull optimized at
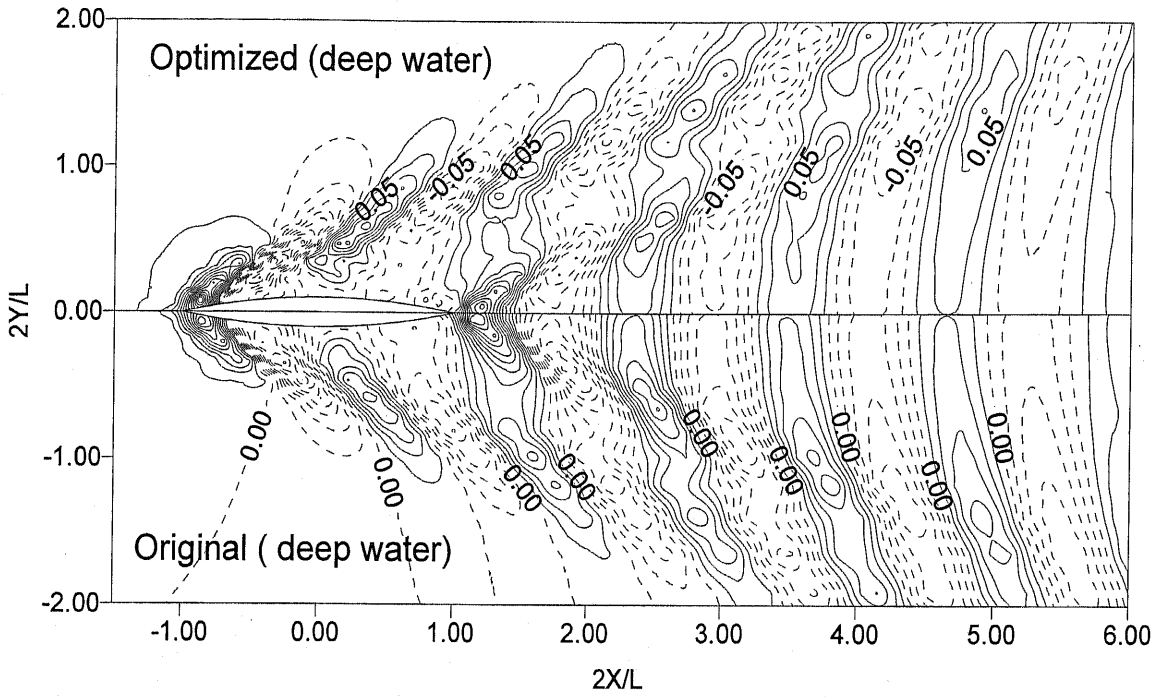$F_n = 0.316$ at depth of water h/T = 5.0.

Fig. 4.20 Comparisons of wave patterns ($2g\zeta/U^2$) of Wigley hull optimized at
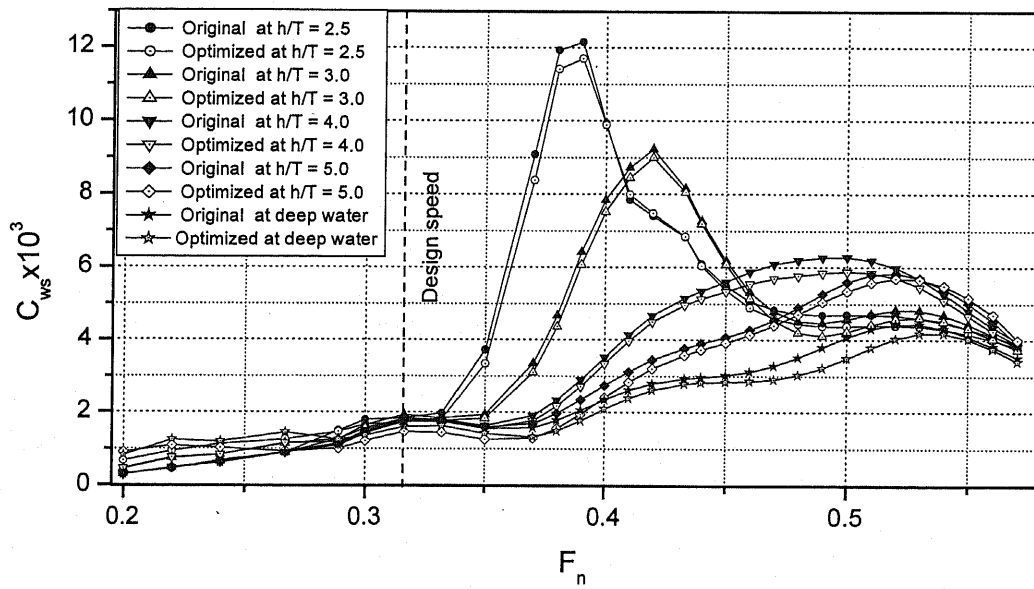$F_n = 0.316$ at deep water.

Fig. 4.21 Comparisons of wavemaking resistance of Wigley hull optimized at
$F_n = 0.316$ for different water depths.

4.4 Optimization of Series 60 (C_B = 0.6) in Shallow Water

For the second example of mono hull in shallow water, a well-known standard ship hull, the Series 60 (C_B =0.6) selected as an initial body shape. The principal particulars and the design speed and constraints for optimization problem of Series 60 hull are shown in Tables 4.3 and 4.4.
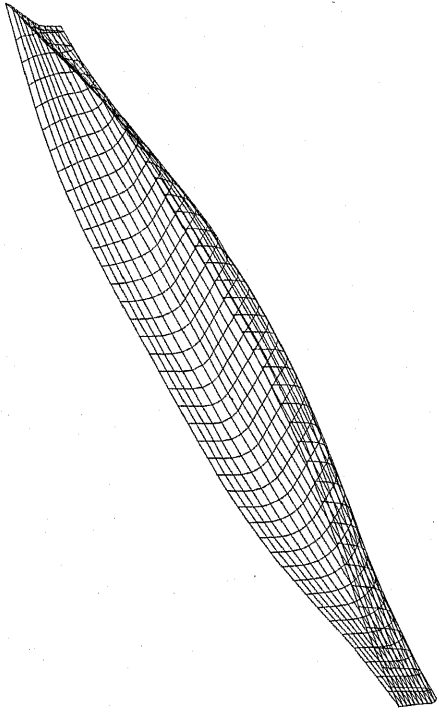
Table 4.3 Principal Particulars of Series 60 Hull

| Particulars	Series 60 hull
L/B	7.5
L/T	18.75
Block coefficient C_B	0.60
Midship coefficient C_M	0.977
Waterplane area coefficient C_W	0.95

The free surface domain for the Series 60 (C_B = 0.60) along the longitudinal direction is $-1.5L \le x \le 3.0L$ and along the transverse directions is $-1.5L \le y \le 0$ respectively. The sea bottom domain are $-3.0L \le x \le 5.0$ and $-2.0L \le y \le 0$ respectively. The number of panel on the ship hull, free surface and bottom surface are 40x10, 70x15 and 40x10 respectively. The panel distributions of Series 60 hull, free surface and sea bottom surface are shown in Figure 4.22. The total number of design variables for Series 60 model is 10.

Table 4.4 Design Speed and Constraints for Series 60 Hull

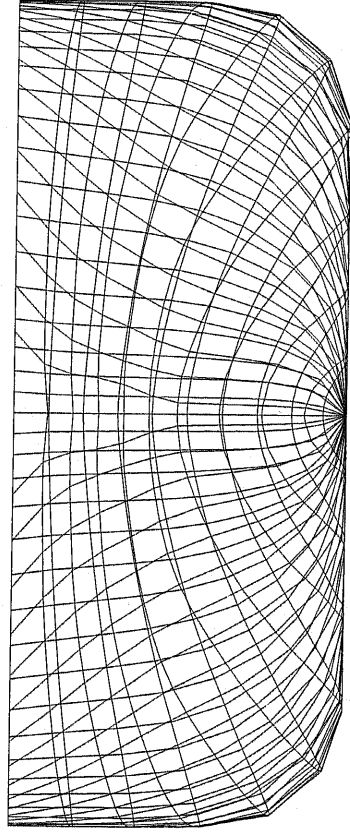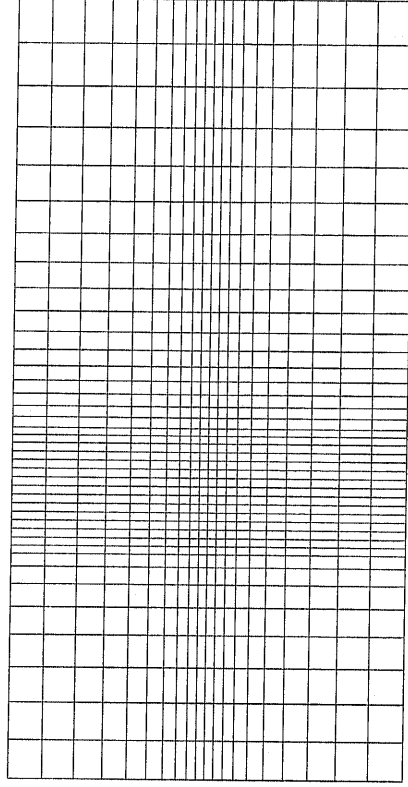| Particulars	Constraints
Hull surface	$y(x,z) > 0$
Volume Displacement (∇)	$0.0995\nabla_0 < \nabla < 1.005\nabla_0$
Longitudinal Center of Buoyancy, LCB	$LCB_0 \pm 0.02\, L_{pp}$
Water plane area coefficient, C_W	$C_W > C_{W0}$
Sinkage, s	$s < s_0$
F_n	0.316

Free Surface

Sea Bottom Surface

3-D view of Series 60 model
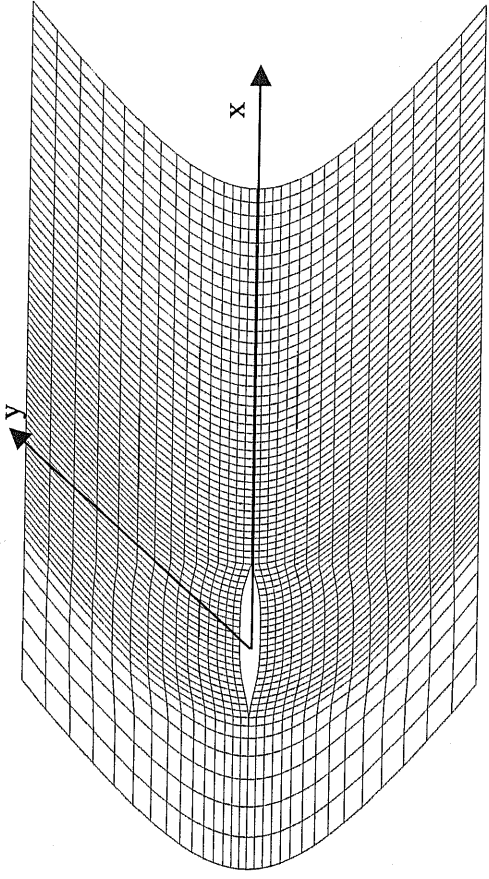
Body plan of Series 60 model

Fig 4.22 Panel distribution of Series 60 model, Free Surface and Sea Bottom Surface in Shallow water

66

The Series 60 hull is optimized at depths of water h/T = 2.5, 3.0, 3.5, 4.0, 4.5, 5.0 and deep water in order to verify the hydrodynamic behavior in shallow and deep water.

Figure 4.23 and 4.24 show the convergence history of wave resistance and sinkage of Series 60 hull. Optimized at h/T =2.5, 3.0, 3.5, 4.0, 4.5, 5.0 and deep water yield converged solution at 20, 32, 25, 27, 44, 36 and 35 optimization cycles respectively. The wave resistance decreased about 17% at depth of water h/T = 2.5, about 27% at depth of water h/T = 3.0, about 29% at depth of water h/T = 3.5, about 30% at depth of water h/T = 4.0, about 31% at depth of water h/T = 4.5, about 32% at depth of water h/T = 5.0 and about 33% at depth of water h/T = ∞.

The application of the optimization procedure produced optimal hulls with original body-plans shown in Figure 4.25, Figure 4.26, Figure 4.27, Figure 4.28 Figure 4.29, Figure 4.30 and Figure 4.31 at depth of water h/T =2.5, 3.0 3.5, 4.0, 4.5, 5.0 and deep water respectively. The frame lines of the fore part become U-shaped for the modified hull this effectively makes a water plane narrower and moves the volume from upper region to lower region. The frame lines of the aft part of the optimized hull become U shape to V-types that's means the water-plane wider than the original hull to compensate a displacement loss at bow part and the volume shift from lower region to upper region.

Figure 4.32 shows difference of sectional areas between the original one and optimized hull at different depth of water. The sectional area is decreased near amidships region and is increased towards the FP and AP.

The comparisons between the calculated wave profiles along the hull are shown in Figure 4.33, Figure 4.34, Figure 4.35, Figure 4.36, Figure 4.37, Figure 4.38 and Figure 4.39 at h/T = 2.5, 3.0, 3.5, 4.0, 4.5, 5.0 and deep water respectively. The wave profiles were taken from the free surface elevation at panels adjacent to the ship surface. The optimized hull generates a slightly greater bow wave than the original hull. The increase of the bow wave steepness is one of the reasons. The amplitude of stern waves is lower than the original hull and this is due to the reduction of transverse wave system.

Figure 4.40, Figure 4.41, Figure 4.42, Figure 4.43, Figure 4.44, Figure 4.45 and Figure 4.46 give the contours of the calculated non-dimensional wave pattern for optimized hulls (upper) and the corresponding wave patterns for original hull (lower) at

h/T =2.5, 3.0 3.5, 4.0, 4.5, 5.0 and deep water respectively. The difference of wave fields generated by modified hulls and original hull are clearly observed.

Lastly Figure 4.47 shows the comparisons of the wavemaking resistance coefficient for the modified hull and original Series 60 (C_B = 0.6). It is seen that the reduction in the wavemaking resistance coefficient has been achieved. Although bow wave height is greater the original values and the hull form has been optimized for a single speed (F_n =0.316) corresponds to lower critical speed for different depth of water, the optimized forms have less wavemaking resistance over the wide range of design speed.
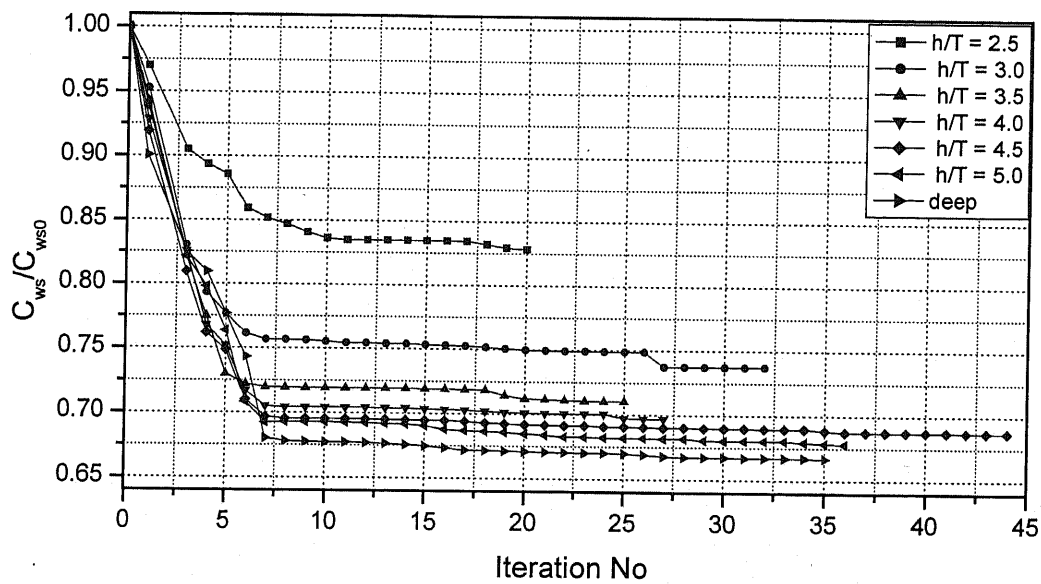

Fig. 4.23 Convergence history of wavemaking resistance of Series 60 hull optimized at F_n = 0.316 for different depth of water.
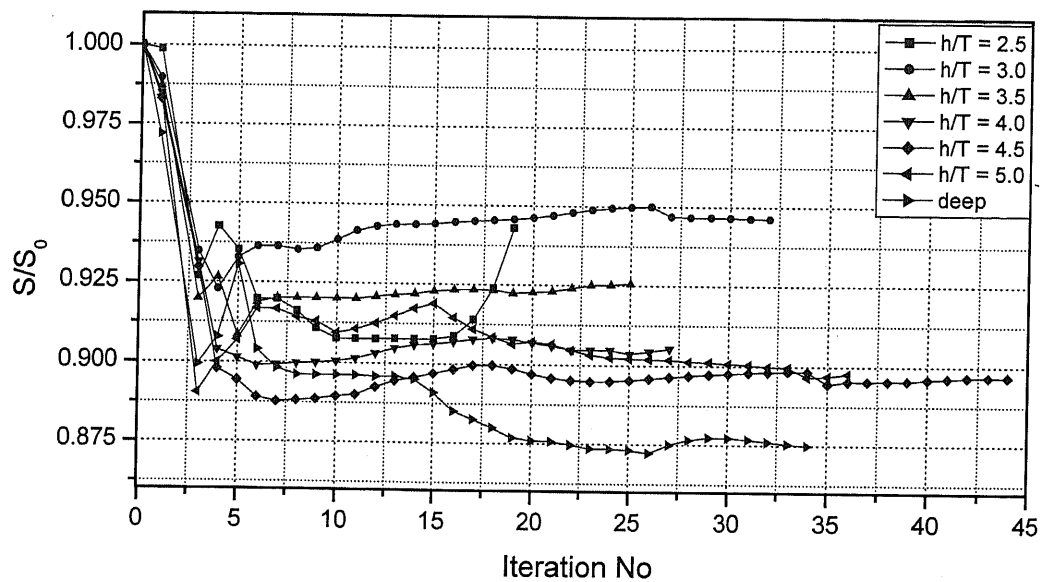
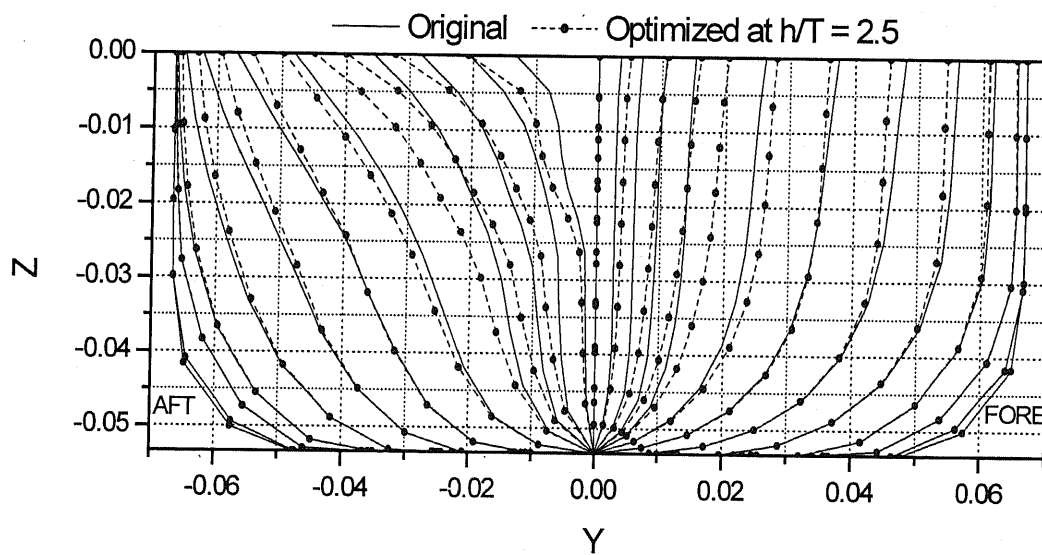Fig. 4.24 Convergence history of sinkage of Series 60 hull optimized at $F_n = 0.316$ for different depth of water.

Fig. 4.25 Comparisons of body plans of the Series 60 optimized at $F_n = 0.316$ at depth of water, $h/T = 2.5$.
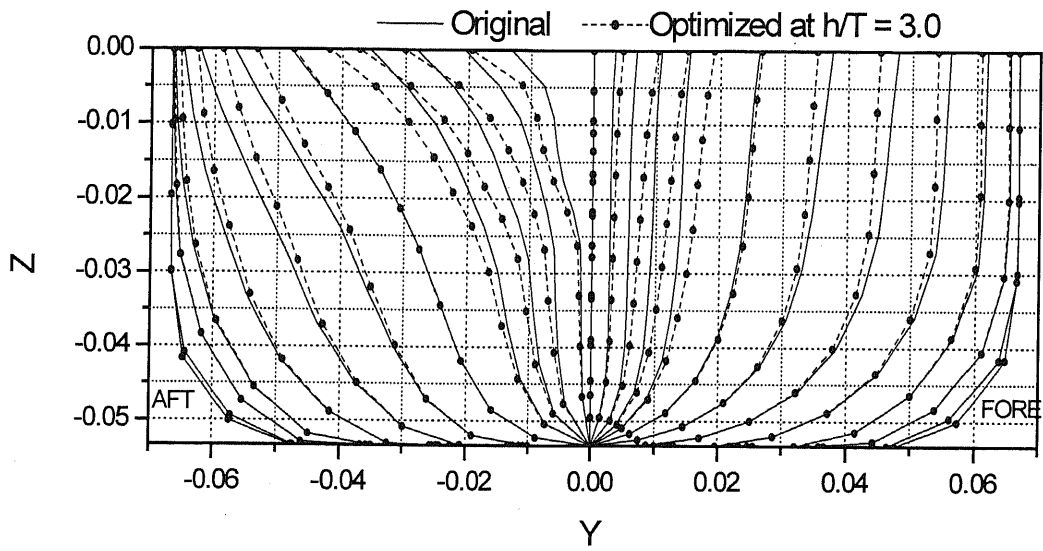
Fig. 4.26 Comparisons of body plans of the Series 60 optimized at $F_n = 0.316$ at depth of water, h/T = 3.0.

Fig. 4.27 Comparisons of body plans of the Series 60 optimized at $F_n = 0.316$ at depth of water, h/T = 3.5.

70

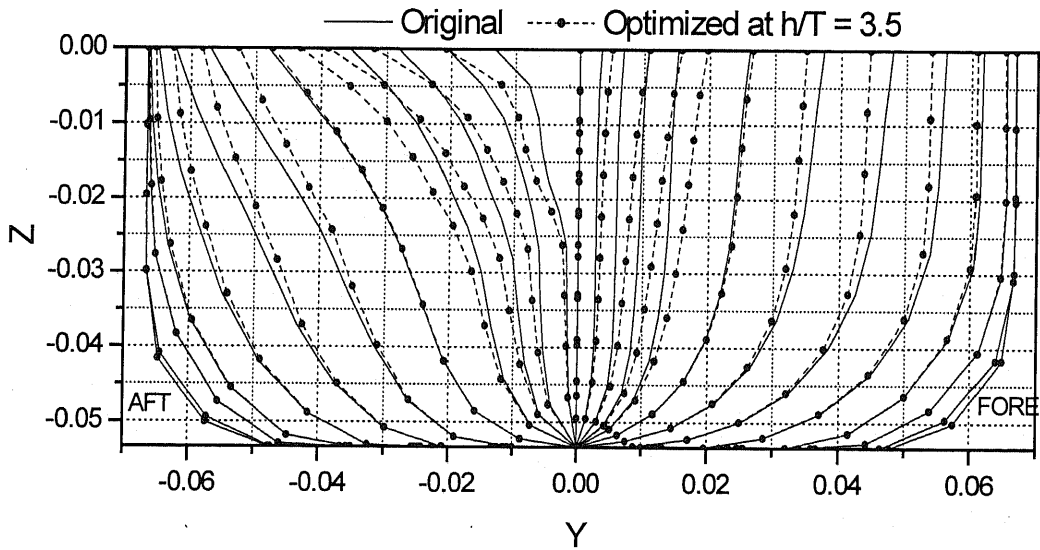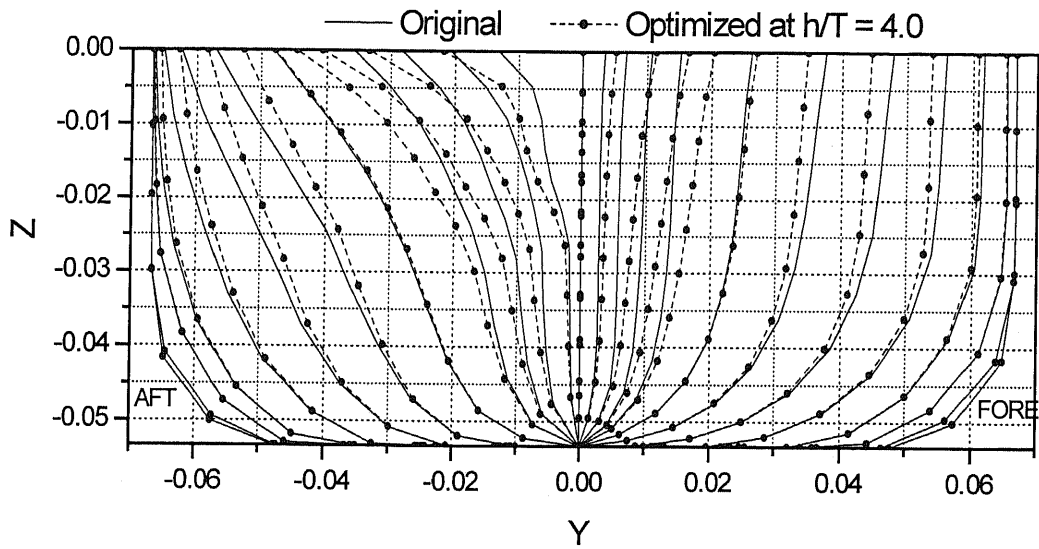Fig. 4.28 Comparisons of body plans of the Series 60 optimized at $F_n = 0.316$ at depth of water, h/T = 4.0.
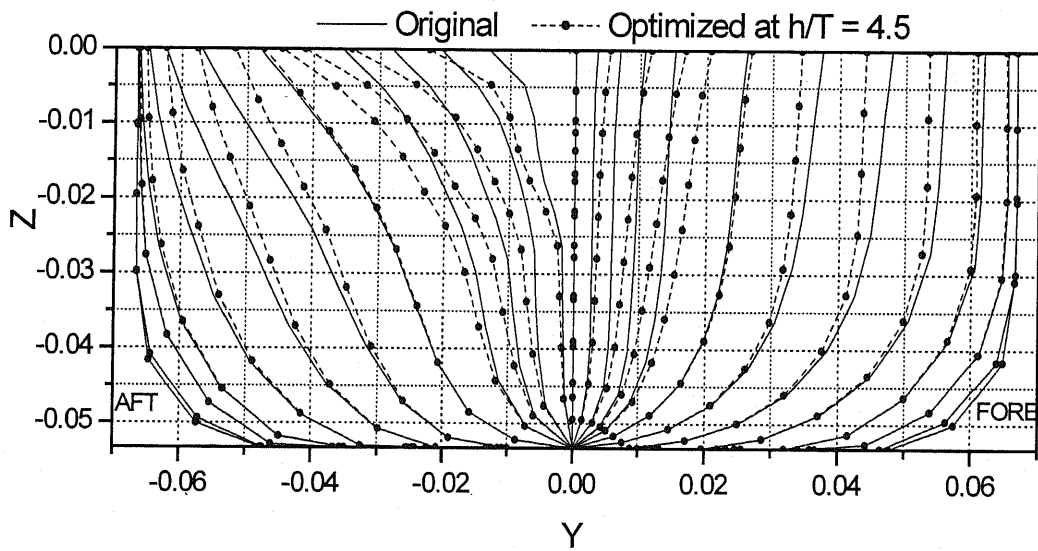
Fig. 4.29 Comparisons of body plans of the Series 60 optimized at $F_n = 0.316$ at depth of water, h/T = 4.5.
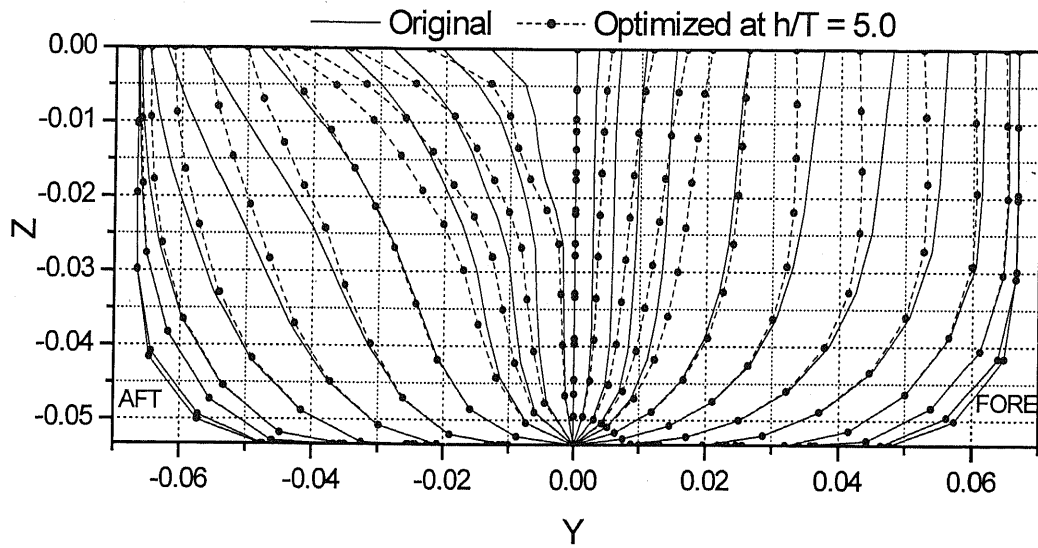
Fig. 4.30 Comparisons of body plans of the Series 60 optimized at $F_n = 0.316$ at depth of water, $h/T = 5.0$
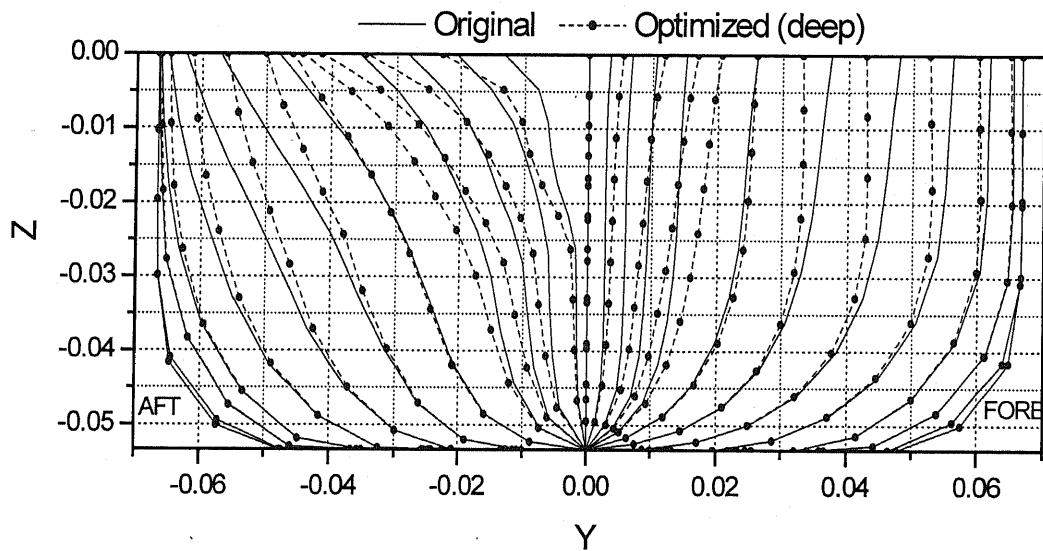
Fig. 4.31 Comparisons of body plans of the Series 60 optimized at $F_n = 0.316$ at deep water.
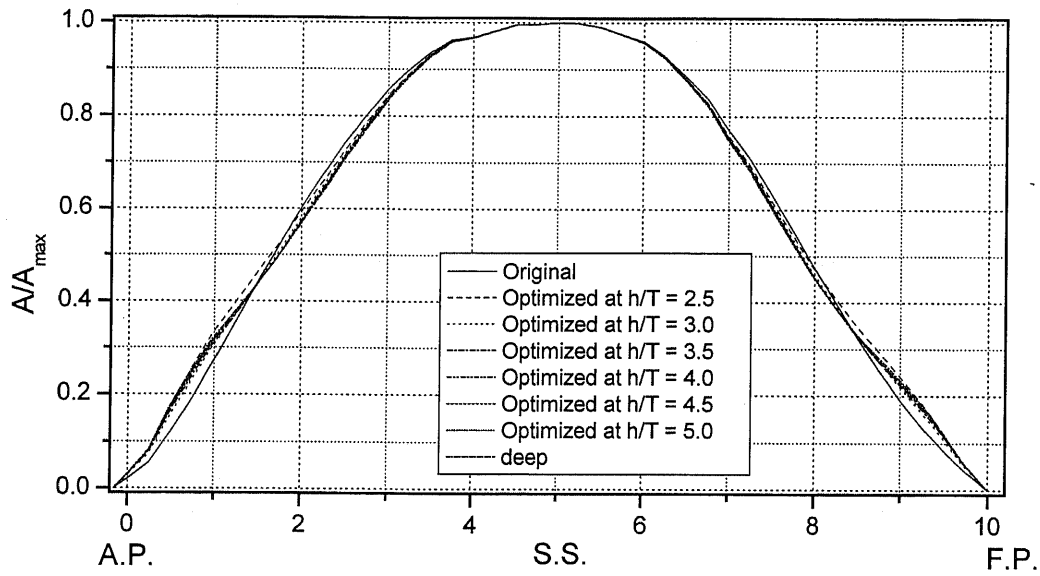
Fig. 4.32 Comparisons of sectional areas of the Series 60 optimized at $F_n = 0.316$ for different depth of water.

Fig. 4.33 Comparisons of wave profiles along the hull of the Series 60 optimized at $F_n = 0.316$ at depth of water, $h/T = 2.5$.

73

Fig. 4.34 Comparisons of wave profiles along the hull of the Series 60 optimized at $F_n = 0.316$ at depth of water, $h/T = 3.0$.
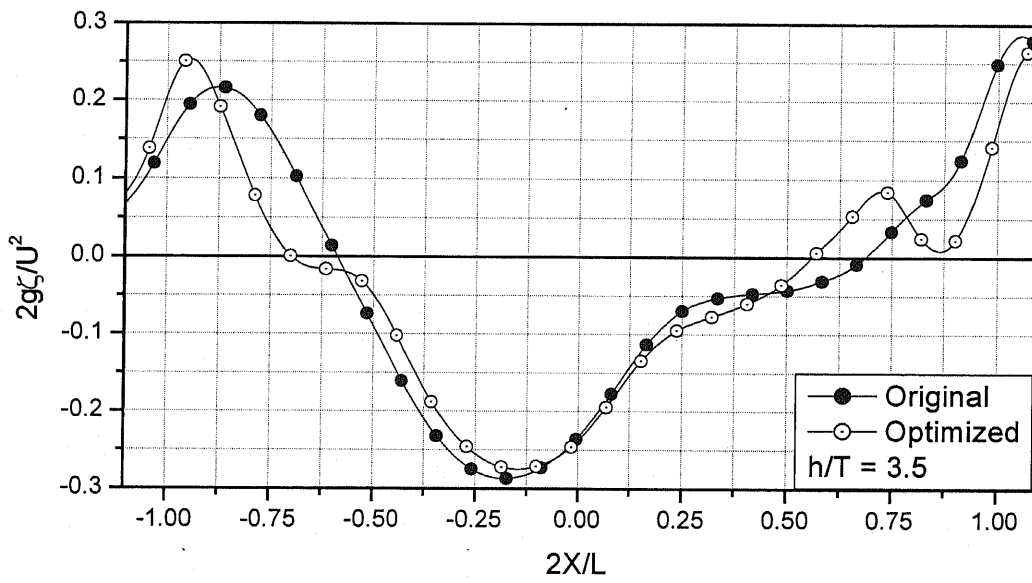
Fig. 4.35 Comparisons of wave profiles along the hull of the Series 60 optimized at $F_n = 0.316$ at depth of water, $h/T = 3.5$.
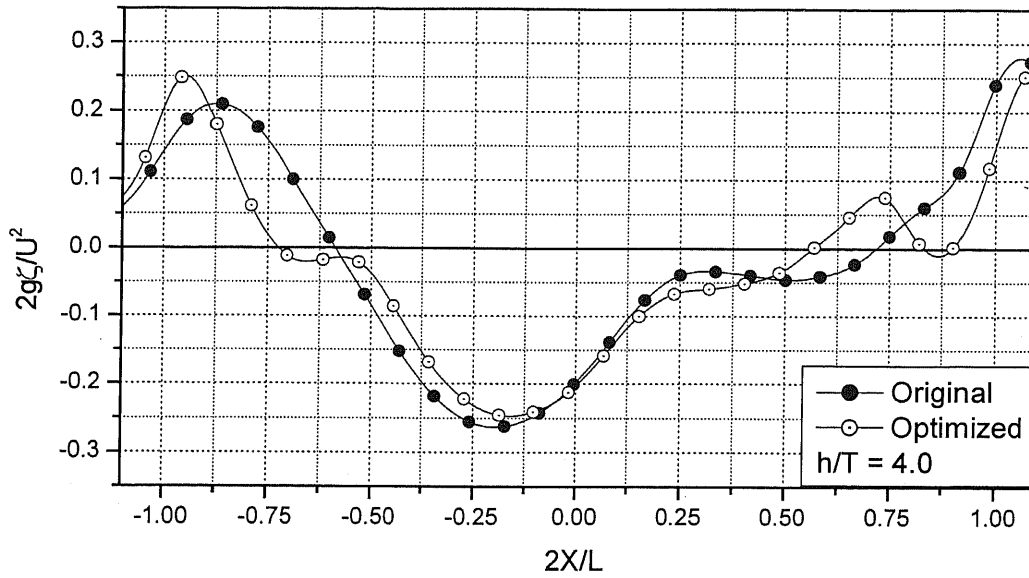
Fig. 4.36 Comparisons of wave profiles along the hull of the Series 60 optimized at
$F_n = 0.316$ at depth of water, h/T = 4.0.
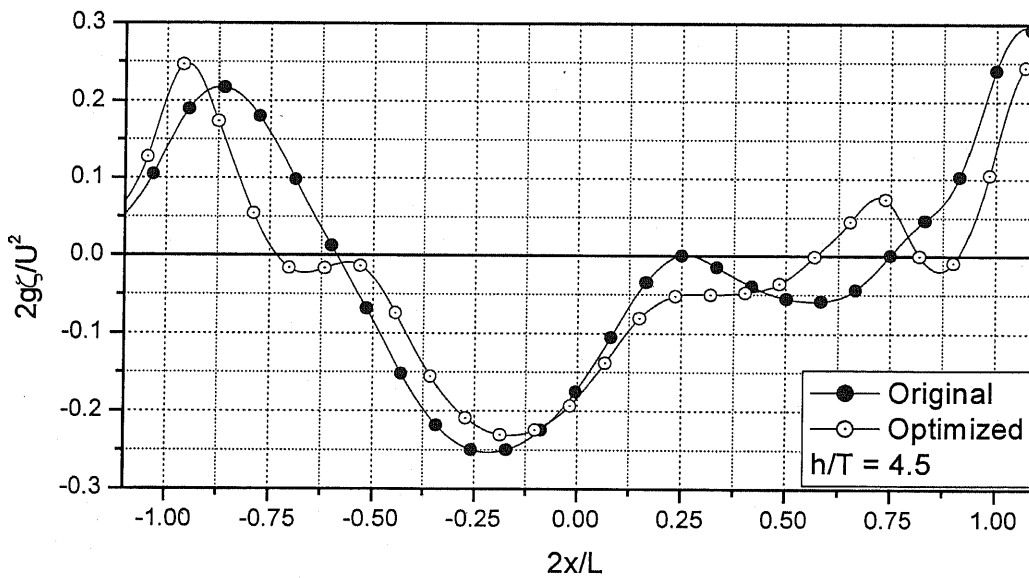
Fig. 4.37 Comparisons of wave profiles along the hull of the Series 60 optimized at
$F_n = 0.316$ at depth of water, h/T = 4.5.
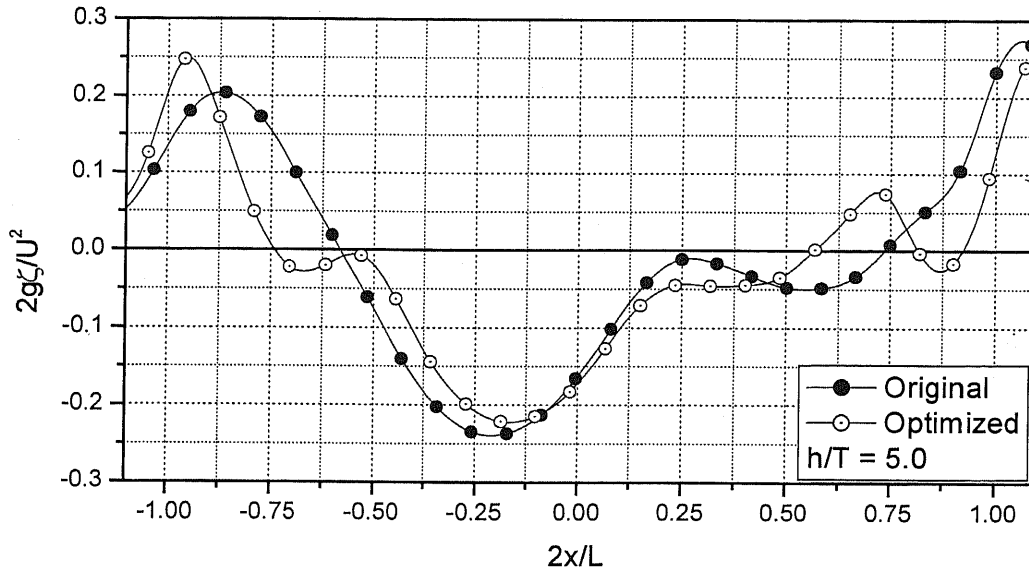
Fig. 4.38 Comparisons of wave profiles along the hull of the Series 60 optimized at $F_n = 0.316$ at depth of water, $h/T = 5.0$.

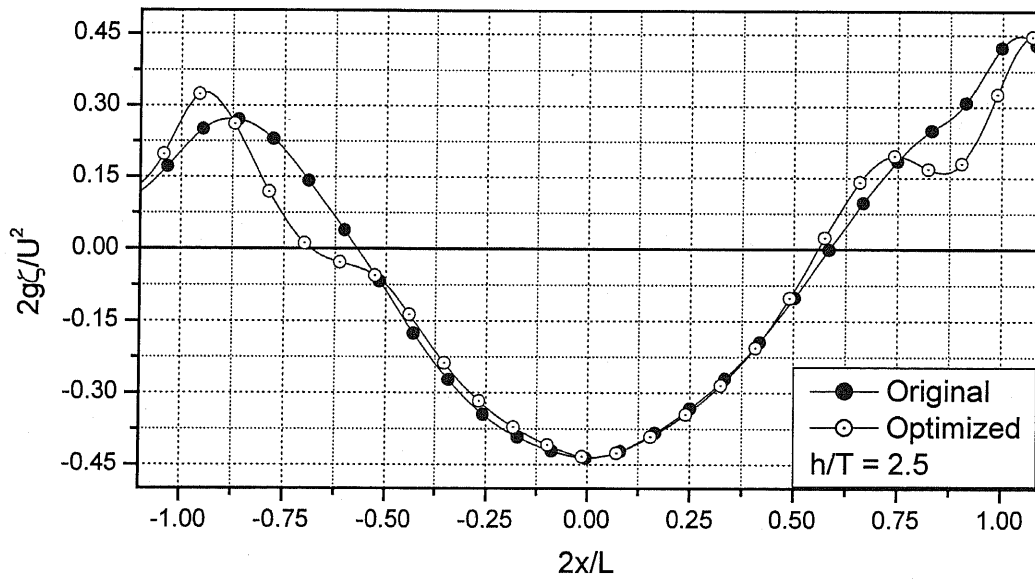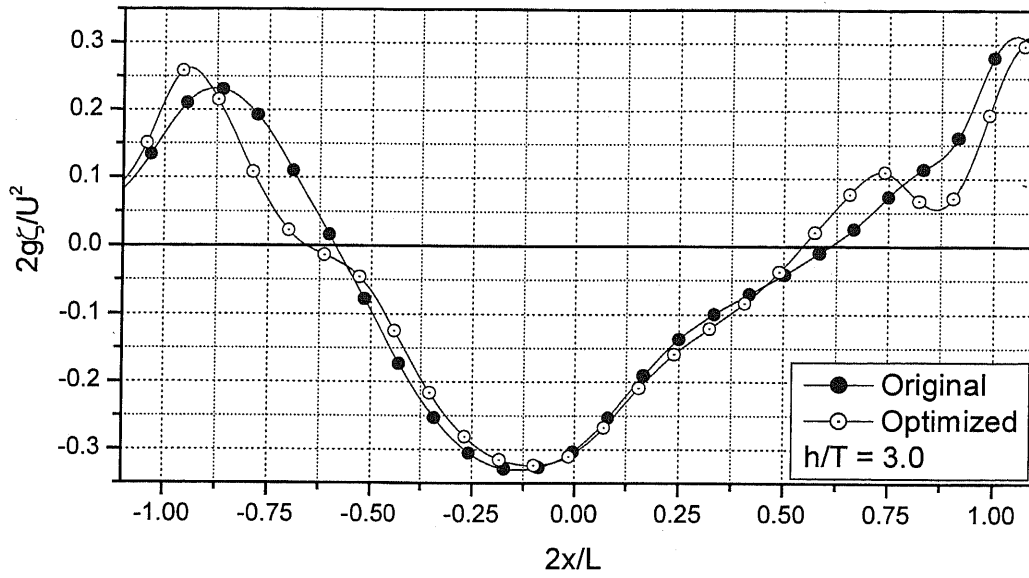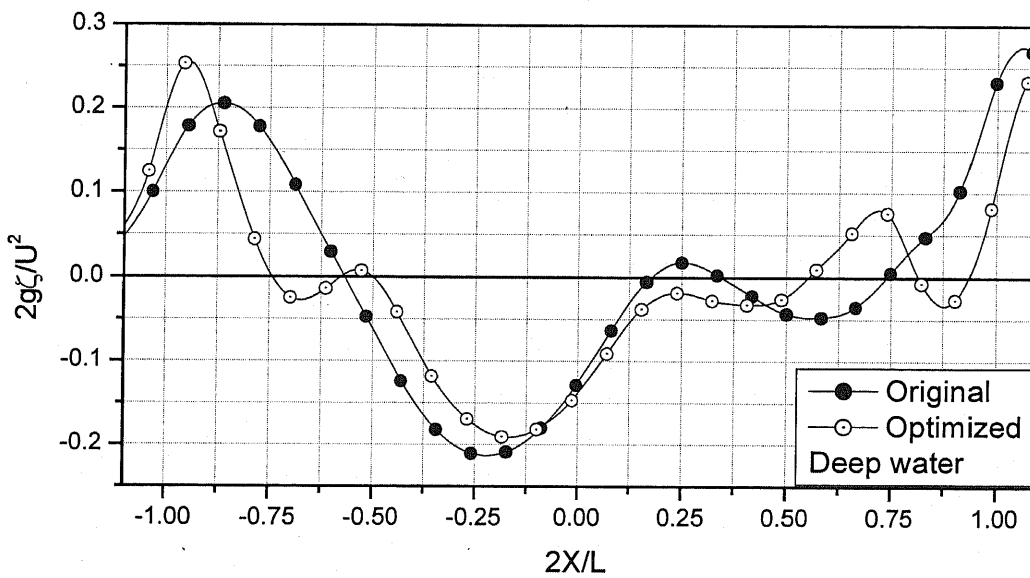Fig. 4.39 Comparisons of wave profiles along the hull of the Series 60 optimized at $F_n = 0.316$ at deep water.

Fig. 4.40 Comparisons of wave patterns ($2g\zeta/U^2$) of the Series 60 hull optimized at
$F_n = 0.316$ at depth of water, h/T = 2.5.
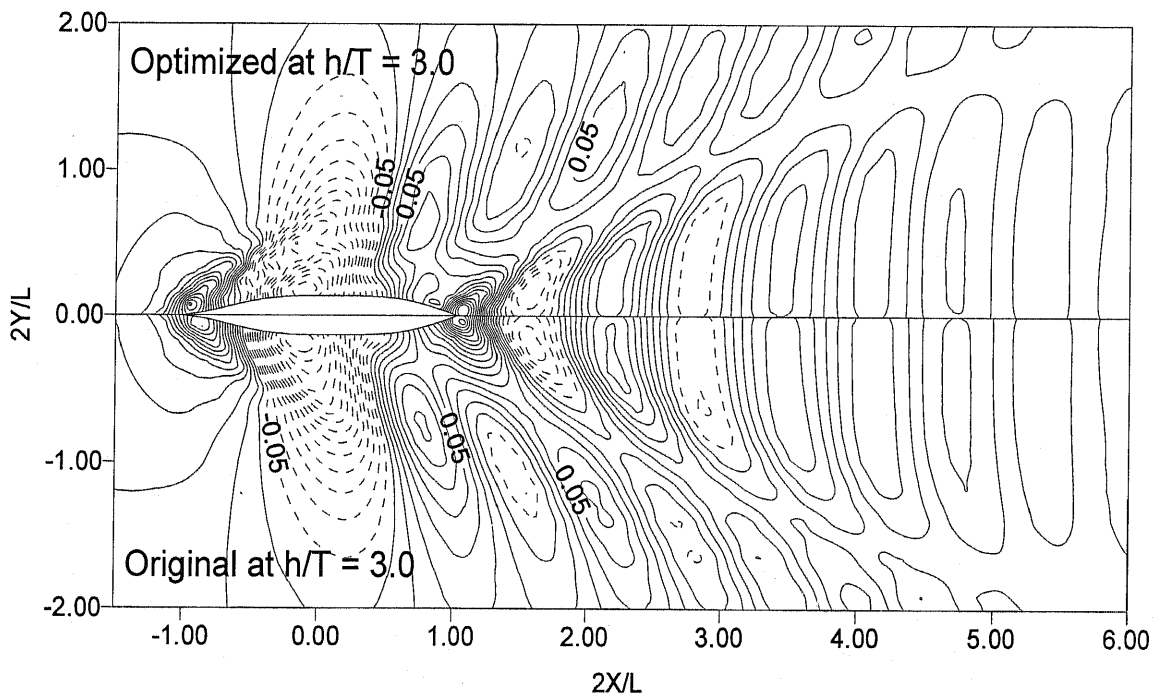
Fig. 4.41 Comparisons of wave patterns ($2g\zeta/U^2$) of the Series 60 hull optimized at
$F_n = 0.316$ at depth of water, h/T = 3.0.
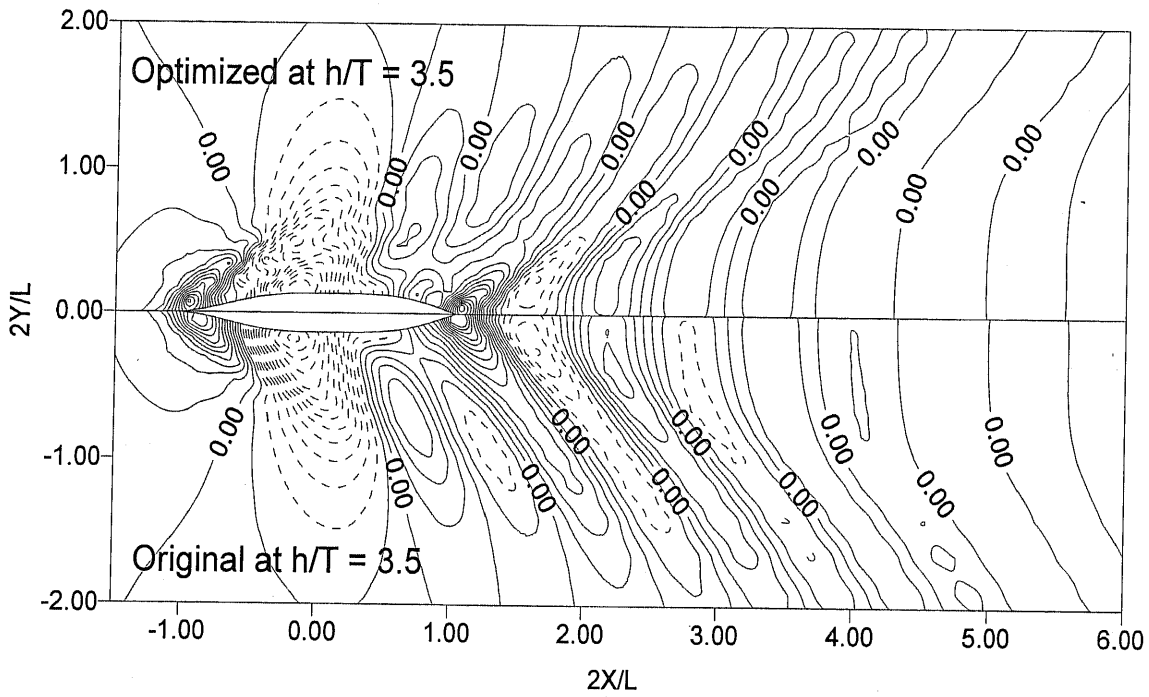
Fig. 4.42 Comparisons of wave patterns $(2g\zeta/U^2)$ of the Series 60 hull optimized at
$F_n = 0.316$ at depth of water, h/T = 3.5.
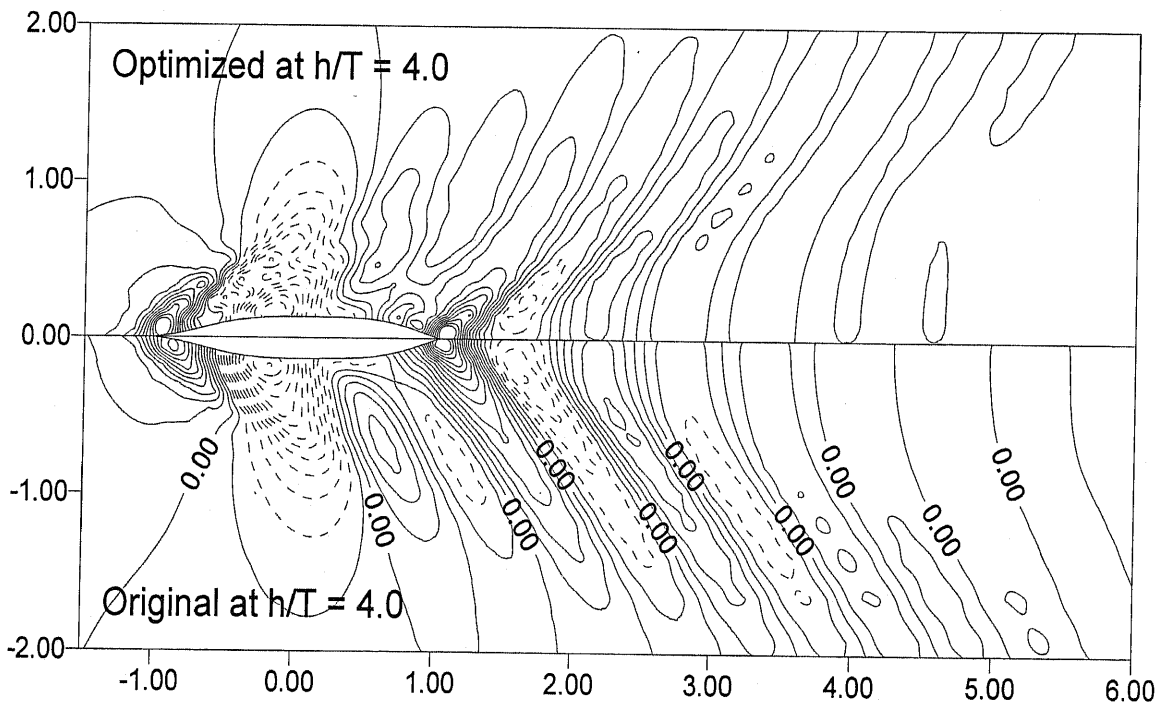
Fig. 4.43 Comparisons of wave patterns $(2g\zeta/U^2)$ of the Series 60 hull optimized at
$F_n = 0.316$ at depth of water, h/T = 4.0.
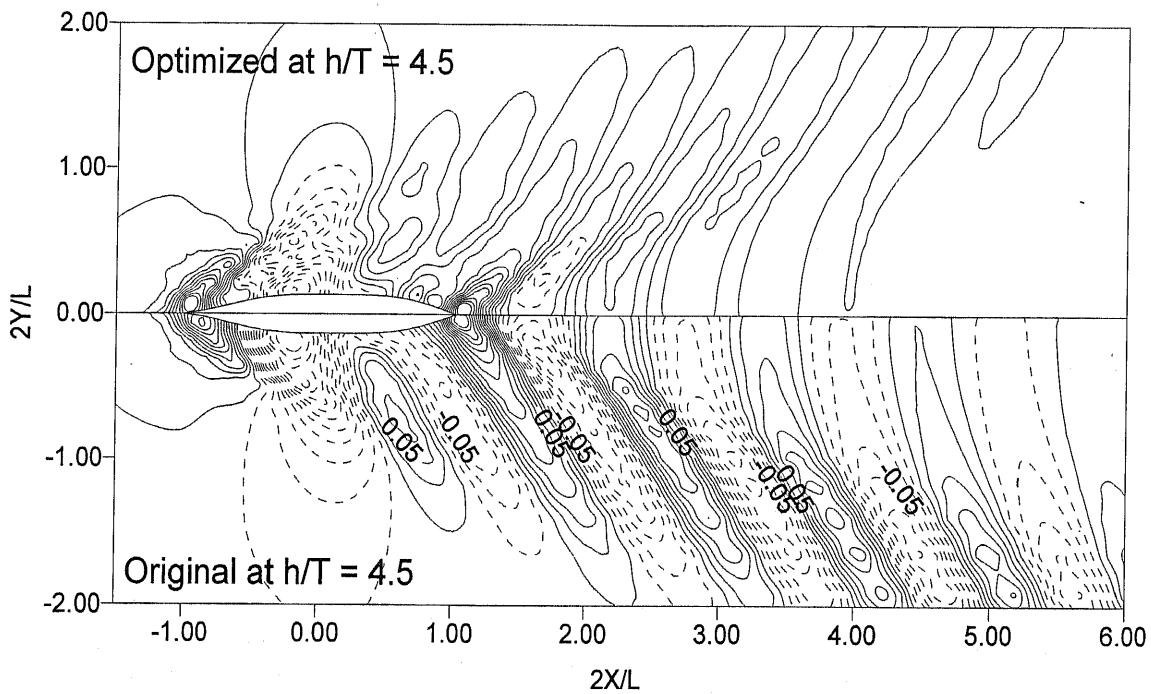
Fig. 4.44 Comparisons of wave patterns ($2g\zeta/U^2$) of the Series 60 hull optimized at
$F_n = 0.316$ at depth of water, h/T = 4.5.
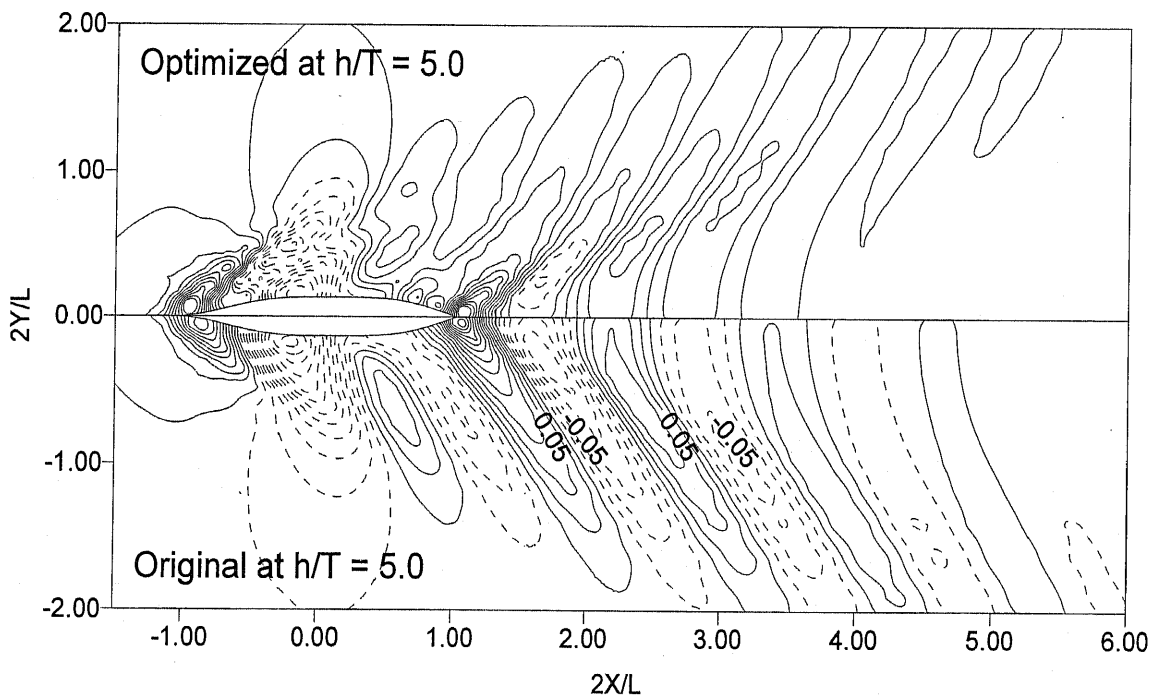
Fig. 4.45 Comparisons of wave patterns ($2g\zeta/U^2$) of the Series 60 hull optimized at
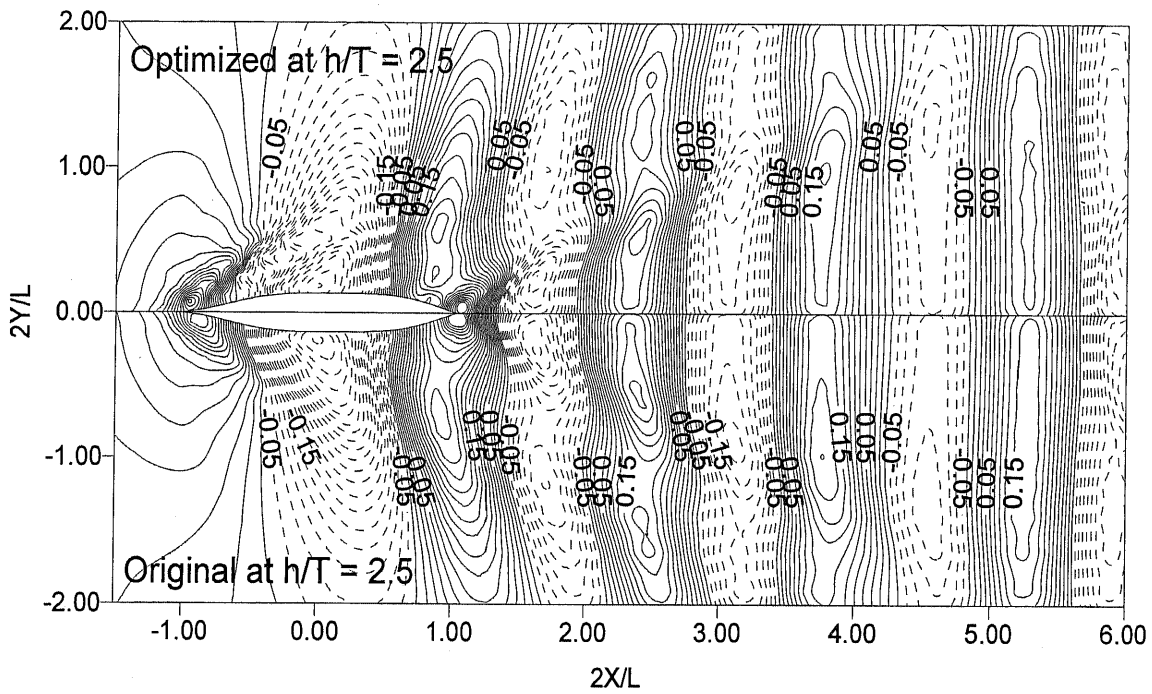$F_n = 0.316$ at depth of water, h/T = 5.0.
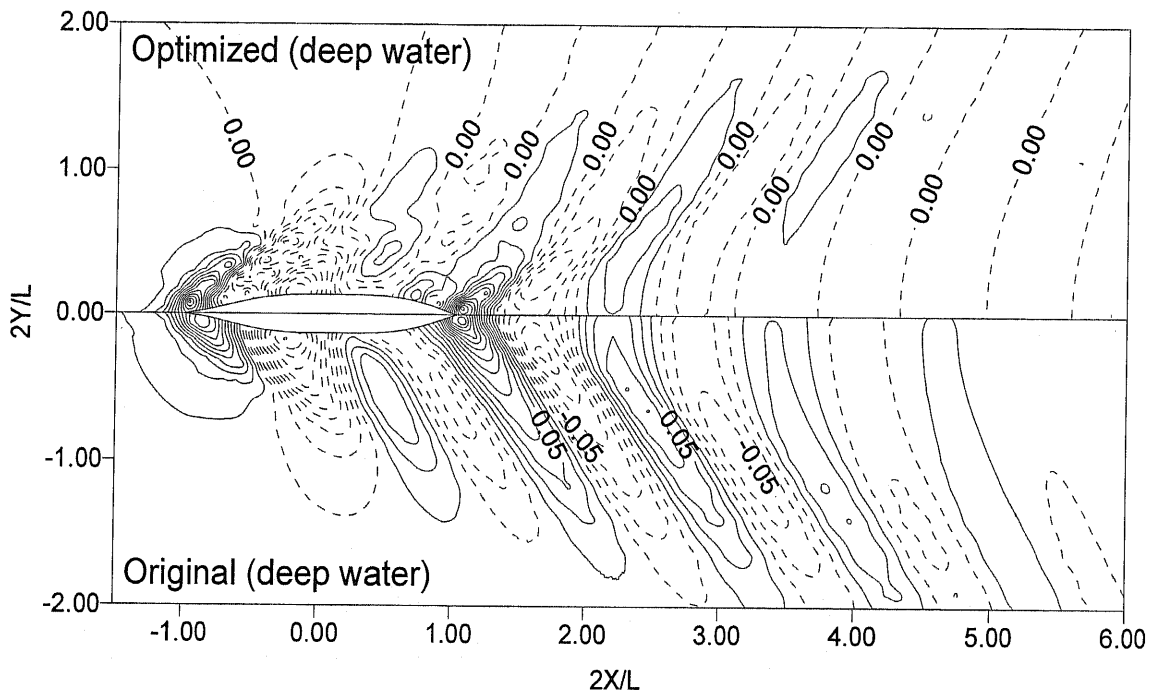
Fig. 4.46 Comparisons of wave patterns ($2g\zeta/U^2$) of the Series 60 hull optimized at $F_n = 0.316$ at deep water.
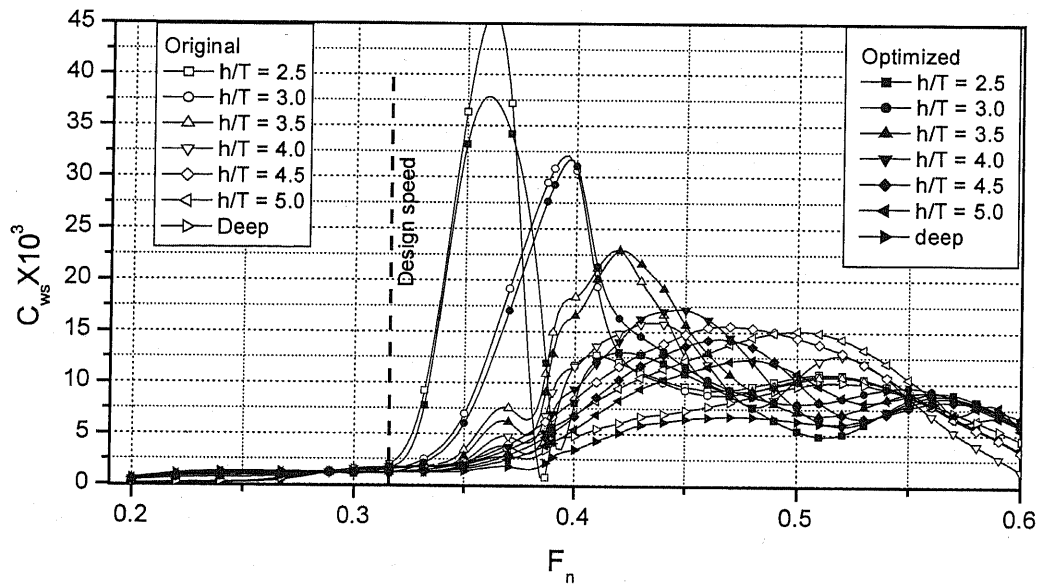
Fig. 4.47 Comparisons of wavemaking resistance of the Series 60 hull optimized at $F_n = 0.316$ for different depths of water.

4.5 Optimization of Catamaran Hull

In the optimization of catamaran ship hull paper, a mathematical hull is employed as demi- hulls of catamarans and airship form bulbs defined from a hydrodynamic point source and a line sink (Thompson, 1968) are employed as large bulbs. The catamaran with airship form bulb configuration is shown in Figure 4.48. For the purpose of fundamental studies, the following simple mathematical hull form is employed as the demi-hulls of catamaran,

$$y = \pm \frac{B}{2} \cos \frac{\pi x}{L} \left\{ 1 - \left(\frac{z}{T} \right)^4 \right\} \tag{4.8}$$

where L, B, and T are length, breath and draft of demi-hulls. In the present case the maximum sectional area of airship bulb is 40% area of the maximum sectional area of both demi-hulls. The principal particulars of Catamaran hull, Airship forms bulbs and design constraints for optimization problem are shown in Table 4.5, 4.6 and 4.7.
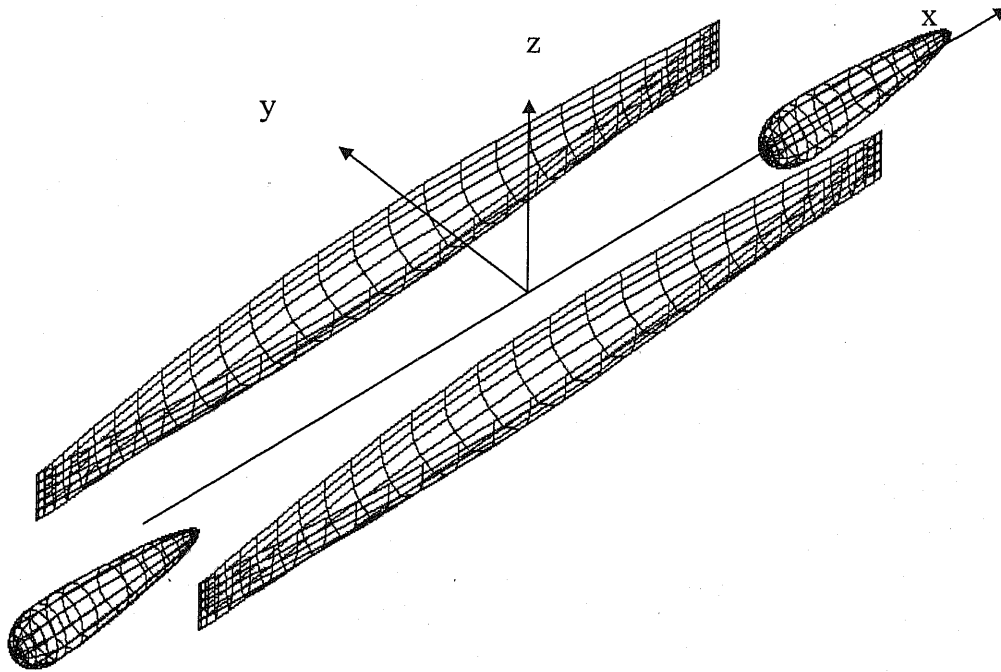
Figure 4.48. Arrangement of Catamaran ship hull with airship forms bulbs

Table 4.5 Principal Particulars of Catamaran Hull

Length, L	1.500 m
Breadth, B	0.1178 m
Draft, T	0.075 m
Volume displacement, ∇	0.006750 m^3
Midship Area, A_M	0.007068 m^2
Midship coefficient, C_M	0.80
Block Coefficient, C_B	0.5093
Prismatic Coefficient, C_p	0.6366

Table 4.6 Principal Particulars of Airship Forms Bulb

Length, L_b	405.55 mm
Maximum Radius, R_{max}	42.5 mm
Volume displacement, ∇_b	0.001244
Maximum Sectional Area, A_{bmax}	0.005654 m^2
Sectional Area Ratio, $A_{bmax}/2A_M$	0.40 (40%)
Point source strength, m	0.0006124 m^3/s
Line sink, 2a	380 mm

The free surface domain for the catamaran hull along the longitudinal direction is $-3.36L \leq x \leq 6.0L$ and along the transverse directions is $-2.80L \leq y \leq 0$ respectively. The number of panel on the ship hull, bow bulb, stern bulb, free surface and wake surface are 2x30x5, 15x6, 15x6, 75x20 and 1x5 respectively. The panel distributions of catamaran hull, bulb40, free surface and wake surface are shown in Figure 4.49. The total number of design variables for catamaran model is 10 (inside part 5 and outside part 5).

Table 4.7 Design Speed and Constraints for Catamaran Hull

Particulars	Constraints
Hull surface	y(x,z) >0
Volume Displacement (∇)	$0.995\nabla_0 < \nabla < 1.005\nabla_0$
F_n	0.45, 0.50

Free Surface

Wake
Surface

x

z

y
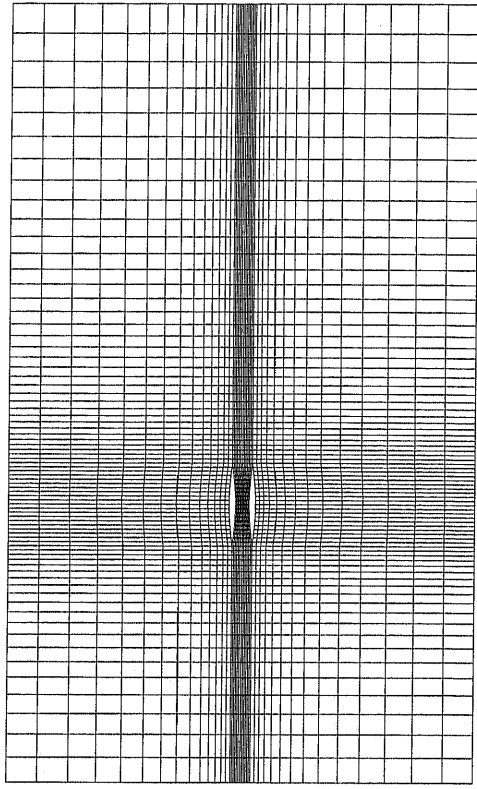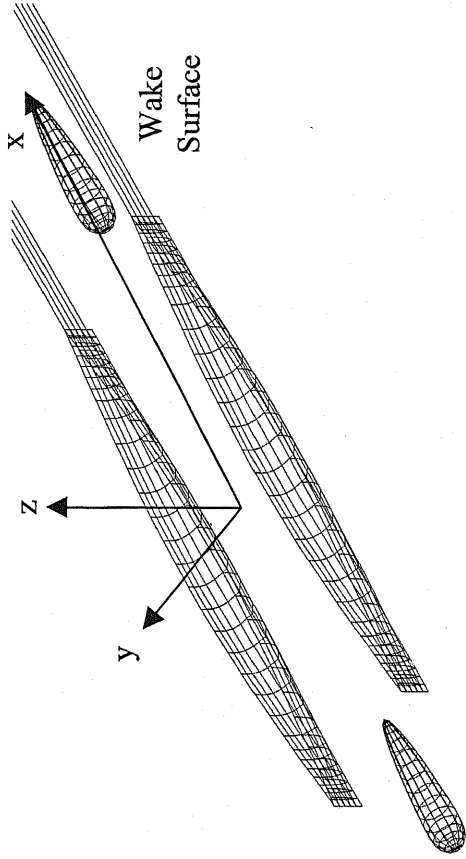
3-D view of Catamaran hull, Airship forms bulbs

● Point Source
— Line Sink

Outline of Bulb 40

0.24L

0.06L
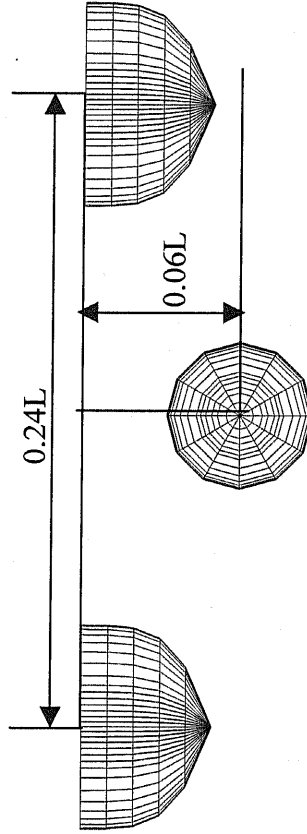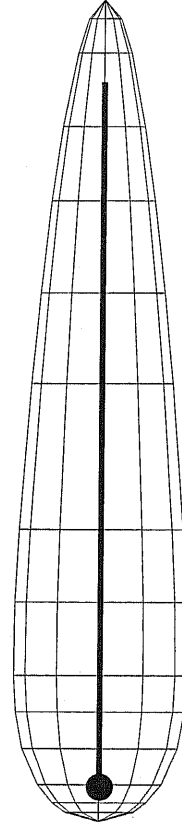
Body Plan of Catamaran hull and Bulb 40

Fig. 4.49 Panel distribution of Catamaran hull, Bulb40, Free surface and Wake Surface

The conventional minimum wavemaking resistance theory shows extremely large bulbs are required to reduce wavemaking resistance for high Froude numbers. In the present case, Bulb 40 means 40% area of maximum sectional of catamaran hulls has been chosen and placed on the center plane of demi-hulls. The bulb position is defined as the position of a point source to form an air ship form. The position of bow bulb is 0.633L from the midship towards the F.P and 0.06L from the water plane in downward direction. The position of stern bulb is 0.466L from midship towards A.P. and 0.06L from the water plane in downward direction. The distance between demi-hulls is 0.24L. The optimization is carried out at two Froude number s0.45 and 0.5, respectively.

Figure 4.50 shows the convergence history of wavemaking resistance of catamaran hull with and without bow and stern bulbs installed on the center plane of demi-hulls at F_n =0.45 and 0.50, respectively. The catamaran hull without bulbs optimized at F_n =0.45 yield converged solution at 10 optimization cycles of SQP process and the wavemaking resistance decreased approximately by 16% of the original value. At F_n = 0.50 the catamaran without center plane bow and aft bulbs, the optimized body is obtained after 10 iteration of SQP process and about 25% reduction of wave resistance is achieved. The wavemaking resistance of the catamaran hulls with bow and stern bulbs at F_n =0.45 was reduced about 28% of the original value of catamaran without bulbs and at F_n = 0.5 was reduced about 40% of the original value of catamaran without bulbs. The catamaran hull with bow and stern bulbs at F_n = 0.45 and 0.50 yield converged solution at 5 and 8 optimization cycles of SQP process, respectively. At Fn = 0.45, the optimized body with bulbs shows about 65 % reduction of wavemaking resistance compared to the original hull without bulbs. The optimized body plans of catamaran hulls at F_n = 0.5 show that about more than 50% reduction of wave resistance is achieved compared to the original value of catamaran without bulbs.

Figure 4.51 and Figure 4.52 show the optimized body (outside and inside) plans of catamaran hulls without bow and stern center plane bulbs of fore and aft part at F_n = 0.45. The frame lines of modified hull (inside part) of catamaran without bulbs become V-shape and the frame lines of outside part of catamaran hulls slightly modified. This is due to the fact that the wavemaking interaction of the inner hull is more significant than the outer hull. Figure 4.53 and Figure 4.54 show the optimized body (outside and inside)

plans of catamaran hulls with bow and stern bulbs installed on center plane of demi-hulls at F_n= 0.45. The frame lines of inside body become U-shape and deformed to streamlined body around F.P. and A.P. The frame lines of outside body become V-shape.

Figure 4.55 and Figure 4.56 show the optimized body plans of catamaran hulls without bulbs at F_n = 0.50 and show similar properties like the frame lines optimized (no bulbs) at F_n = 0.45. Optimized body plans with bulbs at F_n = 0.50 are shown in Figures 4.57 and 4.58 respectively. The inside body frame lines optimized at F_n =0.5 become U-shape and slightly deformed to streamlined body around F.P. and A.P Outside frame lines become U-shape.

Figures 4.59 and 4.60 show the comparison of sectional areas of original and optimized catamaran (inside and outside) with and without center plane bulbs at F_n =0.45 and 0.50 respectively and differences between original and optimized are clearly observed. According to Figure 4.59 and 4.60, the volume displacement of catamaran hull with center plane bow and aft bulbs shifted towards the outside part.

Figure 4.61 shows the non-dimensional wave pattern of original catamaran hulls without (upper) and with (lower) center plane bow and stern bulbs at F_n = 0.45. Figure 4.62 and 4.63 give the calculated non-dimensional wave contours of the original (upper) and optimized (lower) body of catamaran without and with center plane bow and stern bulbs at F_n = 0.45 respectively and the difference of wave fields generated by optimized and original hull with and without center plane bow and aft bulbs are clearly observed. Figure 4.64 shows the non-dimensional wave pattern of original catamaran hulls without (upper) and with (lower) center plane bow and stern bulbs at F_n = 0.5.

Figure 4.65 and 4.66 give the calculated non-dimensional wave contours of the original (upper) and optimized (lower) body of catamaran without and with center plane bow and stern bulbs at F_n = 0.5 respectively and the difference of wave fields generated by optimized and original hull with and without center plane bow and aft bulbs are clearly observed.

Figure 4.67 and Figure 4.68 show the comparison of the wavemaking resistance optimized and original catamaran hulls with and without center plane bow and stern bulbs at F_n=0.45 and F_n = 0.50 respectively. It is seen that the reduction in wave resistance coefficient has been achieved around the design speed but for lower Froude no

the optimized body with bulb shows greater resistance with original one. The optimized body plans of catamaran with and without air ship form bulbs have less wave resistance over the wide range of design speed.
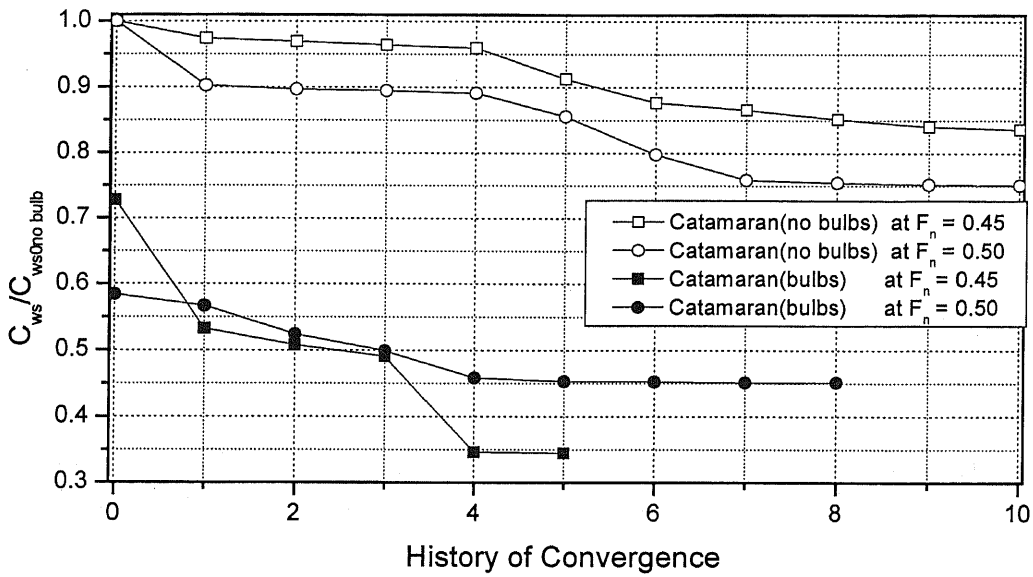
Fig. 4.50 Convergence history of wavemaking resistance of catamaran hulls with and without center plane bow and stern airship form bulbs optimized at $F_n = 0.45$ and 0.50 respectively.
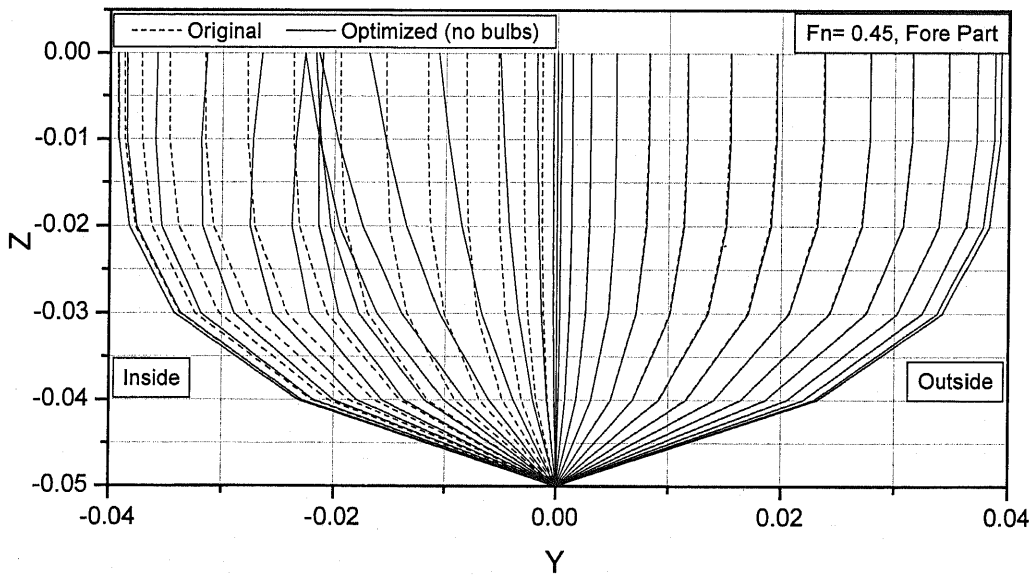
Fig. 4.51 Comparisons of body plans of fore part of catamaran without center plane bow and stern airship form bulbs optimized at $F_n = 0.45$.
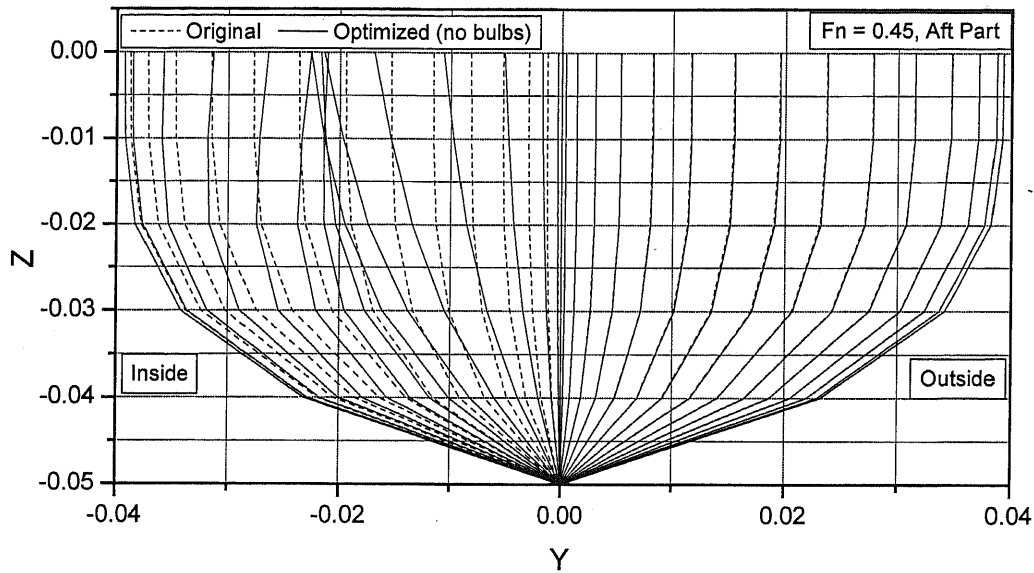
Fig. 4.52 Comparisons of body plans of aft part of catamaran without center plane bow and stern airship form bulbs optimized at $F_n = 0.45$.
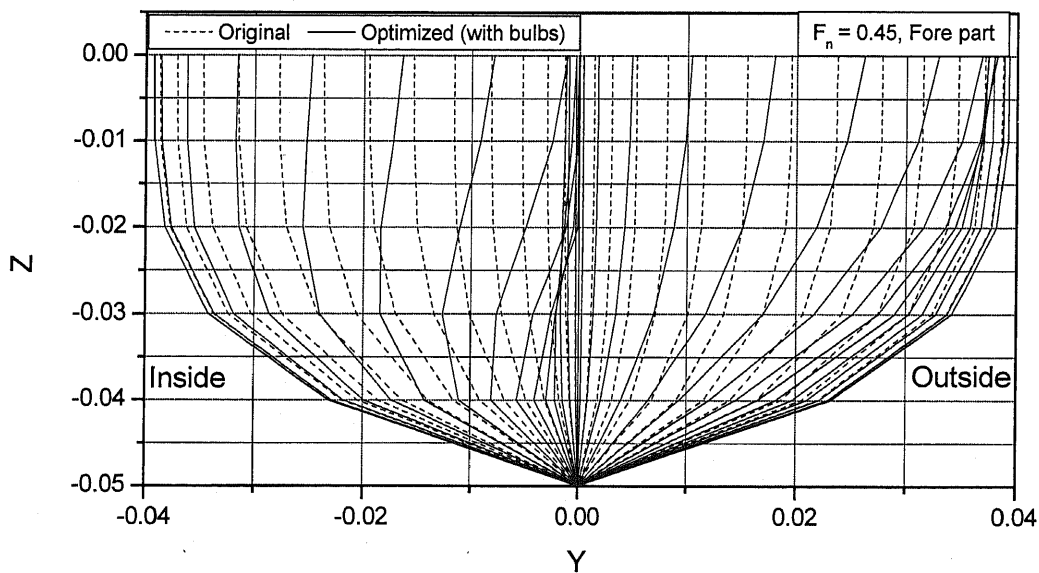
Fig. 4.53 Comparisons of body plans of fore part of catamaran with center plane bow and stern airship form bulbs optimized at $F_n = 0.45$.
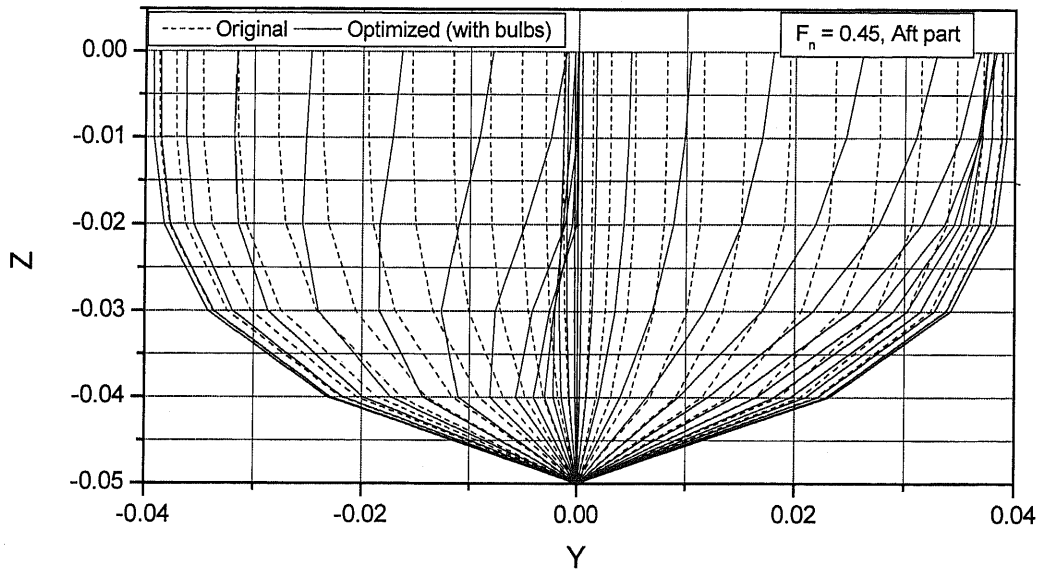
Fig. 4.54 Comparisons of body plans of aft part of catamaran with center plane bow and stern airship form bulbs optimized at $F_n = 0.45$.
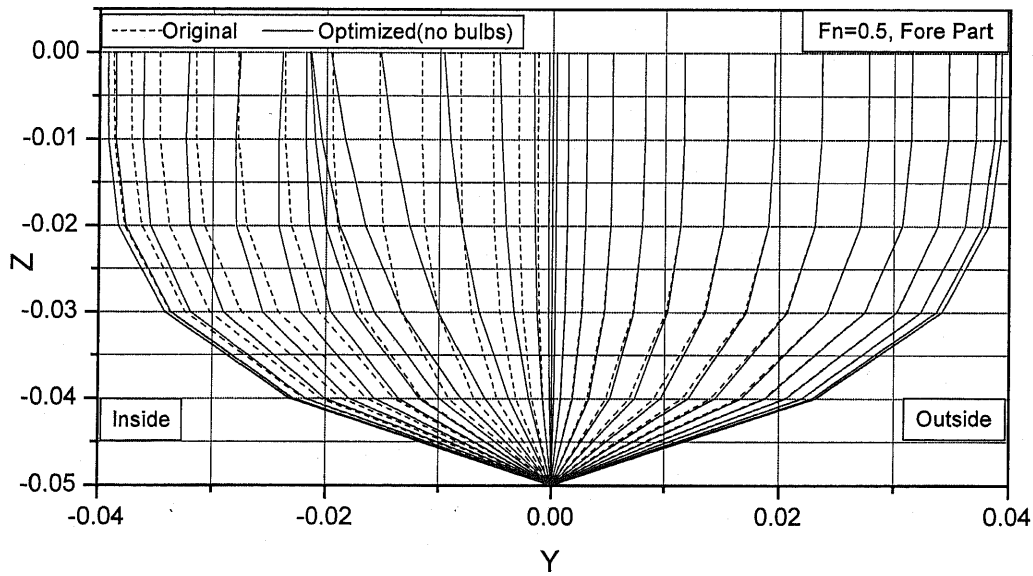
Fig. 4.55 Comparisons of body plans of fore part of catamaran without center plane bow and stern airship form bulbs optimized at $F_n = 0.50$.
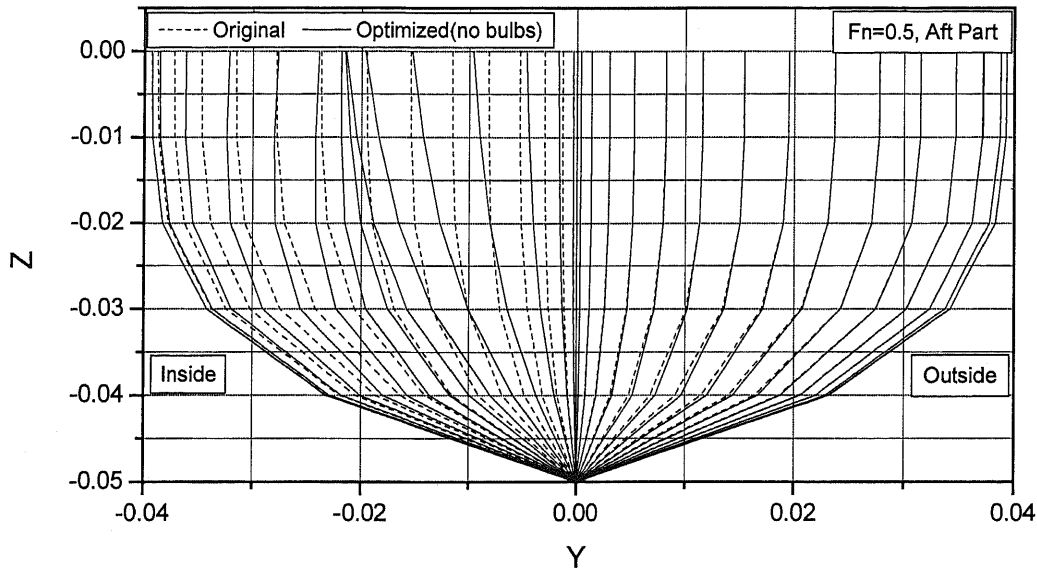
Fig. 4.56 Comparisons of body plans of aft part of catamaran without center plane bow and stern airship form bulbs optimized at $F_n = 0.50$.
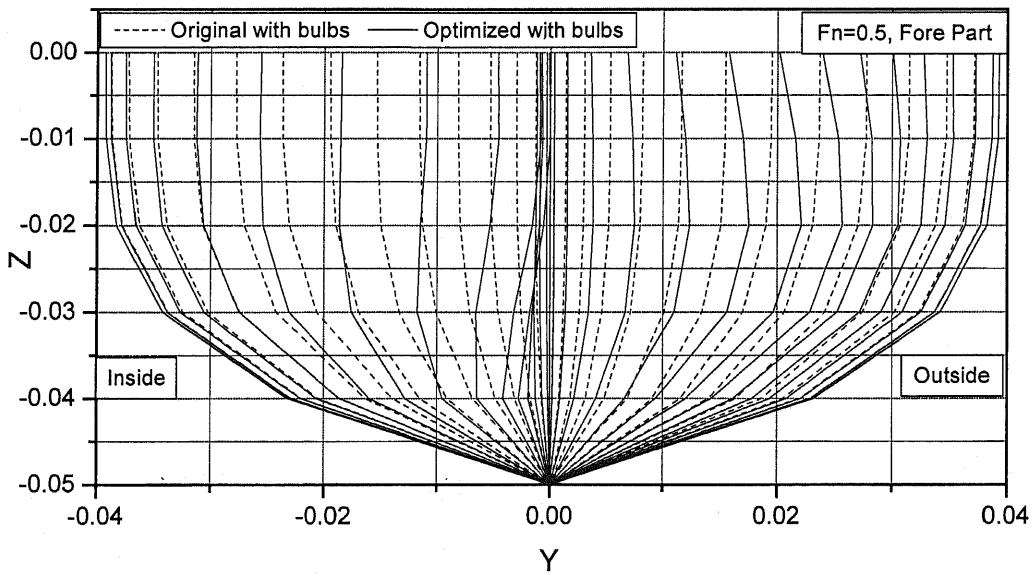
Fig. 4.57 Comparisons of body plans of fore part of catamaran with center plane bow and stern airship form bulbs optimized at $F_n = 0.50$.
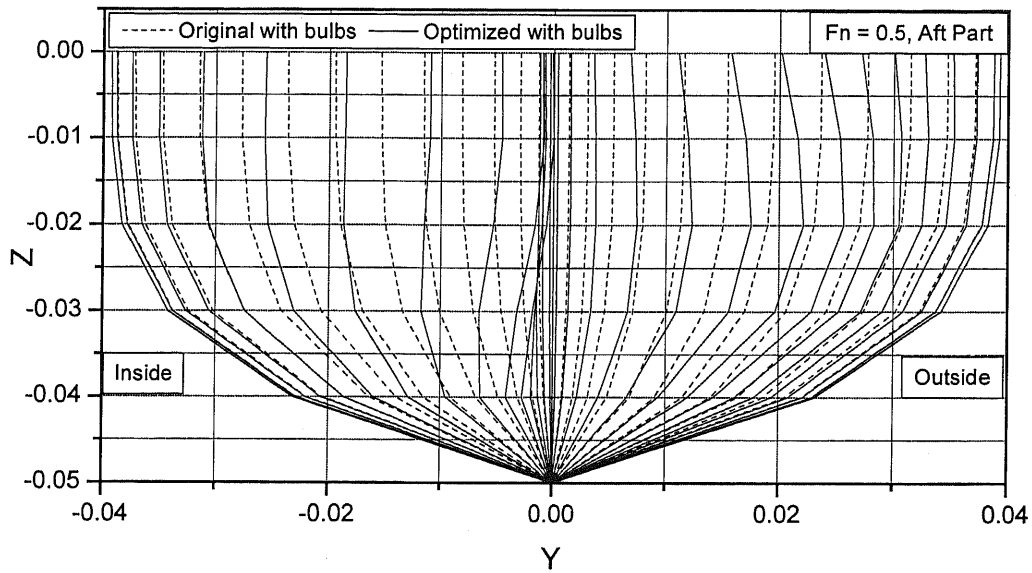
Fig. 4.58 Comparisons of body plans of aft part of catamaran with center plane bow and stern airship form bulbs optimized at $F_n = 0.50$.
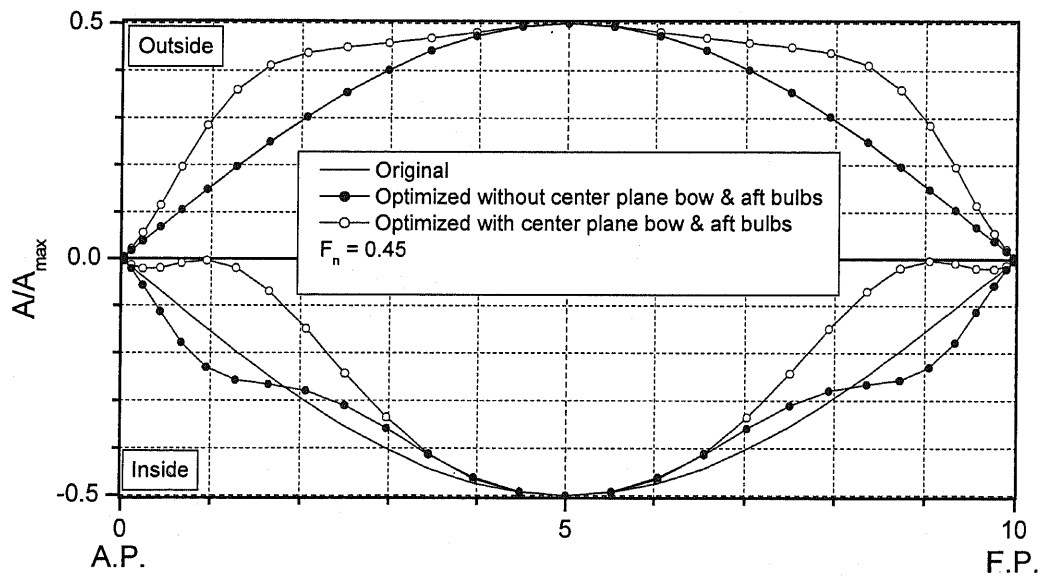
Fig. 4.59 Comparisons of sectional areas of catamaran hull without and with center plane bow and stern airship form bulbs optimized at $F_n = 0.45$.
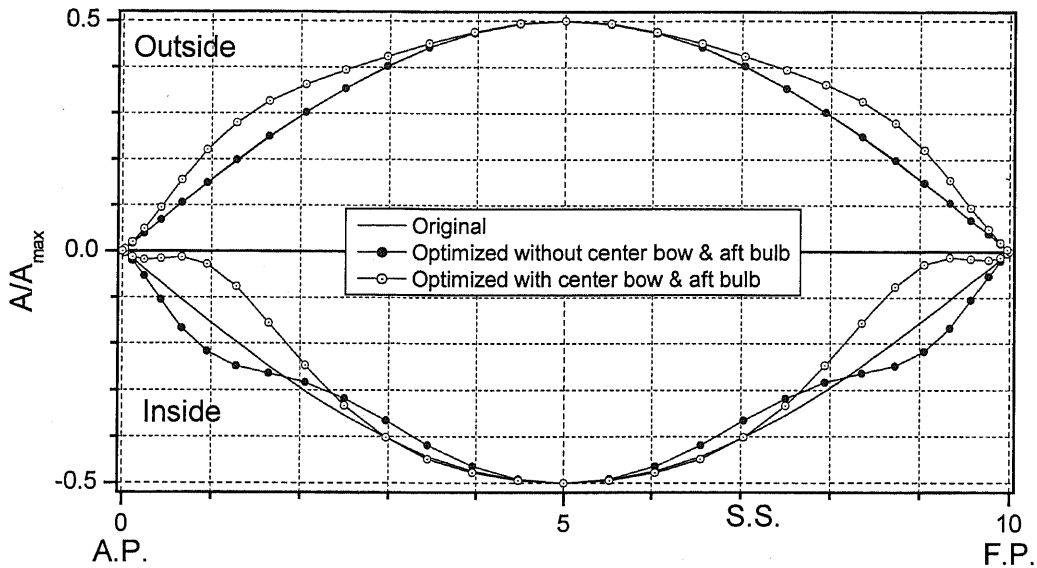
Fig. 4.60 Comparisons of sectional areas of catamaran hull without and with center plane bow and stern airship form bulbs optimized at $F_n = 0.50$.
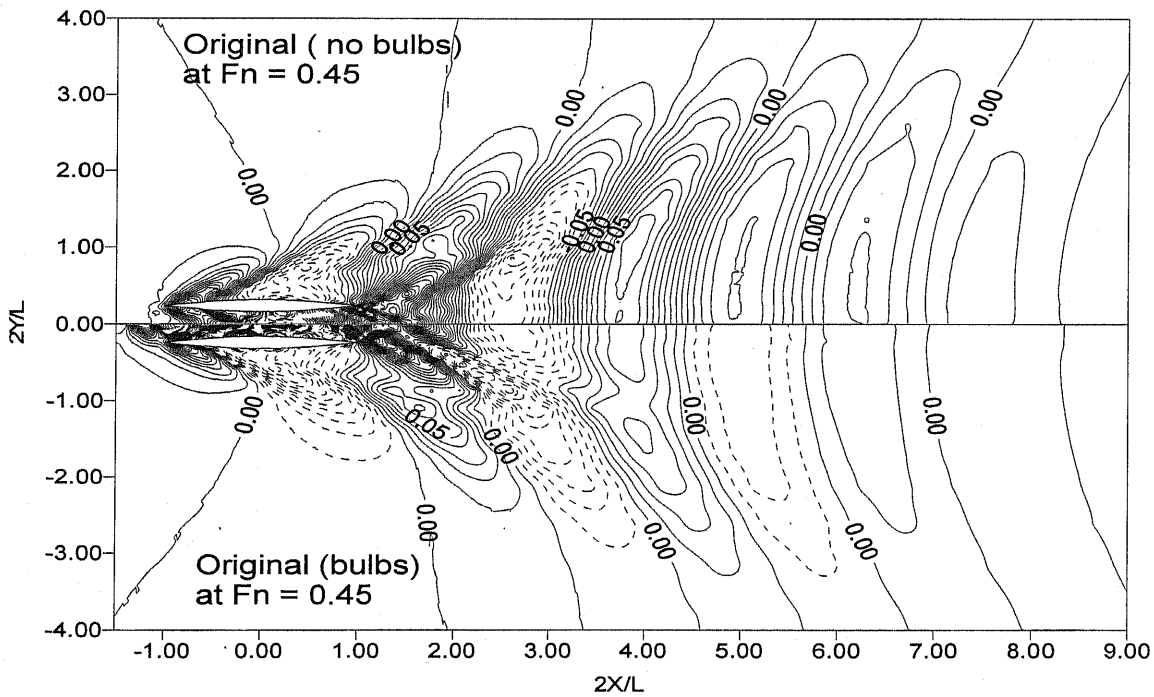
Fig. 4.61 Comparisons of wave pattern ($2g\zeta/U^2$) of original catamaran hull without (upper) and with (lower) center plane bow and stern airship form bulbs at $F_n = 0.45$.

91
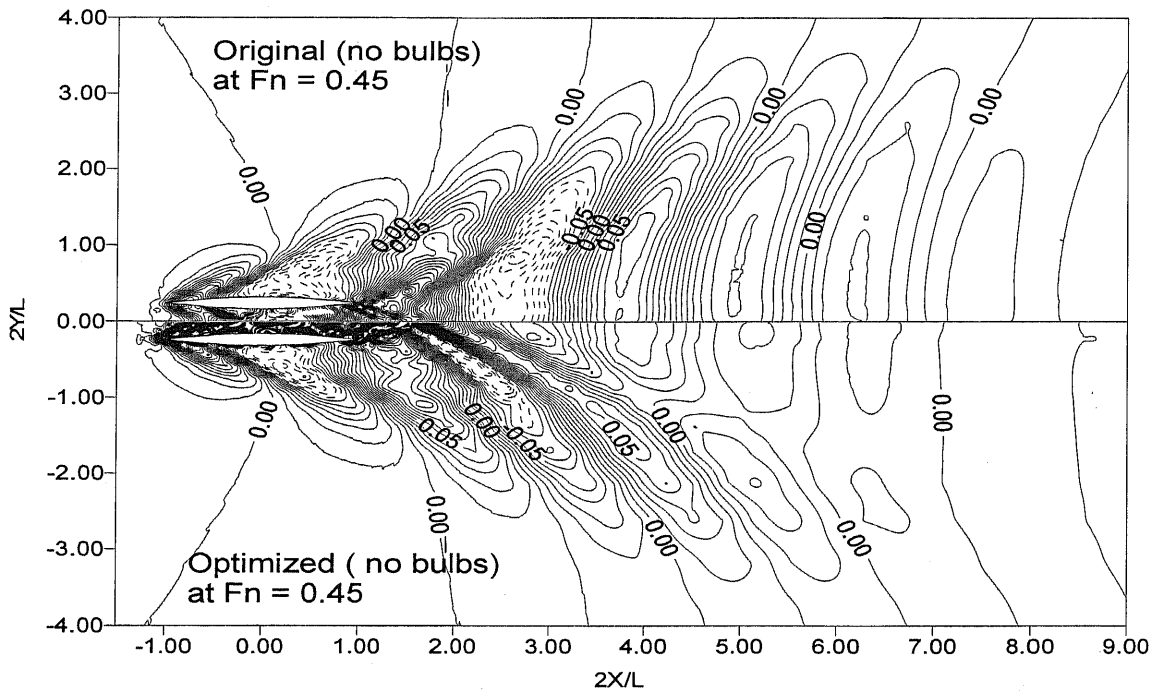
Fig. 4.62 Comparisons of wave pattern ($2g\zeta/U^2$) of original catamaran hull (upper) and modified catamaran (lower) without center plane bow and stern airship form bulbs optimized at $F_n = 0.45$.
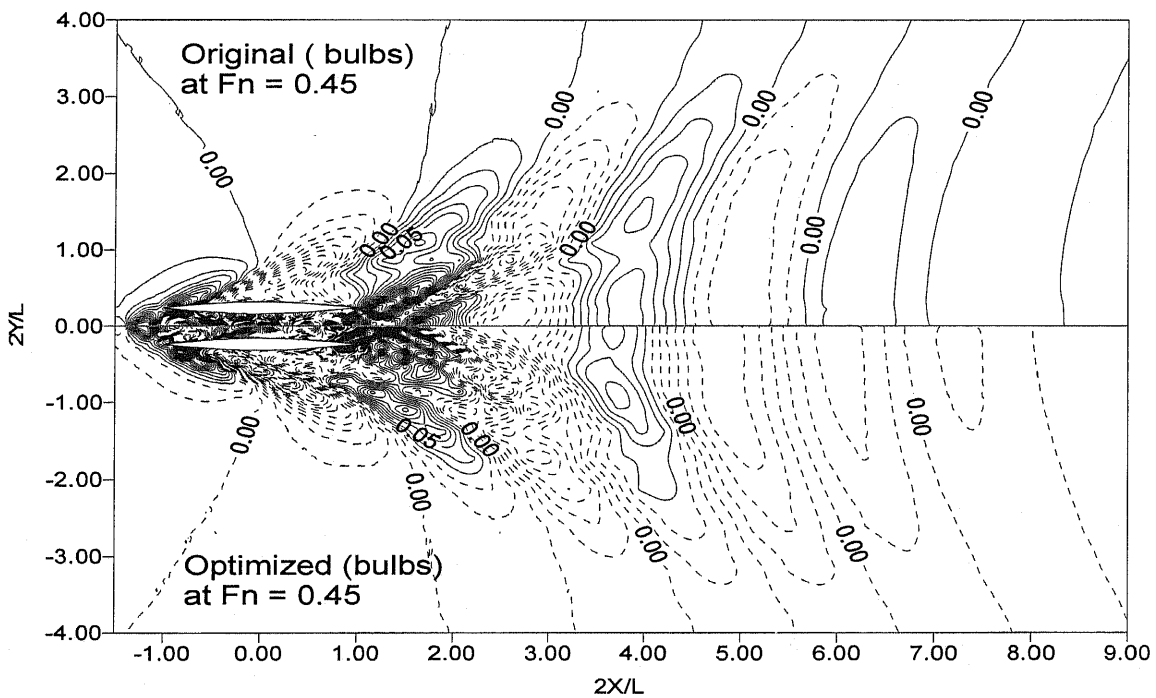
Fig. 4.63 Comparisons of wave pattern ($2g\zeta/U^2$) of original catamaran hull (upper) and modified catamaran (lower) with center plane bow and stern airship form bulbs optimized at $F_n = 0.45$.
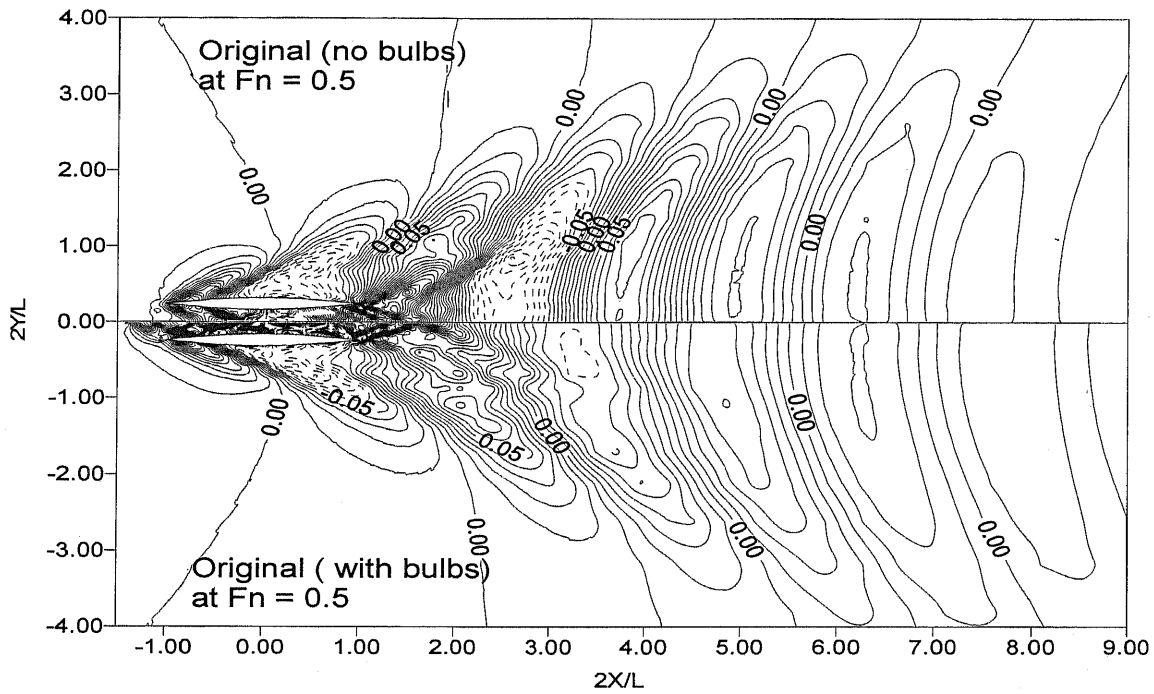
Fig. 4.64 Comparisons of wave pattern $(2g\zeta/U^2)$ of original catamaran hull without (upper) and with (lower) center plane bow and stern airship form bulbs at $F_n = 0.50$.
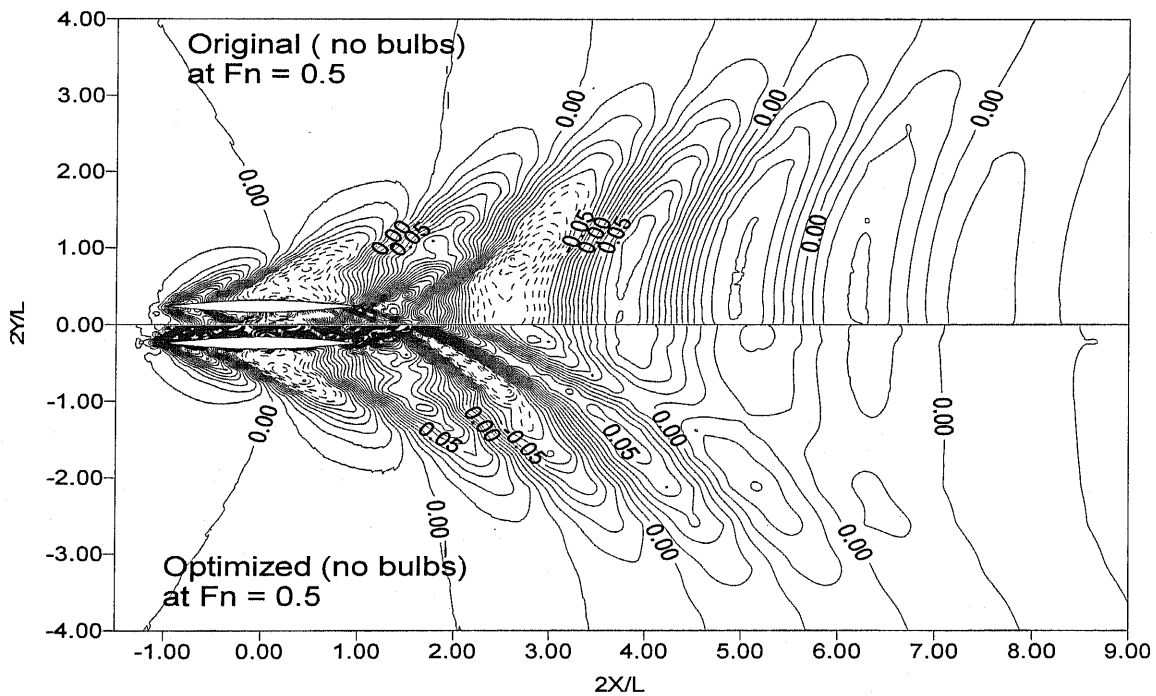
Fig. 4.65 Comparisons of wave pattern $(2g\zeta/U^2)$ of original catamaran hull (upper) and modified catamaran (lower) without center plane bow and stern airship form bulbs optimized at $F_n = 0.50$.
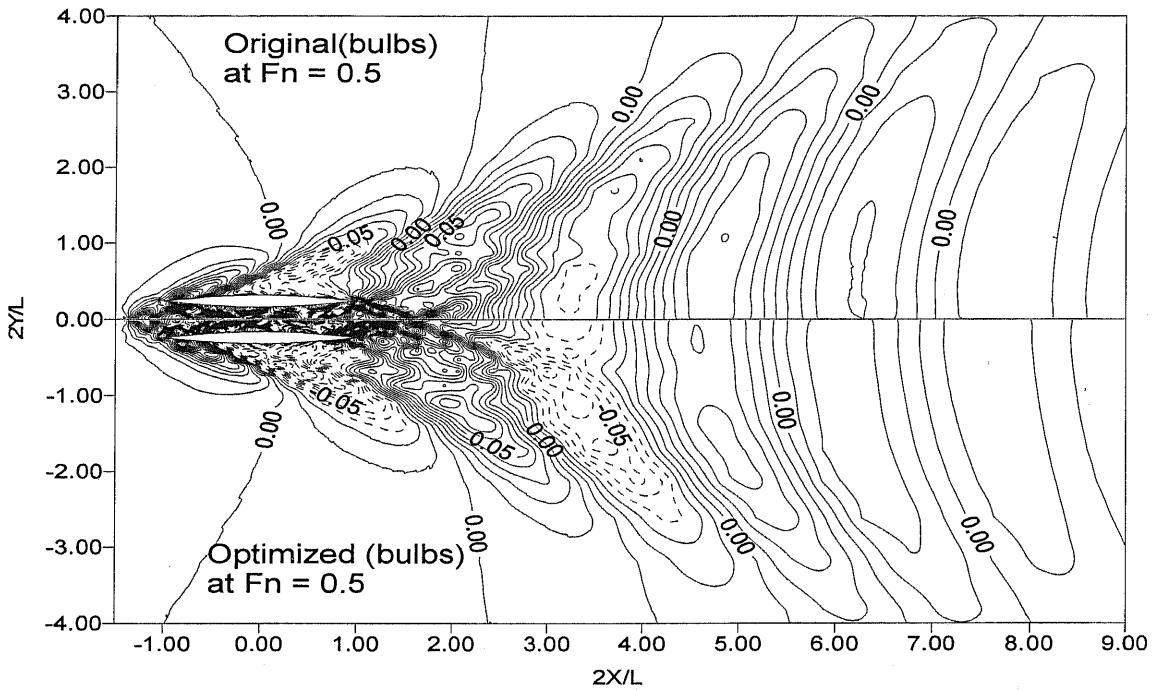
Fig. 4.66 Comparisons of wave pattern ($2g\zeta/U^2$) of original catamaran hull (upper) and modified catamaran (lower) with center plane bow and stern airship form bulbs optimized at $F_n = 0.50$.
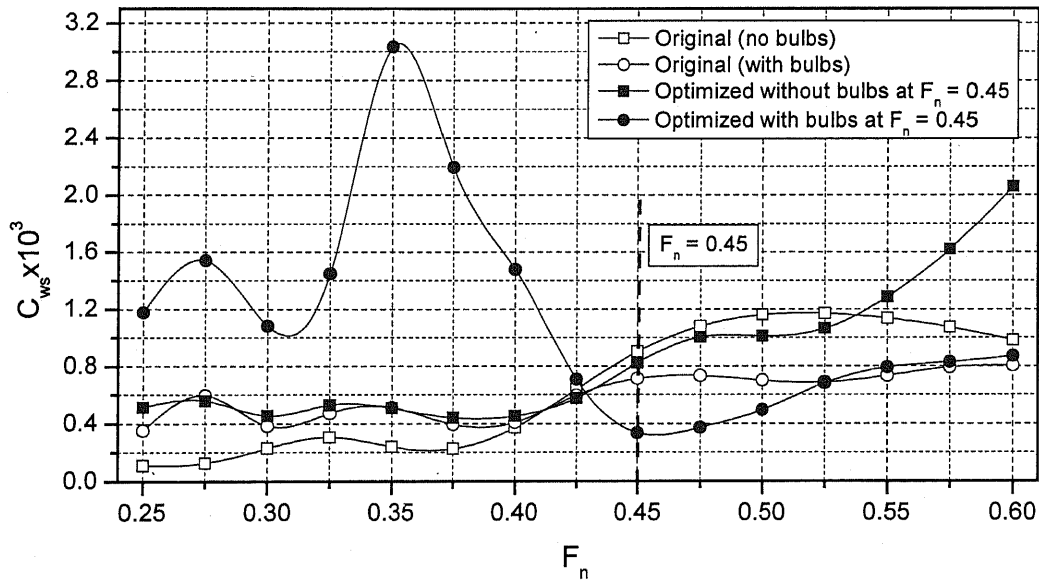
Fig. 4.67 Comparisons of wavemaking resistance original catamaran hull and modified catamaran without and with center plane bow and stern airship form bulbs optimized at $F_n = 0.45$.

94
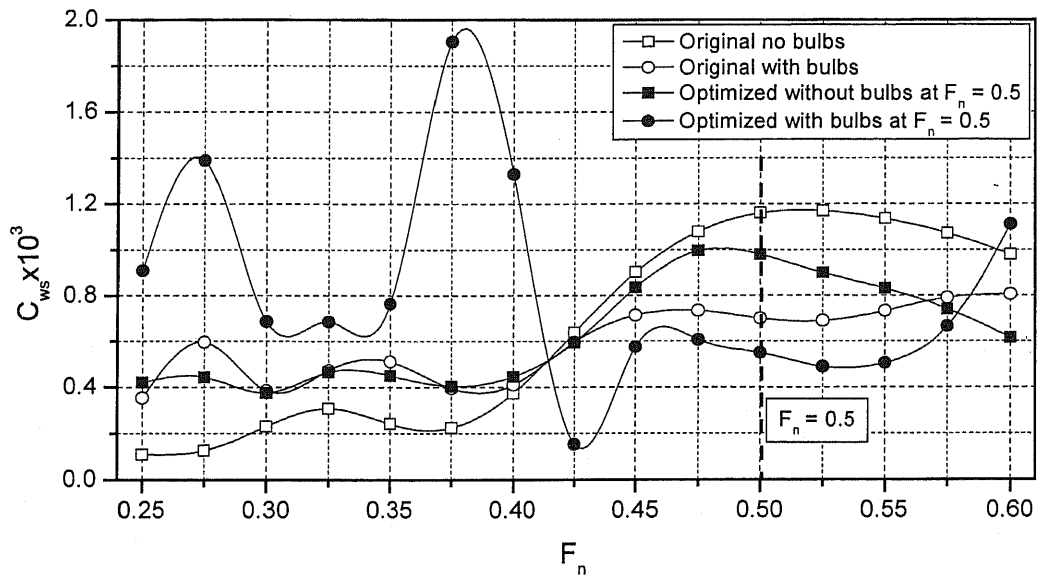
Fig. 4.68 Comparisons of wavemaking resistance original catamaran hull and modified catamaran without and with center plane bow and stern airship form bulbs optimized at $F_n = 0.50$.

Conclusions and Future Works

A numerical method has been proposed for hull form optimization of mono hull (Wigley and Series 60) in shallow water and catamaran hull with airship forms installed on the center plane of catamaran in deep water with respect to wave resistance. Combining the numerical method for solving the three dimensional potential flow around a ship moving at constant speed in calm water in shallow water and deep water with the Sequential Quadratic Programming (SQP) technique, an improved hull form of lower resistance can be generated through a series of iteration computation.

The following conclusion can be drawn from the numerical analysis.

- The optimized body plans of Wigley hull and the Series 60 hull in shallow water show lower resistance with the original ones at all water depths.

- The optimized body plans of Wigley hull and Series 60 hull show lower sinkage with original values at all water depth.

- The sectional area of optimized Wigley hull decreased near amidships region and is increased towards the fore and aft perpendiculars.

- The frame lines of the fore part of modified Series 60 hull become U-shaped. This effectively makes a water plane narrower and moves the volume from upper region to lower region. The frame lines of the aft part of the optimized Series 60 hull become U shape to V-types that's means the water-plane wider than the original hull to compensate a displacement loss at bow part and the volume shift from lower region to upper region.

- The optimized hull both Wigley and Series 60 generates a slightly greater wave height at bow than the original hull. This is due to the increase of steepness of creative waves at the bow. The amplitude of stern waves is lower than the original hull and this is due to the reduction of transverse wave system.

- The modified body of Wigley hull and Series 60 generate small wave height at far field region.

- Significant difference is not observed in the optimized hull forms in deep and shallow waters. This is due to the selection of hull form modification function only in beam-wise direction, not in depth-wise. But in shallow water depth-wise modification is important.

- The modified catamaran hulls in absence of airship form bulb show lower wavemaking resistance than original ones. The optimized catamaran hull with center plane bow and aft airship form bulbs show lower resistance around design Froude number but below Froude number 0.425 show greater resistance than original values.

- The frame lines of modified hull (inside part) of catamaran without bulbs become V-shape and the frame lines of outside part of catamaran hulls slightly modified. The frame lines of inside optimized body plans of catamaran hulls with bow and stern bulbs installed on center plane of demi-hulls become U-shape and deformed to streamlined body around Fore Perpendicular and Aft Perpendicular. The frame lines of outside body become V-shape.

- The volume displacement of optimized catamaran hull with center plane bow and aft bulbs shifted towards the outside part.

From this study, it is seen that the maxima of the wavemaking resistance coefficient for the optimized hull forms (with bulbs) are much bigger than the local maxima of original ones. If the optimized hull form is to be practically meaningful, it is necessary to impose some constraints on the maximum of the object function over the whole range of Froude numbers. . The wavemaking resistance of catamaran hull with bulbs depends on the wavemaking interactions of hulls, the size of the bulb, the relative position of the bulb with respect to main catamaran hull, the wavemaking interaction of bulb etc. Since SQP is based on single object function, and the optimization is carried out at a single Froude number, it is difficult to impose some constraints on the maximum of the object function over the whole range of Froude numbers. The problem will be solved by the use of the multi object function based nonlinear programming technique and the optimized hull forms will be practically meaningful over the whole range of Froude numbers.

The present study is the fundamental study on the fast catamaran hull form design. When the bulb position and the bulbs size are also optimized in the body shape optimization process as will be done as future works, a new concept of fast catamaran operating in high Froude number with extremely small wave resistance can be obtained

The method presented here is only the beginning of the work done in the development of a complete optimum hull form design system. No fairness criteria for hull surface imposed on the optimization process. All the important factors for determining a ship's performance have not yet been incorporated in this system. In particular, it is important in the design of ships that the considerations of propulsion and sea keeping are included at an early design stage. Besides, the determination of the optimal principal particulars of the ship is also an integral part of the design process. Further investigation on shape modification methods and the combination with more complicated flow models such as self-propulsion or sea-keeping analyzes will enable the system to be applicable to practical ship hull designs. Although the presented method has not yet been exploited and tested under enough broad conditions and number of cases, the results point out that the optimization procedure works and that an optimum hull form can be obtained.

The following future works may expected:
- Optimization of practical river ships operating in shallow water
- Optimization of bulb position and bulb size and after that optimization of catamaran ship hull.
- Optimization of ship hull with respect to total resistance (viscous and wavemaking).
- Fairness criteria for ship hull surface should be imposed during the optimization.
- Optimization of submerged ship hull operating near free surface.
- Compare the optimization results with others flow model (Rankine source method, linear wave resistance theory based on thin ship approximation) and others numerical optimization tools.

Bibliography

Ando, J. and Nakatake, K. (2004) A trial to reduce wavemaking resistance of catamaran – Hull form improvement using real-coded genetic algorithm, Transactions of The West – Japan Society of Naval Architects, No. 107, March, pp (1-13) (in Japanese)

ASNOP (1991) research group: Application Systems for Nonlinear Optimization Problems, Nikkan Kogyo Shimbun. (in Japanese)

Bhatti, M. Asghar, (2000) Practical optimization methods with mathematica applications, First edition, Springer –Verlag New York, Inc.

Chun, H. H. and McGregor, R.C. (1991) First and second order forces on Swath ships in waves, Dynamics of Marine Vehicles and Structures in Waves, Elsevier Science Publishers, B.V., pp.65-80.

Dawson, C.W. (1977) A practical computer method for solving ship wave problems, Proceedings of 2nd International Conference on Numerical Ship Hydrodynamics, pp.30-38.

Havelock, T.H. (1922) The effect of shallow water on wave resistance, Proceeding of Royal Society, London, Vol. 100, pp. 499-505.

Hino, T. (1996) Fluid dynamic shape optimization using sensitivity analysis of Navier-Stokes solutions, Journal of Kansai Society of Naval Architects, Japan.

Hino, T., Kodama, Y. and Hirata, N. (1998) Hydrodynamic shape optimization of ships hull forms using CFD, Proceedings of the 3rd Osaka Colloquium on Advanced CFD Applications to Ship Flow and Hull Form Design, Japan, pp.533- 541.

Hoshino, T. (1989) Hydrodynamic analysis of propellers in steady flow using a surface panel method, Journal of the Society of Naval Architects of Japan, Vol. 165, pp. 55-70.

Ikehata, M. and Suzuki, K., (1995) Introduction of airship form bulbs and further studies on its resistance characteristics by means of experiments and Rankine Source method, Proceedings of PRADS95, Vol. 1 pp.12-23.

Kerwin, J., Kinnas, S. A., Lee, J-T, and Shih, W-Z (1987) A surface panel method for the hydrodynamics analysis of ducted propellers, Transactions of the Society of Naval Architecture and Marine Engineers, Vol. 95, pp. 93-122.

Kim, K., Choi, Y., Janson, C. and Larsson, L. (1996) Linear and nonlinear calculations of the free surface potential flow around ships in shallow water, 20th Symposium on Naval Hydrodynamics, pp.408-425.

Kinoshita, M. & Inui, T. (1953) Wavemaking resistance of submerged spheroid ellipsoid and ship in shallow sea, Journal of the Society of Naval Architects of Japan, Vol. 75, pp. 119-135.

Kirsch, M. (1966) Shallow water and channel effects on wave resistance, Journal of Ship Research, pp. 164-181.

Lee, S. J.,(1992) Computation of wave resistance in the water of finite depth using a panel method, Journal of the Society of Naval Architects of Korea, pp.130-135.

Maruo, H. (1966) A note on the higher order theory of thin ships, Bulletin of the Faculty of Engineering, Yokohama National University, Vol.15, pp.1-21.

Maruo, H. and Tachibana, T. (1981) An investigation into the sinkage of a ship at the transcritical speed in shallow water, Journal of the Society of Naval Architects of Japan, Vol. 150, pp.56-62.

Michell, J.H.,(1898) The wave resistance of a ship, Philosophical Magazine Vol.45, pp.106-123.

Milne Thompson, L. M. (1968) Theoretical Hydrodynamics, 5th edition, Macmillan, p.482.

Morino, L., Chen, L.T. and Sucie, E.O., (1974) Steady and oscillatory subsonic and supersonic aerodynamics around complex configurations, AIAA Journal, Vol. 13, No. 3, pp.368-374.

Muller, E., (1985) Analysis of potential flow field and of ship resistance in water of finite depth, International Shipbuilding Progress, Vol. 32, No. 376, pp. 266-277.

Park, K. D. and Suzuki, K., (1998) Numerical analysis of higher order theory based on panel method for free surface flow, Proceedings of ICHD 98, Vol. 1, pp. (97-102), Seoul, Korea.

Newman, J.N.(1977) Marine Hydrodynamics, The MIT press, Massachusetts, pp.290-295.

Newman, J.N., (1978) Advances in Applied Mechanics (Edited by Chia-Shun Yih), Academic Press Inc. Vol.18, pp.222-283.

Ogilve, T.F. and Tuck E.O. (1969) A rational strip theory for ship motions, Part 1, Report No, 013, Department of naval Architecture and Marine Engineering, University of Michigan, Ann Arbor, Michigan, USA.

Peri, D., Rossetti, M. and Campana, E.F. (2001) Design optimization of ship hulls Via CFD technologies, Journal of Ship research, Vol. 45, No.2, pp. 140-149.

Saha, G. K., Suzuki, K., and Kai, H. (2004) Hydrodynamic optimization of ship hull forms in shallow water, Journal of Marine Science and Technology, Vol.9 No. 2, pp. 51-62.

Söding, S.(1997) Drastic resistance reduction in catamarans of staggered hulls, proceedings of FAST'97, pp. 225 - 230.

Suciu, E. O. and Morino, L. (1976) A nonlinear finite element analysis for wings in steady imcompressible flows with wake roll-up, AIAA paper, No. 76-64, pp. 1-10.

Suzuki, K., Kai, H. and Tatsunami, H. (2003) Large bow and stern bulbs installed on center plane of catamaran and their wavemaking characteristics, Proceedings of FAST2003, vol. 2, pp.d2 (1-6), Ischia, Italy.

Suzuki, K., Kai, H. and Tatsunami, H. (2003) Suggestion of catamaran with large bow and stern bulbs on its center plane and numerical analysis of free surface flow, Transactions of The West –Japan Society of Naval Architects, No. 105, March, pp (85-95) (in Japanese)

Suzuki, K., Ikehata, M., Mizutani, N., Inoue, T. and Hosoi, H. (1994) Resistance characteristics of high speed hull form with airship form bulb, Naval Architecture and Ocean Engineering, SNAJ, Vol. 31, pp. 39-48.

Tahara, Y. and Himeno, Y. (1998) An Application of computational fluid dynamics to ship hull optimization problem, Proceedings of the 3rd Osaka Colloquium on Advanced CFD Applications to Ship Flow and Hull Form Design, Japan, pp. 515 -531.

Tarafder, M.D., Suzuki, K. and Kai, H. (2002) Wavemaking resistance of ships in shallow water based on second order free surface condition with sinkage and trim effects, Journal of Kansai Society of Naval Architecture, Japan, No. 237, pp. 9-17, March.

Tarafder, M.D., Suzuki, K. and Kai, H. (2002) Free surface potential flow around multi-hulls in shallow water using a potential based panel method, Journal of Kansai Society of Naval Architecture, Japan, No. 238, pp. 29-38, September.

Timman, R., Hermans, A. J. and Hsiao, G. C. (1985) Water waves and Ship Hydrodynamics, Delft University Press, The Netherlands, pp.71-81.

Timman, R. and Newman, J.N., (1962) The coupled damping coefficients for symmetric ship, Journal of Ship Research, Vol. 5, No. 4, pp. 1-6.

Yasukawa, T. (1989) Calculation of free surface flow around a ship in shallow water by Rankine source method, 5th international Conference on Numerical Ship Hydrodynamics, pp. 643-653.

Zotti, I. (1997) Some experimental investigations into the wave resistance of catamaran hulls, Proceedings of HSMV congress, pp.1-35, -1-44, Sorrento, 18-21, March.

Zotti, I. (2003) Hydrodynamics improvements of catamaran hulls when using streamlined bodies of revolution, Proceedings of FAST2003, vol. 1, pp. a1 (9-18), Ischia, Italy.

Appendices

Appendix A: Transformation of Matrix

The position of the ship relative to x-y-z system is to be determined by means of a vector transformation. For vector α is a structure-fixed system of coordinate the representation of the vector x' in relation to steady moving system x, is found by a linear transformation α of the center of structure to steady moving system and a rotation R according to the following equation (see Figure a1):
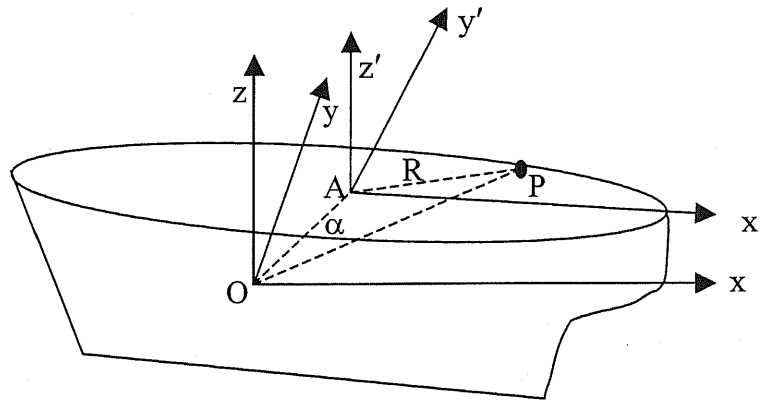
Fig. A1 Definition sketch of a co-ordinate system for transformation of matrix

$$\vec{OP} = \vec{OA} + \vec{AP}$$ (A1)
$$x = \alpha + Rx'$$

in which x' is known relative to the body fixed system of coordinate $x' = (x', y', z')$. In case one is interested in obtaining the vector x' relative to the structure fixed coordinate system for a vector x known in steady moving system, the Equation (A1) is written as

$$x' = R^{-1}(x - \alpha)$$ (A2)

in which R^{-1} is the inversion of the transformation R. The oscillatory motions of the ship are represented by $\xi(\xi_1, \xi_2, \xi_3)$ and $\Omega(\xi_4, \xi_5, \xi_6)$ in which ξ are the displacements of the center of gravity and Ω are the Eulerian angles of ship in space. The Eulerian angles are the measurements of the ship's rotation about the axes, which pass through the center of gravity of the ship. The angular motions due to roll, pitch and yaw are given below:

(a) Rolling: motions about x axis (anticlockwise positive)

$$A = \begin{bmatrix} 1 & 0 & 0 \\ 0 & \cos\xi_4 & \sin\xi_4 \\ 0 & -\sin\xi_4 & \cos\xi_4 \end{bmatrix}$$

(b) Pitching: motions about y axis

$$B = \begin{bmatrix} \cos\xi_5 & 0 & -\sin\xi_5 \\ 0 & 1 & 0 \\ \sin\xi_4 & 0 & \cos\xi_5 \end{bmatrix}$$

(c) Yawing: motion about z axis

$$C = \begin{bmatrix} \cos\xi_6 & \sin\xi_6 & 0 \\ -\sin\xi_6 & \cos\xi_6 & 0 \\ 0 & 0 & 1 \end{bmatrix}$$

The combined transformation matrix below:

$$D = Rx' = CBAx' \tag{A3}$$

$$R = \begin{bmatrix} (\cos\xi_5 \cos\xi_6) & \begin{pmatrix} \cos\xi_4 \sin\xi_6 + \\ \sin\xi_4 \sin\xi_5 \sin\xi_6 \end{pmatrix} & \begin{pmatrix} \sin\xi_4 \sin\xi_6 - \\ \cos\xi_4 \sin\xi_5 \cos\xi_6 \end{pmatrix} \\ -(\cos\xi_5 \sin\xi_6) & \begin{pmatrix} \cos\xi_4 \cos\xi_6 - \\ \sin\xi_4 \sin\xi_5 \sin\xi_6 \end{pmatrix} & \begin{pmatrix} \sin\xi_4 \cos\xi_6 + \\ \cos\xi_4 \sin\xi_5 \sin\xi_6 \end{pmatrix} \\ \sin\xi_5 & -(\sin\xi_4 \cos\xi_5) & (\cos\xi_4 \cos\xi_5) \end{bmatrix}$$

Taking first order quantities after expansion we get

$$R = \begin{bmatrix} 1 & \xi_6 & -\xi_4 \\ -\xi_6 & 1 & \xi_5 \\ \xi_5 & -\xi_4 & 1 \end{bmatrix} + O(\delta^2) \tag{A4}$$

Taking first order and second order quantities we get

$$R = \begin{bmatrix} 1 - \frac{1}{2}(\xi_5^2 + \xi_6^2) & (\xi_6 + \xi_4\xi_5) & (-\xi_5 + \xi_4\xi_6) \\ -\xi_6 & 1 - \frac{1}{2}(\xi_4^2 + \xi_6^2) & (\xi_4 + \xi_5\xi_6) \\ \xi_5 & -\xi_4 & 1 - \frac{1}{2}(\xi_4^2 + \xi_5^2) \end{bmatrix} + O(\delta^3) \tag{A5}$$

105

After the decomposition of the above matrix

$$R = \begin{bmatrix} 1 & \xi_6 & -\xi_5 \\ -\xi_6 & 1 & \xi_4 \\ \xi_5 & -\xi_4 & 1 \end{bmatrix} - \frac{1}{2}\begin{bmatrix} \left(\xi_5^2+\xi_6^2\right) & 0 & 0 \\ -2\xi_4\xi_5 & \left(\xi_4^2+\xi_6^2\right) & 0 \\ -2\xi_4\xi_6 & -2\xi_5\xi_6 & \left(\xi_4^2+\xi_5^2\right) \end{bmatrix} + O\left(\delta^3\right) \tag{A6}$$

$$R = \begin{bmatrix} 1 & \xi_6 & -\xi_5 \\ -\xi_6 & 1 & \xi_4 \\ \xi_5 & -\xi_4 & 1 \end{bmatrix} + H$$

where

$$H = \frac{1}{2}\begin{bmatrix} \left(\xi_5^2+\xi_6^2\right) & 0 & 0 \\ -2\xi_4\xi_5 & \left(\xi_4^2+\xi_6^2\right) & 0 \\ -2\xi_4\xi_6 & -2\xi_5\xi_6 & \left(\xi_4^2+\xi_5^2\right) \end{bmatrix} \tag{A7}$$

Let x denote the position vector of a point on the hull surface S_H measured in a steady moving reference system and x' be the position vector of the same point on the hull surface, measured in a body fixed reference system. The two systems of axes are assumed to coincide when the ship in its equilibrium position. When the hull is displaced from the equilibrium position, the deflection α of any point of the hull can be expressed as (Newman, 1977 and Chun, 1991)

$$\begin{aligned} x - x' &= \xi + \Omega \times x' + \delta^2 H x' + O\left(\delta^3\right) \\ \alpha &= \xi(\xi_1,\xi_2,\xi_3) + \Omega(\xi_4,\xi_5,\xi_6) \times x' + \delta^2 H x' \end{aligned} \tag{A8}$$

The instantaneous normal vector on the wetted surface S_H is approximated by

$$n = n' + \Omega \times n' + \delta^2 H n' + O\left(\delta^3\right) \tag{A9}$$

Now the cross product for six oscillatory motions of the ship in relation to steady moving coordinate system is

$$\begin{aligned} x \times n &= \left[x' + \xi + \Omega \times x'\right] \times \left[n' + \Omega \times n' + \delta^2 H n'\right] + O(\delta^3) \\ &= x' \times n' + \xi \times n' + \left(\Omega \times n'\right) \times x' + x' \times \left(\Omega \times n'\right) + \xi \times \left(\Omega \times n'\right) + x' \times \delta^2 H n' + O(\delta^3) \quad \text{(A10)} \\ &= x' \times n' + \xi \times n' + \Omega \times \left(x' \times n'\right) + x' \times \left(\Omega \times n'\right) + \xi \times \Omega \times n' + \delta^2 H\left(x' \times n'\right) + O\left(\delta^3\right) \end{aligned}$$

If we now consider heaving and pitching motions only, the transformation matrix of the body can be write

106

$$R = \begin{bmatrix} 1 & 0 & -\xi_5 \\ 0 & 1 & 0 \\ \xi_5 & 0 & 1 \end{bmatrix} + O(\delta^2) \qquad (A11)$$

From this point we will use the symbol s for sinkage and t for trim instead of ξ_3 and ξ_5 respectively, so the above equation become

$$R = \begin{bmatrix} 1 & 0 & -t \\ 0 & 1 & 0 \\ t & 0 & 1 \end{bmatrix} + O(\delta^2) \qquad (A12)$$

The deflection of any point on the hull due to heaving and pitching motion becomes

$$\alpha = \xi(0,0,\xi_3) + \Omega(0,\xi_5,0) \times x'(x',y',z') + O(\delta^3)$$
$$= (tz',0,s-tx') \qquad (A13)$$

The instantaneous normal vector due to heaving and pitching motion becomes

$$n = n' + \Omega \times n' + O(\delta^2) = (n_1' + tn_3', n_2', n_3' - tn_1') \qquad (A14)$$

Now the cross product due to heaving and pitching motion in reference to steady moving coordinate system

$$x \times n = x' \times n' + \xi \times n' + \Omega \times (x' \times n') + O(\delta^2)$$
$$= (n_4', n_5', n_6') + (-sn_2', sn_1', 0) + (tn_6', 0, tn_4')$$
$$= [(n_4' - sn_2' + tn_6'), (n_5' + sn_1'), (n_6' + tn_4')] \qquad (A15)$$

The cross product in reference to body fixed coordinate system is

$$x' \times n' = (n_4', n_5', n_6') = [(y'n_3' - z'n_2'), (z'n_1' - x'n_3'), (x'n_2' - y'n_1')] \qquad (A16)$$

Appendix B: Influence Coefficients
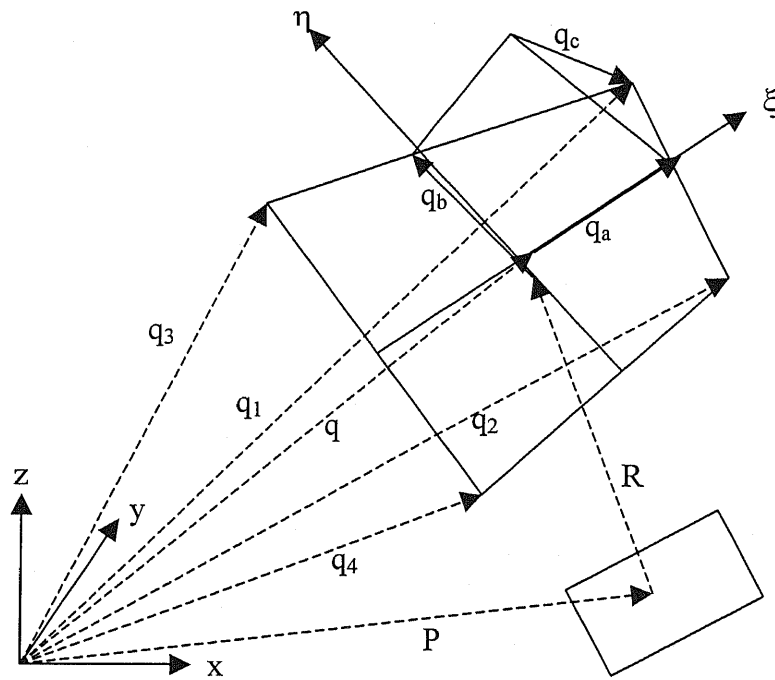
Fig. B1 Quadrilateral element for calculation of influential coefficients .

Based on Morino's Panel method (Morino et al, 1974) all the integrals given in the boundary value problem can be evaluated by assuming that the surface elements are quadrilateral and are approximated by a heperboloidal element. Using position vectors $q_i (i = 1..4)$ of four corner points of a panel any position vector q on the panel can be expressed as (Suciu and Morino, 1976)

$$q = q_0 + \xi q_a + \eta q_b + \xi \eta q_c \quad -1 \le \xi \le 1, \quad -1 \le \eta \le 1 \tag{B1}$$

The position vectors in terms of the locations of four corner points are obtained as:

$$\begin{bmatrix} q_0 \\ q_a \\ q_b \\ q_c \end{bmatrix} = \frac{1}{4} \begin{bmatrix} 1 & 1 & 1 & 1 \\ 1 & 1 & -1 & -1 \\ 1 & -1 & 1 & -1 \\ 1 & -1 & -1 & 1 \end{bmatrix} \begin{bmatrix} q_1 \\ q_2 \\ q_3 \\ q_4 \end{bmatrix} \tag{B2}$$

Introducing the base vectors tangential to surface

$$a_1(\xi,\eta) = \frac{\partial q}{\partial \xi} = q_a + \eta q_c$$

$$a_2(\xi,\eta) = \frac{\partial q}{\partial \eta} = q_b + \xi q_c \qquad (B3)$$

the unit normal vector is given by

$$n(\xi,\eta) = \frac{a_1 \times a_2}{|a_1 \times a_2|} \qquad (B4)$$

whereas the surface element is given by

$$d\sigma = |a_1 \times a_2| d\xi d\eta \qquad (B5)$$

All the integral appeared in the influence coefficients will be of the form

$$I = \int_{-1}^{1} \int_{-1}^{1} f(\xi,\eta) d\xi d\eta \qquad (B6)$$

Note that is

$$f(\xi,\eta) = \frac{\partial^2 D}{\partial \xi \partial \eta}$$

Then

$$I = D(1,1) - D(1,-1) - D(-1,1) + D(-1,-1)$$

Similarly

$$I = S(1,1) - S(1,-1) - S(-1,1) + S(-1,-1) \qquad -\frac{\pi}{2} \le \tan^{-1}(\ ) \le \frac{\pi}{2}$$

$$D = \frac{1}{2\pi} \int \frac{\partial}{\partial n}\left(\frac{1}{R}\right) dS \qquad (B7)$$

$$S = \frac{1}{2\pi} \int \frac{1}{R} dS \qquad (B8)$$

The coefficients of the integral equations are evaluated by using the relationships

$$D(\xi,\eta) = \frac{1}{2\pi} \tan^{-1}\left(\frac{(R \times a_1) \cdot (R \times a_2)}{|R|R \cdot (a_1 \times a_2)}\right) \qquad (B9)$$

$$S(\xi,\eta) = \frac{1}{2\pi}\left\{ -R \times a_1 \cdot n \frac{1}{|a_1|} \sinh^{-1}\left(\frac{R \cdot a_1}{|R \cdot a_1|}\right)\right.$$

$$+ R \times a_2 \cdot n \frac{1}{|a_2|} \sinh^{-1}\left(\frac{R \cdot a_2}{|R.a_2|}\right) \tag{B10}$$

$$\left. + R \cdot n \tan^{-1}\left(\frac{(R \times a_1) \cdot (R \times a_2)}{|R|R \cdot (a_1 \times a_2)}\right)\right\}$$

where

$$R(\xi,\eta) = q - p = q_0 + \xi q_a + \eta q_b + \xi\eta q_c - p \tag{B11}$$

$$\nabla_p D = \frac{1}{2\pi}\int \nabla_p \frac{\partial}{\partial n_q}\left(\frac{1}{R}\right) dS \tag{B12}$$

$$\nabla_p S = \frac{1}{2\pi}\int \nabla_p\left(\frac{1}{R}\right) dS \tag{B13}$$

In addition the coefficients of $\nabla_p D$ and $\nabla_p S$ are evaluated by using the relationships

$$\nabla_p D = \frac{1}{2\pi}\left[\frac{1}{|R|}\left(\frac{R \cdot a_1 \cdot (R \times a_1)}{|R \times a_1|^2} - \frac{R \cdot a_2 \cdot (R \times a_2)}{|R \times a_2|^2}\right)\right] \tag{B14}$$

$$\nabla_p S = \frac{1}{2\pi}\left\{\begin{array}{l} \dfrac{a_1 \times n}{|a_1|}\sinh^{-1}\left(\dfrac{R \cdot a_1}{|R \times a_1|}\right) - \dfrac{a_2 \times n}{|a_2|}\sinh^{-1}\left(\dfrac{R \cdot a_2}{|R \times a_2|}\right) + \\[3mm] n \tan^{-1}\left(\dfrac{(R \cdot a_1) \cdot (R \cdot a_2)}{|R|R \cdot a_1 \times a_2}\right) \end{array}\right\} \tag{B15}$$

Appendix C: Radiation Condition

The coefficients D_H, D_W, D_B, S_H, S_F and their first derivatives are calculated according to Morino's analytical formula based on the assumption of quadrilateral element. In order to satisfy the radiation condition the second derivative D_H, D_W, D_B, S_H and S_F are computed by upstream finite difference operator as recommended by Dawson C.W. (Dawson, 1977)

$$
\left.
\begin{aligned}
D_{Hxx} &= \frac{1}{2\pi} \int_{S_H} \frac{\partial^2}{\partial x_p^2}\left(\frac{\partial G}{\partial n_q}\right) dS \\
D_{Hxx} &= \frac{\partial}{\partial x_p}\left[\frac{1}{2\pi} \int_{S_H} \frac{\partial}{\partial x_p}\left(\frac{\partial G}{\partial n_q}\right) dS\right] = \frac{\partial}{\partial x_p}\left[D_{Hx}\right]
\end{aligned}
\right\}
\tag{C1}
$$

In general the derivative of a function $f(x)$ at any point x can be written in the form:

$$
f_x(x) = \sum_{k=0}^{N-1} e_k f_{i-k}
\tag{C2}
$$

where e_k are determined by means of Taylor's expansion. The values of e_k for 2-point, 3-point and 4-point finite difference operator are obtained from the distance between the points and given in Park(1998) as below:

[1] **Two-point finite difference operator (N=2)**

$$
\left.
\begin{aligned}
e_1 &= \frac{1}{x_{i-1} - x_i} \\
e_0 &= -e_1
\end{aligned}
\right\}
\tag{C3}
$$

[2] **Three- point finite difference operator (N=3)**

$$
\left.
\begin{aligned}
e_2 &= \frac{-(x_{i-2} - x_i)^2}{(x_{i-1} - x_i)(x_{i-2} - x_i)(x_{i-2} - x_{i-1})} \\
e_1 &= \frac{(x_{i-1} - x_i)^2}{(x_{i-1} - x_i)(x_{i-2} - x_i)(x_{i-2} - x_{i-1})} \\
e_0 &= -(e_2 + e_1)
\end{aligned}
\right\}
\tag{C4}
$$

[3] Four- Point finite difference operator (N=4)

$$D_i = \{(x_{i-1} - x_i)(x_{i-2} - x_i)(x_{i-3} - x_i)\} \times$$
$$\{(x_{i-3} - x_{i-1})(x_{i-2} - x_{i-1})(x_{i-3} - x_{i-2})\} \times$$
$$(x_{i-3} + x_{i-2} + x_{i-1} - 3x_i)$$

$$
\left.
\begin{aligned}
e_3 &= \frac{(x_{i-1} - x_i)^2 (x_{i-2} - x_i)^2 (x_{i-2} - x_{i-1})(x_{i-2} + x_{i-1} - 2x_i)}{D_i} \\[2mm]
e_2 &= \frac{-(x_{i-1} - x_i)^2 (x_{i-3} - x_i)^2 (x_{i-3} - x_{i-1})(x_{i-3} + x_{i-1} - 2x_i)}{D_i} \\[2mm]
e_1 &= \frac{(x_{i-2} - x_i)^2 (x_{i-3} - x_i)^2 (x_{i-3} - x_{i-3})(x_{i-3} + x_{i-3} - 2x_i)}{D_i} \\[2mm]
e_0 &= -(e_3 + e_2 + e_1)
\end{aligned}
\right\}
\qquad (C5)
$$

The tangential derivatives of a function can be expressed in terms of local coordinate system (ξ, η) as

$$\nabla_t f = \frac{\frac{\partial f}{\partial \xi}[\xi - (\xi \cdot \eta)\eta] + \frac{\partial f}{\partial \eta}[\eta - (\eta \cdot \xi)\xi]}{|\xi \times \eta|^2} \qquad (C6)$$

Now the derivative of the function in the x −direction can be obtained as

$$\nabla_t f = \nabla_x f + \nabla_y f \qquad (C7)$$

The second derivative of a function is obtained by substituting the first derivative of the function in equation (C2). We shall get the second derivative with respect to xyz coordinate system using equations (C6) and (C7)

Appendix D: Kutta Condition

The perturbation velocity potential on the boundary surface for first order approximation in deep water is discretized as follows

$$\begin{bmatrix} (\delta - D_H) & S_F \\ -D_{Hxx} & 0.5(K_0\delta + S_{Fxx}) \end{bmatrix} \begin{Bmatrix} \phi_{1j} \\ \sigma_{1j} \end{Bmatrix} = \begin{bmatrix} S_H \\ S_{Hxx} \end{bmatrix} \{U \cdot n_x\} + \begin{bmatrix} D_W \\ D_{Wxx} \end{bmatrix} \{\Delta\phi_{1j}\} \tag{D1}$$

The Kutta condition requires that the velocity at the trailing edge of the body be finite. In the numerical formulation of the problem, we will implement the Kutta condition by requiring that the pressure at the upper and lower control points be equal and this can be expressed as

$$\Delta p_j = p_j^U - p_j^L = 0 \quad \text{for } j = 1 \ldots \ldots N \tag{D2}$$

where N is the number of elements (one side) at the trailing edge of the body. A direct solution of the resulting system of equations (D1) and (D2) is difficult due to the nonlinear character of equation (D2). Therefore, an iterative solution algorithm (Kerwin etal, 1987) is employed. At the kth iteration, first solve the linear system of equations (D1) with the values of $\Delta\phi_j^{(k)}$ determined from the $(k-1)^{th}$ iteration. The values of $\Delta p_j^{(k)}$ are given by equation (D2), with the values of pressures p_j^U and p_j^L determined as described in section of pressure calculation. If $\Delta p_j^{(k)}$ is not equal to zero with desired tolerance ($\varepsilon = 10^{-5}$), then proceed to another iteration with $\Delta\phi_j^{(k+1)}$ determined as follows:

$$[\Delta\phi]^{k+1} = [\Delta\phi]^k - [J]^{-1} \cdot [\Delta p]^k \tag{D3}$$

where

$$[\Delta p] = [\Delta p_1, \Delta p_2, \ldots \ldots \ldots \Delta p_N]^T$$

$$[\Delta\phi] = [\Delta\phi_1, \Delta\phi_2, \ldots \ldots \ldots \Delta\phi_N]^T$$

and

$[J]^{-1}$ is the inverse of the Jacobian matrix, the elements of which are defined as

$$J_{ij} = \begin{bmatrix} \dfrac{\partial(\Delta p_i)}{\partial(\Delta\phi_j)} \end{bmatrix} \quad \begin{cases} i = 1 \ldots \ldots N \\ j = 1 \ldots \ldots L \end{cases}$$

with the values of partial derivatives approximated numerically as:

$$\frac{\partial(\Delta p_i)}{\partial(\Delta\phi_j)} \approx \frac{\Delta p_i^{(\beta)} - \Delta p_i^{(0)}}{\Delta\phi_j^{(\beta)} - \Delta\phi_j^{(0)}}$$

where $\varDelta p_i{}^{(0)}$ corresponds to the initial guess $\varDelta \phi_j{}^{(0)}$ and $\varDelta p_j{}^{(\beta)}$ corresponding to $\varDelta \phi_j{}^{(\beta)}$, a perturbation to initial guess defined as

$$\Delta\phi_j^{(\beta)} = (1-\beta)\Delta\phi_j^{(0)} \quad L = j$$

and

$$\Delta\phi_1^{(\beta)} = \Delta\phi_1^{(0)} \quad \text{for} \quad L \neq j$$

where β is a very small number, which can be 10^{-2}. The initial guess $\varDelta \phi_j{}^{(0)}$ is taken as the difference of the potential at the upper and lower control points at the trailing edge of the body.

$$\Delta\phi_j^{(0)} = \Delta\phi_j^{U} - \Delta\phi_j^{L} \tag{D4}$$

The initial guess is therefore the original Morino Kutta condition.